# Centre for Maintenance Optimization & Reliability Engineering

Director
Chi-Guhn Lee

## Semi-annual report

December 11, 2018
Michael E. Charles Council Chamber

Mechanical & Industrial Engineering
UNIVERSITY OF TORONTO

cmore.mie.utoronto.ca | 416·946·7867

# Contents

# C-MORE progress meeting agenda

Michael E. Charles council chambers
35 St. George St. University of Toronto, Room 202
Tuesday December 11, 2018

| | |
|---|---|
| **Registration and coffee** | |
| 8:30–9:00 | |
| **Executive summary, introduction of attendees** | Chi-Guhn Lee |
| 9:00–9:20 | |
| **Presentations by consortium members** | |
| 9:20–10:20 | |
| Barrick | Joe Ashun |
| Department of National Defence | Lt. (N) Ian Clarke & Jamie Dreyer |
| **Coffee break** | |
| 10:20–10:50 | |
| **Collaborations with consortium members** | |
| 10:50–12:10 | |
| UK MOD: A minimal digital twin for asset health monitoring | Danish Anis |
| UK MOD: A real-options approach for long term procurement | Jing Cao |
| Kinross: Significant variable selection for haul truck engines | Dragan Banjevic |
| Barrick: Regression analysis of pump vibration data | Gaoyang Li |
| **Lunch** | |
| 12:10–1:00 | |
| **Collaborations with consortium members, continued** | |
| 1:00–2:20 | |
| Teck: Komatsu replacement decisions and salvage value sensitivity | Janet Lam |
| TTC: NDT inspections by track type and structure | Janet Lam & Sophie Tian |
| Toronto Hydro: Investment smoothing solution approaches | Gary Wang |
| Veoneer: Predictive maintenance strategies for process improvement | Akshay Vishwakarma |
| **Coffee break** | |
| 2:20–2:50 | |
| **Theoretical research developments** | |
| 2:50–3:50 | |
| Sequential decision making using multiple sources of information | Mike Gimelfarb |
| Data driven prognostics for CBM and health management | Li Yang |
| Research overview | Gaoyang Li |

# Executive summary

**Chi-Guhn Lee, C-MORE Director**

The following report summarizes work undertaken between C-MORE and collaborating companies and notes the major changes at C-MORE since the meeting in June 2018. As Director of the Centre for Maintenance Optimization and Reliability Engineering (C-MORE), I have continued to expand the service and research portfolio of the Centre by ensuring the continuous engagement of consortium members and driving the research program in new directions, such as data analytics and machine learning. Since the last progress meeting, the Consortium is in the process of signing up two new members: Metrolinx, and Department National Defence.

At the same time, I have been supervising both undergraduate and graduate projects, in digital twin, reinforcement learning, robust optimal stopping problem, and Markov decision processes.

I was invited as a keynote speaker at several conferences in the fall of 2018, including the 2nd Symposium on the Physical Asset Management by Centre for TAMS of Inha University in South Korea on November 16, 2018. I also had the pleasure of being a speaker at the International Operations & Maintenance Conference in the Arab Countries (OMAINTEC) in Cairo on November 18, 2018, and as a distinguished speaker in the seminar series on Digital Innovation by LG CNS in Seoul on November 22, 2018.

The C-MORE team has been busy since the June meeting. I am very happy that Professor Fae Azhari, MIE, University of Toronto, Professor Scott Sanner, MIE, University of Toronto, and Professor Sharareh Taghipour, MIE, Ryerson University, continue to be affiliated with C-MORE.

## The C-MORE team

**Janet Lam, Assistant Director**

Janet has continued working on projects with member companies, as well as developing research projects with other organizations, such as Veoneer and the Canadian Electricity Association. She visited the CEA generation committee workshop at Fredericton in October where she delivered a presentation on predictive analytics.

**Ali Zuashkiani, Director of educational programs**
Ali has been active in providing consulting services to various industries such as oil and gas, power generation and distribution, mining, and petrochemical. He has been busy delivering PAM, RCM3 and Spart Part Management programs to asset management professionals across the globe, and is serving on a team of five members developing guidelines on Management of Change for Institute of Asset Management.

He graduated from Harvard Kennedy School Executive Program in Public Leadership in March 2018 and graduated from Said Oxford Business School Executive Program in Leadership and Management in August 2018.

**Andrew K. S. Jardine, Professor emeritus**
In the fall of 2018, Andrew was appointed as an Adjunct Professor at Ryerson University, Department of Mechanical and Industrial Engineering, 2018 – 2021. At the University of Toronto, he is teaching a graduate course in Engineering Asset Management, and also delivered a 5-day course in Physical Asset Management through the School of Continuing Studies.

Across the globe, Andrew has been honoured with the keynote presentation at the International Operations & Maintenance Conference in the Arab Countries (OMAINTEC) in Cairo on November 18, 2018. The presentation is titled ”An Analytic Tool Box for Evidence Based Asset Management”. At the same conference, he also delivered a workshop titled ”The Role of Analytics to Optimise Maintenance and Replacement Decisions”. In September, Andrew attended the World Conference on Engineering Asset Management (WCEAM) in Stavanger, Norway.

In serving on the member awards committee for the Plant Engineering and Maintenance Association of Canada (PEMAC), Andrew made site visits to Cameco Corporation’s facility in Port Hope and the City of Mississauga maintenance facilities for the Maintenance Team of the Year award.

**Professor Fae Azhari**
While Fae has been on leave since June, her research group has remained active. Her current projects include: complex naval asset management using sensor data, optimizing the fabrication and performance of multifunctional cementitious composites, the application of digital image correlation for effective non-contact strain measurements in SHM, developing a sensing device for monitoring lateral soil pressure, the application of fibre optic sensors in torsional vibration monitoring, developing a sensing mat for gait analysis, bridge scour monitoring, and SHM of prestressed concrete beams using cementitious sensors.

Fae was awarded an NSERC Engage grant on fault detection in electronic packaging components and

an IC-IMPACTS grant on field implementation of a bridge scour monitoring scheme.

**Professor Scott Sanner**

Scott Sanner has wrapped up a project with TTC involving MEng student Tuocheng Liu. The aim of the project was to apply deep learning tools to train visual object detection methods to detect thermal anomalies on the TTC rail system. The project demonstrated relatively high accuracy and precision was achievable with under 300 labeled example images. A final report and all project source code required to reproduce results, train, and evaluate on future data were delivered to TTC.

Beyond this TTC project, Scott has been involved in a range of applied projects covering network and power grid security, predictive modeling for residential HVAC, prediction of hospital readmission for Sunnybrook hospital, uses of social media in financial applications, and a number of projects involving recommender systems for eCommerce applications. Scott also continues to engage in fundamental research on machine learning, reinforcement learning, deep learning, constraint satisfaction (with a best paper award at CPAIOR), and sequential decision-making in support of the aforementioned applications.

**Professor Sharareh Taghipour**

Sharareh's nomination as Canada Research Chair in Physical Asset Management was approved for five years (2018-2023). Sharareh has been teaching two courses at Ryerson in Fall 2018: Advanced Reliability Modeling for graduate students and Experimental Design and Quality Assurance for undergraduate students. She finished two collaborative projects entitled "Common Framework for Risk-Based Optimization of Gas Pipeline Integrity Inspections" and "Development of equipment repair/replacement decision making tool with economic and environmental considerations" with Jana Laboratories Inc. and with Fiix Inc., respectively. She also started a new collaboration with Intelerad Medical Systems Incorporated on a project entitled "Model recipes for incoming workload prediction". Moreover, she started collaboration with Wind Energy Institute of Canada for a project which aims to develop a digital twin of the wind turbines for their predictive maintenance. The data have been already shared with Ryerson and the plan is to conduct the project by Danish Anis (PhD student) at the University of Toronto under co-supervision of Sharareh and myself.

**Li Yang, Postdoctoral Fellow**

Li Yang joined C-MORE as a postdoctoral fellow in October, 2018. He got his Ph.D. degree in the School of Reliability and Systems Engineering at Beihang University in the same year. He is now working on the development of prognostics, condition-based maintenance and health management theories, with applications in wind turbines, production lines and transportation systems, etc.

**Dragan Banjevic, C-MORE Consultant**
Though officially retired, Dragan continued to collaborated mostly with Janet on projects with consortium members, notably with Kinross Gold, Barrick Gold, and TTC, under his new title of C-MORE consultant. He also provided help in some projects with C-MORE students.

## C-MORE students

We welcomed several new graduate students to C-MORE this fall:

*Danish Anis* started his Ph.D. under the joint supervision of Professors Chi-Guhn Lee and Sharareh Taghipour with a research focus on development of a digital twin for military vehicles.

*Kuilin Chen* began his Ph.D. program in September 2018 and is supervised by Prof. Chi-Guhn Lee. He completed his M.A.Sc. degree in statistical process control and optimization at McMaster University. He's currently a senior process automation engineer at ArcelorMittal Dofasco. His research topic is development of digital twin for reheat furnace.

*Michael Gimelfarb* began his Ph.D. program in September 2018 under co-supervision of Professors Scott Sanner and Chi-Guhn Lee. His recent paper, entitled "Reinforcement Learning with Multiple Experts: A Bayesian Model Combination Approach", was presented at the NIPS 2018 conference. Currently, he is working on adaptive exploration and model-based transfer learning.

*Avi Sokol* started his Ph.D. program in September 2018 under the supervision of Professor Chi-Guhn Lee with a research interest to use Machine Learning and Artificial Intelligence to reduce waste in supply chains. With a background in Industrial Engineering and Operations Research, Avi is currently employed as an Engineering Project Manager at Canadian Bearings.

*Gaoyang Li* started his Ph.D. program in Electric Machines and Electric Apparatus from March 2016 in Xi'an Jiaotong University and is now a visiting student in C-MORE since September 2018 under the supervision of Prof. Chi-Guhn Lee. His research interests include the condition monitoring, intelligent diagnosis, and remaining useful life prediction of power apparatus.

*Akshay Vishwakarma* collaborated with the engineering team at Veoneer and C-MORE to develop a predictive/statistical model for testing equipment at Veoneer.

*Jing Cao* is a fourth-year Engineering Science thesis student. She has submitted the proposal discussing how she would implement the real-option theory for optimizing UKMOD aircraft long-term procurement strategies.

*Gary Wang* is a fourth-year Engineering Science thesis student. After completing his PEY at Toronto Hydro, Gary joins C-MORE for this engineering thesis, continuing his work on the investment spike smoothing problem proposed by Toronto Hydro.

*Songhuan Huang* and *Tun Li* completed their MEng projects in Machine learning approaches for maintenance and co-authored a paper commissioned by the Canadian Electricity Association.

*Sophie Tian* is a undergraduate student in industrial engineering, currently on PEY at CIBC. She is currently working on the NDT inspection project with TTC, under the supervision of Dr. Janet Lam, to update the asset register and create an augmented database.

## C-MORE activities with consortium members

C-MORE is currently involved in the following projects with industry partners. All projects will be presented at the progress meeting and details are found in this report:

**Barrick Gold**

Following a meeting in late June, C-MORE received additional data for the Veladero barren pump project. The discharge pressure for each pump as well as the cause of downtime were included. Based on Thomas' recommendations, a multiple regression approach as taken to deduce relationships between the different variables in the data. We were able to identify some variables that are good predictors of flow and pressure of the pump system.

**Kinross Gold**

Further work on the significance of different measurement variables was done in the second half of 2018. As iron measurements did not originally return significant values, the predictive value of previous iron measurements, as well as the difference between iron measurements was investigated. Both were found to be significant. Using the additional cost information available, we were able to develop a decision policy for replacing the engines.

**Teck Coal**

Graeme proposed a project to analyse the optimal replacement age of their Komatsu haul trucks based on the capital investment plan. The problem was found to be highly sensitive to salvage values that could be obtained at retiring the asset. A software tool was developed to enable Teck to explore possible outcomes based on Teck's expected salvage value schedule. David Williams and his team received a SMS training session over Skype in August.

**Toronto Hydro**

Formulation of an optimization problem for the investment smoothing project took place. A linear and non-linear programming approach was explored. The next challenge is to address the size of the problem, as number of assets within a type of equipment can range in the hundreds of thousands.

**Toronto Transit Commission**
An extension of the NDT inspection project including the geometry and construction of tracks was proposed. Further details on the asset register were developed. We were able to compute an optimal inspection schedule for the Bloor-Danforth line (Line 2).

**UK MOD**
There are two on-going projects with UK MOD. Danish is building a statistics-based digital twin for vehicles to better model repair and maintenance strategies. Jing is formulating a real-options approach to long-term procurement problems. A web-based reactive application is to be built for this project.

## C-MORE Educational programs

Andrew Jardine has continued to offer courses in asset management around the world. The most recent Physical Asset Management course at the University of Toronto (in conjunction with the School of Continuing Studies) ran November 5 - 9, 2018. Based on ongoing changes in the workplace, the content has been revised; there is less focus on asset management, but continuing emphasis on data analytics, and a new section on machine learning.

In 2019, C-MORE is hosting a 3-day course featuring machine learning and asset management 4.0. It is scheduled for June 10-12 to coincide with the next consortium meeting.

## Conclusion

I have enjoyed the past year, working with the collaborating companies and learning about their specific needs. I am confident C-MORE will continue to maintain the support of current industry members through the hard work and dedication of its staff and students.

Chi-Guhn Lee
December 2018

# 1 Visits and interactions

**June 2018–December 2018**

| Date | Company | Location | Topic |
|---|---|---|---|
| Jun 5 | Team Eagle | Conference call | Project initiation meeting |
| Jun 13 | Team Eagle | U of T | Adaptive braking project meeting |
| Jun 15 | Veoneer | U of T | Project initiation meeting: Testing equipment reliability |
| Jun 20 | LG CNS, Korean Ministry of Science | U of T | University-level collaboration meeting |
| Jun 25 | Barrick | Barrick Toronto office | Veladero barren pump follow up |
| Jun 27 | DND | Conference call | Consortium membership discussion |
| Jun 27 | Teck | Conference call | Project initiation meeting: Capital asset replacement plan |
| Jun 28 | Kinross | Kinross Toronto office | CAT engines significant variables update |
| Jul 4 | Kishore Jhagroo | U of T | Educational programs collaboration |
| Jul 4 | Princess Margaret Hospital | U of T | Technical project proposal |
| Jul 5 | Toromont | Toromont Brampton office | Qualifying meeting |
| Jul 10 | Kishore Jhagroo | U of T | Educational programs follow-up |
| Jul 16 | Niroo research institute | U of T | Qualifying meeting |

*Continues on next page*

| Date | Company | Location | Topic |
|---|---|---|---|
| Jul 17 | Inanibus | U of T | Qualifying meeting |
| Jul 26 | TTC | TTC Dundas office | NDT weighting factors next phase |
| Aug 10 | Ontario centres of excellence | Conference call | Fund leveraging options |
| Aug 10 | Toronto Hydro | U of T | Investment smoothing follow-up |
| Aug 15 | Teck | Conference call | SMS software tutorial |
| Aug 21 | Toronto Hydro | 500 Commissioners office | Investment smoothing follow-up |
| Sep 10 – 20 | Scale AI | University of Montereal | Supercluster on AI for supply chain management |
| Sep 14 | Weir group | U of T | University-level collaboration meeting |
| Sep 21 | CEA | U of T | Conference preparation |
| Sep 24 – 26 | WCEAM | Stavanger, Norway | World Conference on Engineering Asset Management |
| Sep 26 | Toronto Hydro | U of T | Investment smoothing follow-up |
| Oct 1 | Nestlé | Nestlé Toronto office | Faculty-level collaboration meeting |
| Oct 5 | UK MOD | Conference call | Digital twin project details |
| Oct 9 | Defence Research and Development Canada | Conference call | Qualifying meeting |
| Oct 9 | TTC | U of T | NDT further stratification details |
| Oct 15 – 17 | CEA | Fredericton, NB | Generating unit meeting |
| Oct 18 | UK MOD | Conference call | Procurement project details |
| Oct 19 | COMAC | U of T | Faculty-level collaboration meeting on machine learning for manufacturing |
| Oct 29 | TTC | Bathurst office | NDT next phase and Line 1 train addition project |

*Continues on next page*

| Date | Company | Location | Topic |
|---|---|---|---|
| Nov 1 | Titan | Conference call | Qualifying meeting |
| Nov 5 – 9 | C-MORE | U of T | 5-day program on Physical Asset Management |
| Nov 6 | Inanibus | U of T | Collaboration |
| Nov 7 | Kinross | Kinross Toronto office | Significant variables follow-up |
| Nov 8 | Capital Power | Conference call | Qualifying meeting |
| Nov 14 | TAMS | Inha University | Inter-centre collaboration meeting for MOU |
| Nov 18 – 21 | OMAINTEC | Cairo, Egypt | Presentation and delegate |
| Nov 21 | Barrick | Barrick Toronto office | Veladero pump regression results |
| Nov 28 | Titan | U of T | Collaboration meeting |
| Nov 28 | Longyuan Canada Renewables | Longyuan ScotiaPlaza Office | Collaboration meeting |
| Nov 28 | CN | Conference call | Qualifying meeting |
| Dec 3 – 7 | NIPS Conference | Montreal | Presentation and delegate |

# 2 C-MORE publications and presentations 2018

## Journal papers published or accepted


[1] Jiang, Z., Banjevic, D., Mingcheng E., Jardine, A., Li, Q., "Remaining useful life estimation of metropolitan train wheels considering measurement error", *Journal of Quality in Maintenance Engineering*, 2018, 24:4, 422-436 DOI: 10.1108/JQME-04-2016-0017.

[2] Sahba, P., Balcıoğlu, B., Banjevic, D., "Multilevel rationing policy for spare parts when demand is state dependent", *OR Spectrum*, 2018.

[3] Safaei, N. and Jardine, AKS. "Aircraft routing with generalized maintenance constraints", *OMEGA: The International Journal of Management Science*, 2018, 80: 111-122. DOI: 10.1016/j.omega.2017.08.013.

[4] Seecharan, T., Labib, A., Jardine, A., "Maintenance strategies: Decision Making Grid vs Jack-Knife Diagram", *Journal of Quality in Maintenance Engineering*, 2018, 24:1, 61–78. DOI: 10.1108/JQME-06-2016-0023.

[5] Qiu Qingan, Cui Lirong, Yang Li*. "Maintenance Policies for Energy System Subject to Complex Failure Processes and Power Purchasing Agreement," *Computers & Industrial Engineering*, 2018, 119: 193-203.

[6] Yang Li, Ye Zhisheng, Chi-Guhn Lee, Yang Sufen, Peng Rui. "A two-phase preventive maintenance policy considering imperfect repair and postponed replacement," *European Journal of Operational Research*, 2018. DOI: 10.1016/j.ejor.2018.10.049.

[7] Yang Li, Zhao Yu, Peng Rui, Ma Xiaobing. "Hybrid preventive maintenance of competing failures under random environment," *Reliability Engineering and System Safety*, 2018, 174: 130-140.

[8] Yang Li, Zhao Yu, Peng Rui, Ma Xiaobing, "Opportunistic maintenance of production systems subject to random wait time and multiple control limits," *Journal of manufacturing systems*, 2018, 47: 12-34.

[9] Yang Li, Zhao Yu, Ma Xiaobing, "Multi-level maintenance strategy of deteriorating systems subject to two-stage inspection," *Computers & Industrial Engineering*, 2018, 118: 160-169.

[10] Yang Li, Zhao Yu, Ma Xiaobing, Qiu Qingan, "An optimal inspection and replacement policy for a two-unit system," *Journal of Risk and Reliability*, 2018, DOI:10.1177/1748006X18761488.

## Journal papers submitted or under review

[1] Yang Li, Sun Qiuzhuang, Ye Zhisheng, "Designing Mission Abort Strategies based on Early-Warning Signal-Application to UAV," *IEEE Transactions on Industrial Informatics*, 2018. Under review.

[2] Yang Li, Zhao Yu, Ma Xiaobing, "Advanced maintenance scheduling of a two-component system with failure interaction," *Applied Mathematical Modeling*, 2018. Under 2nd review.

## Articles in other contexts

[1] Jardine, A.K.S. "An Analytic Toolbox", *Assets*, August 2018, 14–16. Magazine for members of the Institute of Asset Management

[2] Lam, J. Banjevic, D., Huang, S., Li, T. Lee, C. G. "Applications of predictive analytics in assessing power generating unit reliability", 2018. White paper produced for the Canadian Electricity Association.

## Conference presentations

[1] Gimelfarb, M. Sanner, S., Lee, C. G, "Reinforcement Learning with Multiple Experts: A Bayesian Model Combination Approach", *Advances in Neural Information Processing Systems (NeurIPS)*, 2018.

[2] Jardine, A.K.S., "An Analytic Tool Box for Evidence Based Asset Management", *International Operations & Maintenance Conference in the Arab Countries (OMAINTEC)*, Cairo, November 18, 2018, Keynote presentation.

[3] Jardine, A.K.S. "The Role of Analytics to Optimise Maintenance and Replacement Decisions" *OMAINTEC conference*, Cairo, November 19, 2018. Workshop presentation.

[4] Lam, J. "Predictive Analytics in Maintenance of Generating Units" *CCOS Generation Committee Workshop*, Fredericton, October 16, 2018.

# 3 C-MORE leadership activities

**Chi-Guhn Lee, C-MORE director**

Chi-Guhn has lead a team of research graduate students doing research in digital twin, reinforcement learning, robust optimal stopping problem, and Markov decision processes. He was also invited as a keynote speaker at 1° Seminario Integrador, Programa de Pos-Graduacao em Engenharia Civil, Uniersidade Federal de Pernambuco, Recife, Brazil on September 14, 2018, as a keynote speaker in an entrepreneurship event hosted by Kiga Labs in Toronto on November 5, 2018, as a keynote speaker at the 2nd Symposium on the Physical Asset Management by Centre for TAMS of Inha University in South Korea on November 16, 2018, as a speaker at the International Operations & Maintenance Conference in the Arab Countries (OMAINTEC) in Cairo on November 18, 2018, and as a distinguished speaker in the seminar series on Digital Innovation by LG CNS in Seoul on November 22, 2018.

**Janet Lam, Assistant director**

Since June, Janet has continued working on projects with member companies, as well as developing research projects with other organizations, such as Veoneer and the Canadian Electricity Association. She visited the CEA generation committee workshop in October and delivered a presentation on predictive analytics. The progress of the projects will be presented by the graduate students in today's meeting.

**Andrew K. S. Jardine, Professor emeritus**

In the fall of 2018, Andrew was appointed as an Adjunct Professor at Ryerson University, Department of Mechanical and Industrial Engineering, 2018 – 2021. At the University of Toronto, he is teaching a graduate course in Engineering Asset Management, and also delivered a 5-day course in Physical Asset Management through the School of Continuing Studies.

Across the globe, Andrew has been honoured with the keynote presentation at the International Operations & Maintenance Conference in the Arab Countries (OMAINTEC) in Cairo on November 18, 2018. The presentation is titled "An Analytic Tool Box for Evidence Based Asset Management". At the same conference, he also delivered a workshop titled "The Role of Analytics to Optimise Maintenance and Replacement Decisions". In September, Andrew attended the World Conference on Engineering Asset Management (WCEAM) in Stavanger, Norway.

In serving on the member awards committee for the Plant Engineering and Maintenance Association of Canada (PEMAC), Andrew made site visits to Cameco Corporation's facility in Port Hope and the City of Mississauga maintenance facilities for the Maintenance Team of the Year award.

**Dragan Banjevic, C-MORE consultant**

In his work with C-MORE Dragan collaborated mostly with Janet on projects with consortium members, notably with Kinross Gold, Barrick Gold, and TTC. He also provided help in some projects with C-MORE students.

**Sharareh Taghipour, Ryerson, external collaborator**

Sharareh's nomination as Canada Research Chair in Physical Asset Management was approved for five years (2018-2023). Sharareh has been teaching two courses at Ryerson in Fall 2018: Advanced Reliability Modeling for graduate students and Experimental Design and Quality Assurance for undergraduate students. She finished two collaborative projects entitled "Common Framework for Risk-Based Optimization of Gas Pipeline Integrity Inspections" and "Development of equipment repair/replacement decision making tool with economic and environmental considerations" with Jana Laboratories Inc. and with Fiix Inc., respectively. She also started a new collaboration with Intelerad Medical Systems Incorporated on a project entitled "Model recipes for incoming workload prediction". Moreover, she started collaboration with Wind Energy Institute of Canada for a project which aims to develop a digital twin of the wind turbines for their predictive maintenance. The data have been already shared with Ryerson and the plan is to conduct the project by Danish Anis (PhD student) at the University of Toronto under co-supervision of Sharareh and Chi-Guhn Lee.

**Scott Sanner, University of Toronto**

As of August 2018, Scott Sanner has wrapped up a project with TTC involving MEng student Tuocheng Liu. The aim of the project was to apply deep learning tools to train visual object detection methods to detect thermal anomalies on the TTC rail system. The project demonstrated relatively high accuracy and precision was achievable with under 300 labeled example images. A final report and all project source code required to reproduce results, train, and evaluate on future data were delivered to TTC.

Beyond this TTC project, Scott has been involved in a range of applied projects covering network and power grid security, predictive modeling for residential HVAC, prediction of hospital readmission for Sunnybrook hospital, uses of social media in financial applications, and a number of projects involving recommender systems for eCommerce applications. Scott also continues to engage in fundamental research on machine learning, reinforcement learning, deep learning, constraint satisfaction (with a best paper award at CPAIOR), and sequential decision-making in support of the aforementioned applications.

**Fae Azhari, University of Toronto**

While Fae has been on leave since June, her research group has remained active. Four new people joined

her research group, making the current members to 1 post-doc, 4 PhD, 2 MASc., and 2 undergraduate students. Her projects include: complex naval asset management using sensor data, optimizing the fabrication and performance of multifunctional cementitious composites, the application of digital image correlation for effective non-contact strain measurements in SHM, developing a sensing device for monitoring lateral soil pressure, the application of fibre optic sensors in torsional vibration monitoring, developing a sensing mat for gait analysis, bridge scour monitoring, and SHM of prestressed concrete beams using cementitious sensors. Scott Koshman attended CORS and INFORMS conferences in the summer, and presented his work. Fae was awarded an NSERC Engage grant on fault detection in electronic packaging components and an IC-IMPACTS grant on field implementation of a bridge scour monitoring scheme.

**Ali Zuashkiani, Director of educational programs**

Ali has been active in providing consulting services to various industries such as oil and gas, power generation and distribution, mining, and petrochemical.

In educational programs, Ali conducted a five-day PAM course in Dubai , three and ten-day introductory RCM3 facilitation courses to SABIC, a petrochemical company in Saudi Arabia. He also delivered Spare Part Management programs to DP World and to IPEMAN in Peru.

Ali attended the World's Economic Forum conference on Fourth Industrial Revolution in San Francisco, and is on a team of five members developing guidelines on Management of Change for Institute of Asset Management.

He graduated from Harvard Kennedy School Executive Program in Public Leadership in March 2018 and graduated from Said Oxford Business School Executive Program in Leadership and Management in August 2018. **C-MORE Educational programs** In 2018, three main educational program were offered as part of C-MORE.

- Public 5-day PAM course. April
- Life cycle costing and spare parts management to IPEMAN, Peru. October.
- School of continuing studies, 5-day PAM course. November.

In 2019, C-MORE is hosting a 3-day course featuring machine learning and asset management 4.0. It is scheduled for June 10-12 to coincide with the next consortium meeting.

# 4 Overall project direction

**Janet Lam, C-MORE Assistant director**

## Goals and retrospectives

This report gives a short overview of the activities in C-MORE for the period June 2018–December 2018. Professor Chi-Guhn Lee continues his leadership activity as the Director of C-MORE. He established several new contacts with industry, having qualifying meetings with Toromont, DRDC, Nestlé, The Weir Group, COMAC and Titan. Two companies are in the process of joining the Consortium: Metrolinx and DND. Collaboration with the consortium members has continued on the current projects, and we have discussed ideas for new ones.

A major push to submit a grant proposal for an NSERC Collaborative Research and Development (CRD) grant took place in the summer and fall of 2018. This grant leverages consortium membership fees with federal government funding. The partnered members on this grant are Barrick, Kinross and Teck. The title of this proposal is Maintenance and reliability in the face of uncertain data.

An NSERC Engage grant with Veoneer Inc. is also in progress.

Research activity has continued with the addition of a new postdoctoral fellow, PhD student, and a visiting PhD student. Several MEng and undergraduate thesis students are also working on ongoing projects.

## 4.1 Activities

### 4.1.1 Theoretical work

This section on theoretical work is oriented toward students' and postdoctoral fellows' research topics.

| Name | Activity |
|---|---|
| Li Yang, Postdoctoral fellow | Li Yang joined C-MORE as a postdoctoral fellow in October, 2018. He got his Ph.D. degree in the School of Reliability and Systems Engineering at Beihang University in the same year. He is now working on the development of prognostics, condition-based maintenance and health management theories, with applications in wind turbines, production lines and transportation systems, etc. |
| Danish Anis, Ph.D. student | Danish started his Ph.D. under the joint supervision of Prof. Chi-Guhn Lee and Prof. Sharareh Taghipour in September 2018 with a research focus on development of a digital twin for military vehicles. Prior to joining C-MORE, he completed his B.Eng in Mechanical Engineering in 2016 and M.Sc in Reliability Engineering and Asset Management in 2017 from The University of Manchester, UK. |
| Jing Janice Cao, EngSci thesis student | Jing has submitted the proposal discussing how she would implement the real-option theory for optimizing UKMOD aircraft long-term procurement strategies. She is currently working on the formulation of the aircraft procurement utility function with different decision variables and constraints. She plans to submit the formulation with a web based interactive program in December 2018. |
| Kuilin Chen, Ph.D. student | Kuilin began his Ph.D. program in September 2018 and is supervised by Prof. Chi-Guhn Lee. He completed his M.A.Sc. degree in statistical process control and optimization at McMaster University. He's currently a senior process automation engineer at ArcelorMittal Dofasco. His research topic is development of digital twin for reheat furnace. |
| Michael Gimelfarb, Ph.D. candidate | Michael began his Ph.D. program in September 2018 under co-supervision of Professor Scott Sanner and Professor Chi-Guhn Lee. His recent paper, entitled "Reinforcement Learning with Multiple Experts: A Bayesian Model Combination Approach", was accepted to the NIPS 2018 conference and will be presented in December. A more detailed review of this work is included in the report. Currently, he is working on adaptive exploration and model-based transfer learning. |

*Continues on next page*

| Name | Activity |
|---|---|
| Songhuan Huang, M.Eng student | Songhuan co-authored a paper commissioned by the Canadian Electricity Association, with an emphasis on machine learning approaches to multi-class text classification. He graduated from the M.Eng program and is now working at Shiu Pong Developments Ltd as a Project coordinator. |
| Gaoyang Li, Visting PhD student | Gaoyang started his Ph.D. program in Electric Machines and Electric Apparatus from March 2016 in Xi'an Jiaotong University and is now a visiting student in C-MORE since September 2018 under the supervision of Prof. Chi-Guhn Lee. His research interests include the condition monitoring, intelligent diagnosis, and remaining useful life prediction of power apparatus. |
| Tun Li, M.Eng student | Tun co-authored a paper commissioned by the Canadian Electricity Association, with an emphasis on clustering units with machine learning approaches to categorize units by health characteristics. He is scheduled to graduate from the M.Eng program in December 2018. |
| Avi Sokol, Ph.D. student | Avi started his Ph.D. program in September 2018 under the supervision of Professor Chi-Guhn Lee with a research interest to use Machine Learning and Artificial Intelligence to reduce waste in supply chains. With a background in Industrial Engineering and Operations Research, Avi is currently employed as an Engineering Project Manager at Canadian Bearings. |
| Sophie Tian, PEY research student | Sophie is an undergraduate student in industrial engineering, currently on PEY at CIBC. She is currently working on the NDT inspection project with TTC, under the supervision of Dr. Janet Lam, to update the asset register and create an augmented database. |
| Akshay Vishwakarma, MEng student | Akshay is an MEng student working under Prof Chi-Guhn Lee and Dr. Lam for his MEng project. Akshay collaborated with the engineering team at Veoneer and C-MORE to develop a predictive/statistical model for testing equipment at Veoneer. This model will help Veoneer predict upcoming failures in their equipment and plan their resources accordingly. |

*Continues on next page*

| Name | Activity |
|---|---|
| Gary Wang, EngSci thesis student | Gary was a senior technical student at Toronto Hydro. Since the last meeting, Gary, Prof. Lee, and Dr. Lam have met with several engineers and supervisors at Toronto Hydro to discuss detailed approaches to the Toronto Hydro investment spike smoothing problem. After completing his PEY at Toronto Hydro, Gary joins C-MORE for this engineering thesis, continuing his work on the investment spike smoothing problem proposed by Toronto Hydro. In the last few months, detailed mathematical formulations and optimization simulations have been developed. |

### 4.1.2 Collaboration with companies and site visits

This section gives details on pregress in research conducted with consortium members

| Member | Collaboration |
|---|---|
| Barrick | Following a meeting in late June, C-MORE received additional data for the Veladero barren pump project. The discharge pressure for each pump as well as the cause of downtime were included. Based on Thomas' recommendations, a multiple regression approach as taken to deduce relationships between the different variables in the data. |
| Kinross | Further work on the significance of different measurement variables was done in the second half of 2018. As iron measurements did not originally return significant values, the predictive value of previous iron measurements, as well as the difference between iron measurements was investigated. Both were found to be significant. |
| Teck | Graeme proposed a project to analyse the optimal replacement age of their Komatsu haul trucks based on the capital investment plan. The problem was found to be highly sensitive to salvage values that could be obtained at retiring the asset. David Williams and his team received a SMS training session over Skype in August. |
| Toronto Hydro | Formulation of an optimization problem for the investment smoothing project took place. Gary is working on solution approaches to the formulation. There were several on-site meetings throughout the term. |

*Continues on next page*

| Member | Collaboration |
|---|---|
| TTC | An extension of the NDT inspection project including the geometry and construction of tracks was proposed. Sophie has been updating the asset register to ensure accuracy of the track information. |
| UK MOD | There are two on-going projects with UK MOD. Danish is building a statistics-based digital twin for vehicles to better model repair and maintenance strategies. Jing is formulating a real-options approach to long-term procurement problems. A web-based reactive application is to be built for this project. |

# 5 Development of a Digital Twin for Military Vehicles

**Mohamad Danish Anis, C-MORE Ph.D. student**

## 5.1 Background

In September 2018, C-MORE began exploring the opportunity of developing a digital twin as an extension of its existing research in the field of predictive maintenance of critical assets. Mr. Tim Jefferis from the Ministry of Defence UK (MoD UK), a C-MORE consortium member, pitched the idea of investigating the minimum amount of maintenance data necessary for modelling a digital twin for their military vehicles.

Due to the absence of a specified target system, a typical vehicle engine cooling system was chosen for behaviour modelling. The following report discusses the initial work on how a cloud based Simulink model of an engine cooling system can be developed for the purpose of fault detection and maintenance scheduling to facilitate remote diagnostics. The project is currently at its virtual representation stage where sensor data can be used to detect anomalous system behavior and later isolate the root cause.

## 5.2 Introduction

State of the art advancements and evolution in digital technologies are constantly challenging the traditional practices in many industries worldwide. The onset of what is seen by many as the fourth industrial revolution (Industry 4.0) finds its basis in a new generation of virtual reality and big-data driven models [1]. Studies such as [2]–[4] recognize Industry 4.0 as a paradigm shift in investment strategies of companies towards smart technology from an Industrial Internet of Things (IIoT) perspective. This reflects in the strategic responses adopted by organizations to economic crisis, increased market competitiveness and asset maintenance complexity.

For quiet some time now, digital twin (DT) technology has been recognized as a core component of Industry 4.0 with its ability to virtually represent the elements and dynamics of how an IIoT device operates throughout its life. The idea of a DT took shape with the vision of providing a comprehensive

functional mirror of a component, product or system, aiming to replicate the physical asset's performance in virtual space with real-time synchronization [5]. Instead of relying on information based on fleet statistics or other computationally expensive iterations to assess machine reliability, the question now being asked was whether one can determine the system failure modes before actually designing the physical system itself [6]. Essentially, a DT can create a digital feedback loop for remote diagnostics determining when and where failures may occur and how to better prepare for them. Thus, the use of this technology has paved way for a deeper understanding of Prognostics and Health Management (PHM) for accurate diagnosis and prognosis of damaged machinery parts under normal and adverse operating conditions.

### 5.2.1 Motivation

Armed forces in military face life threatening situations in war zones where machinery failure can be catastrophic. With high maintenance costs and dangerous repercussions of an unanticipated failure, there needs to be a high fidelity reference model to predict and analyze the performance of military vehicle systems under harsh conditions.

This study serves to be an applied research with UK's Ministry of Defense (MoD UK), involving multidisciplinary work in industrial operations research, mathematical modelling and maintenance optimization. The motivation is to develop DT algorithms that can integrate, simulate and visualize in the context of maintenance.

### 5.2.2 Literature Review: The Digital Twin Concept

Given the novelty of the DT concept, there exists little but a steadily growing literature on the different application specific definitions of a DT as understood by researchers from around the world. The first formal definition of a DT was proposed by NASA in its integrated technology road map, calling it a virtual equivalent of the physical system replicated for modelling, simulation and analysis purposes [7]. The broader aim was to have an integrated model to simulate, monitor, calculate, regulate and control system processes in a highly quasi-real fashion.

Based on the studies conducted over the last six years, table 5.1 below summarizes the industrial application specific definitions of DT as appeared in the literature.

### 5.2.3 Digital Twin Research Objective

The main objective is to accurately diagnose and predict the upcoming failure in a military vehicle subcomponent and model the repair and maintenance strategies using an appropriate diagnostic/prognostic DT. Therefore, the tasks at hand to develop a DT can be listed as (i) Data pre-processing (Diagnostics to identify failure modes) (ii) Existing failure mode prognosis (Remaining Useful Life Estimation) (iii)

Table 5.1: **Application Specific Literature Review on Digital Twins**

| Ref. No. | Year | Application Description | Comments |
|---|---|---|---|
| [8] | 2012 | DT used to predict aircraft structural reliability over the course of the mission | The developed DT was a life-long model with configurations for sub-models in the entire inventory |
| [9] | 2012 | Used DT for confidence prediction and CBM decision making in an aircraft | The developed numerical simulation model was used for RUL prediction |
| [10] | 2013 | A DT was used to model the life of vehicle materials and structures | The developed high-fidelity model was able to predict cracks with on-board vehicle health management system |
| [11] | 2015 | DT was able to model the relationship between product manufacturing process and the operating environment through simulation | The current state and behaviour of the production system life-cycle was realistically modelled |
| [12] | 2015 | The developed DT was able to incorporate wind turbine blade structural fatigue damage in real-time | The high fidelity model focused on SHM to develop a FEM framework for fatigue damage prediction |
| [13] | 2016 | The study put to use DT for engineering and mechanical design integrity | The model makes use of CAE-based simulations along with Simulink |
| [14] | 2016 | The DT was put to use for virtual commissioning for robot control | Used a Virtual Environment and Robotic Simulation (VERS) for control optimization |
| [15] | 2017 | Integrated DT with cyber-physical system (CPS) and virtual factory for smart manufacturing | The aim of the study was to create an architecture reference model for a cloud based CPS |
| [16] | 2017 | Heuristic optimization algorithm so as to identify key parameters of the model | The fidelity of the model was increased by regularly comparing results against real data |
| [17] | 2017 | In a DT for additive manufacturing, analytical sub-models were used to predict spatial and temporal variations | The predicted variations of metallurgical parameters proved accurate with validation of experimental data |
| [18] | 2018 | A generic DT driven PHM is proposed for interaction mechanism and fused data in a Wind Turbine | The study efficiently explained the building blocks of DT in complex machinery and constructed its framework by taking into account cost, fidelity and large data size |

Future failure mode prognosis (RUL with future failure modes and confidence levels) (iv) Post-action prognosis (Potential actions to eliminate the progression of failure modes).

The role of both diagnosis and prognosis need to be identified in order to understand the process that a system/component goes through from healthy state to final failure. The problem statement here requires a system oriented approach to prognostic based decision support, thereby making the existing failure mode diagnosis of the vehicle's cooling system an important task. Figure 5.1 below is a comprehensive flowchart imbibing the earlier mentioned tasks (ii) - (iv) as prognostics and (i) as diagnostics.

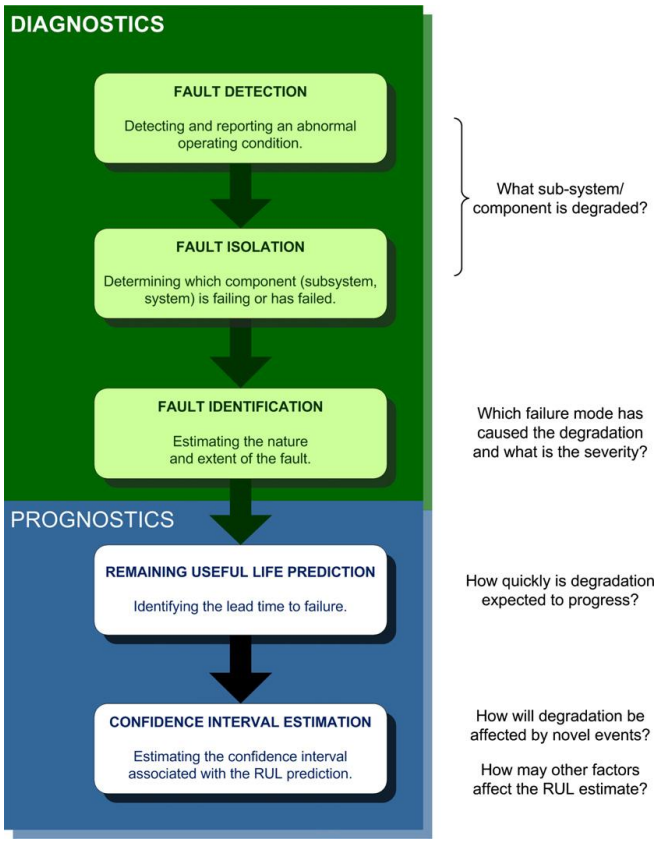


Figure 5.1: Steps involving prognosis results and relationship with diagnosis

## 5.3 Mathematical Modelling

Establishing fault hypothesis for any system requires the representation of its governing thermodynamics and physical laws as mathematical equations first. The main aim of this section is to analytically formulate the problem definition in designing a DT for the military vehicle.

The fundamental goal of our DT is to predict the output of the engine's cooling system (maintaining

desired vehicle temperature) with high fidelity. The equations of the mathematical sub-models governing the engine cooling system, namely the radiator model, fan model, electrical pump model and the engine control unit model, are derived from physical laws and assembled together below.These equations are used to generate a Simulink model of engine cooling system. By comparing faulty signals against healthy components signals, the developed model can be used for accurate and time efficient fault diagnosis.

### 5.3.1 Radiator: Heat Exchange Model

Given that a radiator exchanges heat with the environment to maintain system temperature, it facilitates a heat transfer function initiated when the engine operating temperature exceeds the specified threshold. The mechanisms involved in this heat transfer between the coolant and outside air are defined depending on the involved component surfaces between which the transfer is taking place at a given time. In principle, the radiator model is expressed using heat transfer rates between the engine coolant fluid and air in the following form:

$$\dot{Q}_{\text{total}} = \dot{Q}_{C-S} + \dot{Q}_{S-S} + \dot{Q}_{S-a} \tag{5.1}$$

Where $\dot{Q}_{\text{total}}$ is the total heat transfer between the coolant and outside air. The subsequent heat transfer rates on the RHS are that from coolant to inner wall ($\dot{Q}_{C-S}$), through radiator tube walls ($\dot{Q}_{S-S}$) that is assumed as 0 and radiator wall to the air ($\dot{Q}_{S-a}$). Equation (5.1) can be re-written as

$$\begin{aligned} \dot{m}C_P(T_i - T_0) &= mC_P(T_0 - T_s) + 0 + mC_P\frac{dT_0}{dt} \\ \frac{dT_0}{dt} &= \dot{m}C_P\frac{(T_i - T_0) - UA_r(T_0 - T_s)}{mC_P} \end{aligned} \tag{5.2}$$

Where $\dot{m}$ = Coolant mass flow rate, $m$ = Mass of coolant, $C_P$ = Specific heat capacity, $T_i$ = Engine coolant temperature, $T_s$ = Outside air temperature, $T_0$ = Coolant outlet temperature, $U$ = heat transfer coefficient, $A_t$ = Radiator tube cross section area and $A_r$ = Radiator area. eq. (5.2) basically provides the relation between temperature decrease and the heat transferred to outside air.

The coolant is expected to keep flowing through the pipes until the engine reverts back to its specified normal operating temperature. This is controlled by a temperature set point $sp_t$ through PID controllers (PID to be discussed in section 5.3.4). Specific to the objectives of the vehicle DT in question, the task of the heat exchange model is to predict an appropriate $T_0$ so as to regulate the $\dot{Q}_{C-S}$ with minimum prediction error. This can be done by identifying a transfer function $f_c(\cdot)$ between the measured $T_0$ and

a vector $x_t$ of all previously modelled temperatures $\hat{T_0}$ and set points as follows:

$$T_0 = f_c(\hat{T}_{01}, \hat{T}_{02}, \dots, sp_{t1}, sp_{t2}, \dots) + e_t$$

This can be expressed as

$$T_0 = f_c(x_t, \omega) + e_t$$

Where $e_t$ is an error given by the PID in the form of discontinuous signals or ripples.

Theoretically, the solution to eq. (5.2) should be able to predict the radiator coolant outlet model. However, the heat flow explained through Newton's law of cooling in eq. (5.1) does not accommodate the net energy change with air temperature expressed analytically by the 1st law of Thermodynamics. Therefore, the solution from eqs. (5.1) and (5.2) shall be used to model the next sub-system.

### 5.3.2 Fans: Surface Heat Transfer Model

Newton's Law of cooling states that the heat flow between an object and its surrounding environment can be characterized by a heat transfer coefficient $h$. $\dot{Q}_N$ is the heat flow rate calculated by:

$$\dot{Q}_N = hA(T_s - T_0),$$

where $h$ is in W/m$^2$K, $A$ is the cross sectional area of the surface in m$^2$, $T_S$ is the environmental temperature and $T_0$ is coolant temperature at any given point.

According to first law of thermodynamics, the change in energy with the change in air temperature is given by $\dot{Q}_T$. It is the net heat flow to the outside air, joules/s and given by,

$$\dot{Q}_T = \rho C_v V \frac{d(T_s - T_0)}{dt}$$

where $\rho$ is the air density in kg/m$^3$, $c_v$ is the specific heat of air in kJ/kgC and $V$ is the air volume in m$^3$. For the case where the net heat flow is zero, Newton's Law of Cooling and the First law of Thermodynamics, can be given by,

$$hA(T_s - T_0) = \rho C_v V \frac{d(T_s - T_0)}{dt}.$$

Solving the above provides $\ln(T_0 - T_s) = -\frac{t}{\tau} + C \gg \tau = \frac{\rho C_v V}{hA}$ where $\tau$ is the time constant. Further solution for the coolant temperature and mass flow rate $\dot{m}$ provides the following equation,

$$T_0 = T_s - (T_S - T_i) \exp\left\{\frac{-hA}{\dot{m}C_v}\right\}.$$

As seen in fig. 5.2, the presence of a fan improves the heat transfer rate and helps in achieving the desired temperature of 100°C much quicker.

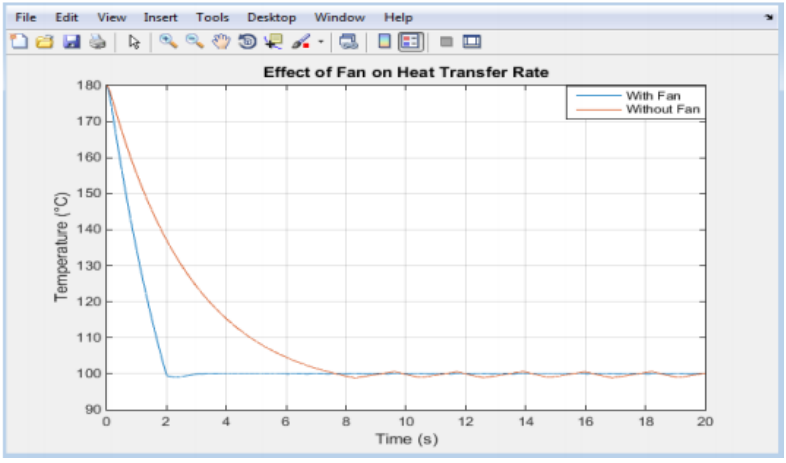


Figure 5.2: Effect of Fan on Heat Transfer Rate

### 5.3.3 Expansion Tank: Combustion Model

The expansion tank maintains system pressure by allowing air into cooling system through a valve. The mass flow rate from the previous model is used as an input,

$$\dot{m}_t = \mu_t(\theta_t) A_t \frac{P_a}{\sqrt{RT}} \phi\left(\frac{Pm}{P_a}\right),$$

where $\mu_t(\theta_t)$ is a flow coefficient at the throttle valve, $A_t$ is an opening cross sectional area of the throttle valve, $\theta_t$ is an opening angle of the throttle valve, $P_a$ is pressure of an atmosphere around the engine and $\phi\left(\frac{Pm}{P_a}\right)$ is a function using the fraction of pressures as a variable with $R$ as gas constant and $T$ as gas temperature respectively.

The heat from the comubstion $Q_{\text{cool}}$ is given by

$$Q_{\text{cool}} = \dot{m}_t(LHV - H_{\text{evp}}),$$

where fuel characteristics LHV (fuel's lower heat value) and $H_{\text{evp}}$ (the evaporation heat of the fuel) are calibration constants. Therefore, heat from the flowing coolant can be given in terms of the material heat capacity $C_p$ by,

$$T_{\text{cool}} = T_S + \frac{1}{C_p} Q_{\text{cool}}.$$

### 5.3.4 Electric Water Pump: DC Motor and PI Controller Model

The electric pump unit is composed of an electric motor and a water pump connected to the same axis, and a speed control device. The variation of rotation is determined by the electronic module which receives a PWM (pulse width modulation). The percentage variation of PWM is directly related to the variable speed electric pump motor [19].

A brushless DC electric motor is used to rotate the coolant inside the cooling system. The velocity of flow of coolant is dependent on the angular velocity of rotation of pump's impeller driven by dc motor. It is given by the relation $w \times r$, where $w$ is angular velocity of rotation of impeller and $r$ is radius of impeller.

**(i) DC Motor Model** - A separately excited DC motor is used as a plant to the control system. There are two methods that can be used to control the speed of a separately excited DC motor. The famous method of armature voltage control has advantage to retain maximum torque capability while the other method of field flux control will reduce maximum torque capability. If $k_m$ is torque constant, $R_m$ is terminal resistance, $L_m$ is terminal inductance and $J_{eq}$ is total moment of inertia, then the DC Motor transfer function is given by

$$G(s) = \frac{P_{\text{dot}}}{V(s)} = \frac{K}{\tau s + 1}$$

**(ii) PI Controller Model** - Control objectives focus on the transient behavior of the system such as to produce a zero steady state error, a fast transient response to a step command, a short settling time and low overshoot. It is also desirable to make the system less sensitive to disturbance [19]. A Proportional Integral Derivate (PID) controller is the best-known controller in industries. This scheme offers simple structure as well as robust performance. 20 For DC motor drive purpose, the use of two term controller so called PI controller is sufficient for best performance. Figure 5.3 represents the error and controlled signals combining with a reference signal to provide the output angular velocity. where error signal $e(t) = r(t) - w_m(t)$ and control signal is given by

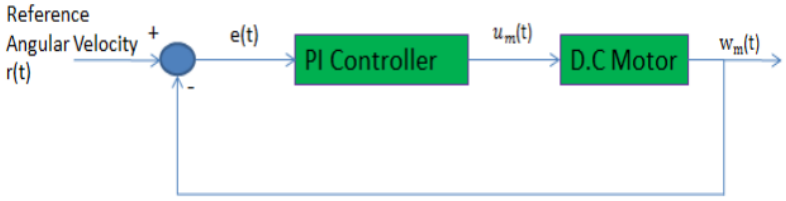


Figure 5.3: Speed Control of DC Motor

$$u_m(t) = k_p[r(t) - w_m(t)] + k_i \int_0^t [r(t) - w_m(\tau)]d\tau,$$

where $k_p$ is proportional gain and $k_i$ is integral gain. Therefore the transfer function of PI controller is given by

$$G_{PI}(s) = k_p + k_i$$

### 5.3.5 Engine Cooling System: Simulink Model

Figure 5.4 below shows the model of an Engine Cooling System in Simulink. It contains an engine where the heat is generated and added to the coolant, a temperature sensor to record the engine temperature, engine control unit to control the cooling of the system, a water pump to circulate the coolant inside the engine cooling system, a thermostat to regulate the flow of the coolant to the radiator and a radiator with an electric fan to dissipate heat from the coolant. The black lines in the figure are the input and

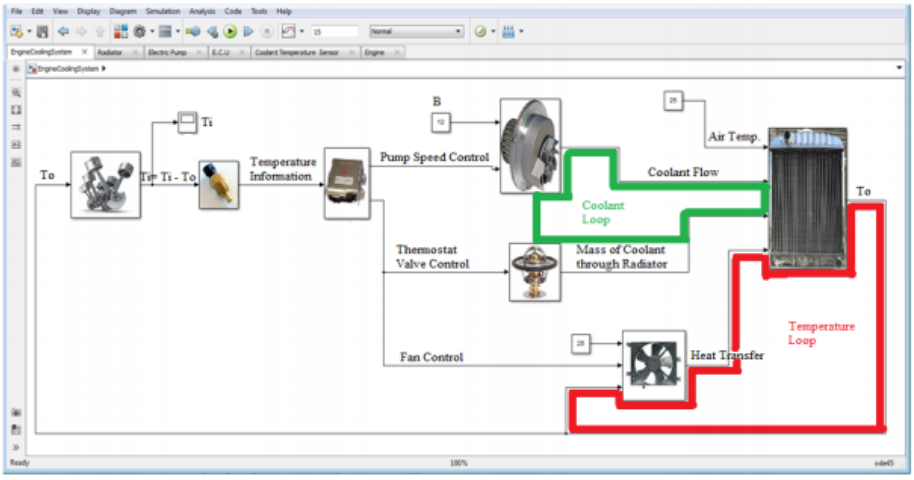


Figure 5.4: Engine Cooling System in Simulink

output signals of the components. The red line shows the coolant temperature loop (where the heat is dissipated) and the green line show the coolant flow loop (pump to radiator). The model contains an ECM which controls the working of the pump, the thermostat and the fan based on the engine temperature. During engine warm up phase, the ECM closes the thermostat completely by-passing the coolant back again to the engine to help achieve its desired working temperature quickly. The ECM also makes the pump move at a slower speed to save energy consumption. However, when the engine temperature becomes high (more than 100°C), ECM opens the thermostat valve to its fullest, increases the speed of pump to its maximum value and switches on the electric fan.

## 5.4 Next steps

Having been able to represent the vehicle cooling system in Simulink, the specified input conditions, data from the engine cooling components (sensor, pump and thermostat) is collected from the ECM of the vehicle under test. The same input conditions are used for the Engine Cooling System Simulink

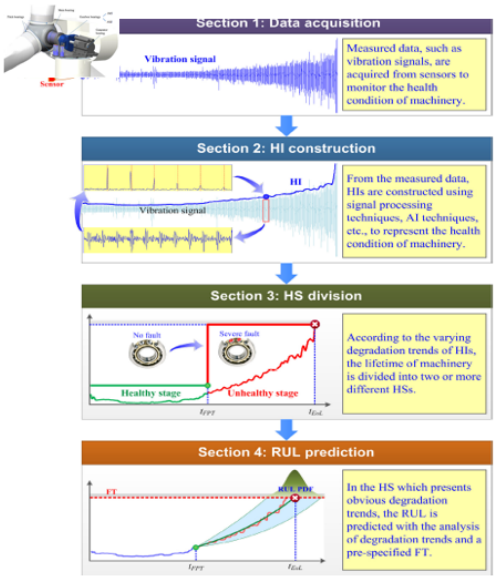


| | |
|---|---|
| **(1) Data Acquisition** | |
| CM Data (Sensors) | • *Vibration, Temperature, Oil Analysis, Voltage, Pressure, Weather/Environment Data* |
| Event Data | • *Installation, breakdowns, overhauls*<br>• *PM Repairs, replacements, oil changes* |
| **(2) Data Processing (Health Indicator Construction)** | |
| Data Cleaning | • *Sensor fault isolation, manual examination* |
| Data Analysis | *Feature extraction (Depends on CM Parameters)*<br>• *Waveform – Time, Frequency & time-freq. domain*<br>• *Value type – Multivariate (PCA, ICA, ARMA etc.)* |
| **(3) Health State Division** | |
| Degradation Modelling | • *Multi-stage (Healthy / Unhealthy) Estimation* |
| Hypothesis Testing | • *Fault detection without intrusive inspection* |
| **(4) Remaining Useful Life Estimation** | |
| Model-based Methods | • *Wiener, Inverse Gaussian, AR, Gamma, PF* |
| Physics-based Models | • *Paris' law, Forman Law, Norton Law* |
| Data-driven Models | • *HMM, ANN, CNN, SVM, Neuro-fuzzy* |
| Hybrid Models | *For Instance:*<br>• *Model-based ARMA used for system identification*<br>• *Hypothesis testing of obtained parameters*<br>• *Prognosis (RUL) using Data-driven HMM* |

Figure 5.5: RUL Estimation flowchart and model categories

model and simulation data are collected. These two sets of data are used to locate any faulty component in engine cooling system of the test vehicle. This is done by comparing the component's data from the vehicle to that generated by the Simulink model and indicate a fault if large deviations are found. Under same outside air temperature, drive cycle, supply voltage and gas pedal pressure, component data is collected from both the model and the vehicle. The fault diagnosis algorithm compares the predicted behavior of the model and behavior and indicate the presence of any fault.

For fault prognosis, the following flowchart in fig. 5.5 can be used to prepare a Remaining Useful Life Estimation model using either model-based, data-driven, physics-based or hybrid models. Currently, work is in progress on how can an RUL estimation model be used to create a cloud based digital twin ecosystem, which can be operated online and where a real-time data acquisition and parameter update can take place. Also to be addressed is the data-information fusion technique (flow of information from raw sensor data to high level understanding) which can help in the implementation of DT for predictive maintenance.

# Bibliography


[1] F. Tao, J. Cheng, Q. Qi, M. Zhang, H. Zhang, and F. Sui, "Digital twin-driven product design, manufacturing and service with big data," *The International Journal of Advanced Manufacturing Technology*, vol. 94, no. 9-12, pp. 3563–3576, 2018.

[2] J. Lee, B. Bagheri, and H.-A. Kao, "A cyber-physical systems architecture for industry 4.0-based manufacturing systems," *Manufacturing Letters*, vol. 3, pp. 18–23, 2015.

[3] K. Ashton, "That 'internet of things' thing.," *RFID Journal*, vol. 11, no. 2, pp. 467–475, 2009.

[4] E. Negri, L. Fumagalli, and M. Macchi, "A review of the roles of digital twin in cps-based production systems," *Procedia Manufacturing*, vol. 11, pp. 939–948, 2017.

[5] S. Boschert and R. Rosen, "Digital twin—the simulation aspect," in *Mechatronic Futures*, Springer, 2016, pp. 59–74.

[6] C. Li, S. Mahadevan, Y. Ling, S. Choze, and L. Wang, "Dynamic bayesian network for aircraft wing health monitoring digital twin," *AIAA Journal*, vol. 55, no. 3, pp. 930–941, 2017.

[7] E. Glaessgen and D. Stargel, "The digital twin paradigm for future nasa and us air force vehicles," in *53rd AIAA/ASME/ASCE/AHS/ASC Structures, Structural Dynamics and Materials Conference 20th AIAA/ASME/AHS Adaptive Structures Conference 14th AIAA*, 2012, p. 1818.

[8] E. Tuegel, "The airframe digital twin: Some challenges to realization," in *53rd AIAA/ASME/ASCE/AHS/ASC Structures, Structural Dynamics and Materials Conference 20th AIAA/ASME/AHS Adaptive Structures Conference 14th AIAA*, 1812, p. 1812.

[9] B. Smarslok, A. Culler, and S. Mahadevan, "Error quantification and confidence assessment of aerothermal model predictions for hypersonic aircraft," in *53rd AIAA/ASME/ASCE/AHS/ASC Structures, Structural Dynamics and Materials Conference 20th AIAA/ASME/AHS Adaptive Structures Conference 14th AIAA*, 2012, p. 1817.

[10] K. Reifsnider and P. Majumdar, "Multiphysics stimulated simulation digital twin methods for fleet management," in *54th AIAA/ASME/ASCE/AHS/ASC Structures, Structural Dynamics, and Materials Conference*, 2013, p. 1578.

[11] R. Rosen, G. Von Wichert, G. Lo, and K. D. Bettenhausen, "About the importance of autonomy and digital twins for the future of manufacturing," *IFAC-PapersOnLine*, vol. 48, no. 3, pp. 567–572, 2015.

[12] Y. Bazilevs, X. Deng, A. Korobenko, F. L. di Scalea, M. Todd, and S. Taylor, "Isogeometric fatigue damage prediction in large-scale composite structures driven by dynamic sensor data," *Journal of Applied Mechanics*, vol. 82, no. 9, p. 091 008, 2015.

[13] A. Canedo, "Industrial iot lifecycle via digital twins," in *Proceedings of the Eleventh IEEE/ACM/IFIP International Conference on Hardware/Software Codesign and System Synthesis*, ACM, 2016, p. 29.

[14] G. Grinshpun, T. Cichon, D. Dipika, and J. Rossmann, "From virtual testbeds to real lightweight robots: Development and deployment of control algorithms for soft robots, with particular reference to," in *ISR 2016: 47st International Symposium on Robotics; Proceedings of*, VDE, 2016, pp. 1–7.

[15] K. M. Alam and A. El Saddik, "C2ps: A digital twin architecture reference model for the cloud-based cyber-physical systems," *IEEE Access*, vol. 5, pp. 2050–2062, 2017.

[16] B. R. Seshadri and T. Krishnamurthy, "Structural health management of damaged aircraft structures using digital twin concept," in *25th AIAA/AHS Adaptive Structures Conference*, 2017, p. 1675.

[17] T. DebRoy, W. Zhang, J. Turner, and S. Babu, "Building digital twins of 3d printing machines," *Scripta Materialia*, vol. 135, pp. 119–124, 2017.

[18] F. Tao, M. Zhang, Y. Liu, and A. Nee, "Digital twin driven prognostics and health management for complex equipment," *CIRP Annals*, 2018.

[19] E. G. Ribeiro, A. P. de Andrade Filho, and J. L. de Carvalho Meira, "Electric water pump for engine cooling," SAE Technical Paper, Tech. Rep., 2007.

# 6 Real-option Approach to UKMOD Procurement Problem

**Jing Cao, EngSci thesis student**

This report presents an ongoing thesis project of real-options analysis on the UK Military of Defense aircraft procurement problem.

## 6.1 Introduction to real-option approach

### 6.1.1 Background and significance of real-option

Running a business requires managers to make wise investment or operation decisions. Real-world projects are often complex and have substantial uncertainties in multiple phases. One decision may totally affect the life of a company and determine the success or failure of a business. As a result, the techniques of making wise decisions became an important topic of research. Convention ways of decision making include statistical and economic methods, Return on Investment (ROI), Net Present Value (NPV) calculations, cost-benefit analysis, etc. These traditional ways of decision making ignore outcome uncertainty, the choice of investment timing and irreversibility of resource commitment [1]. Thus, there needs to be a framework that can evaluate and determine the proper investment/disinvestment and business operation decisions.

### 6.1.2 Objective and hypothesis

One of the most powerful theories in business decision analysis that can address decisions under an extreme form of uncertainty is "Real option analysis". It is derived from financial option theory and offers numerous insights into business decisions with option like features by answering below two questions [2]:

1. How much to pay for a given real option;
2. When if ever to collect on the bet by exercising the option.

The goal of the thesis project is to develop an optimizing process using real option theory and confirm

its role in business investment and procurement decisions. I will investigate a real-world business example and devise an optimization model that will examine risks and uncertainties using real option analysis. The project will demonstrate the power of real options and compare it against traditional decision theory. The example will be based on the assumption that it can be solved using real option analysis and the factors are subject to completely random walk.

## 6.2 UKMOD Procurement Problem Definition

### 6.2.1 Objective

The high-level objective of this problem is to identify an optimized procurement model of aircrafts for UKMOD. We convert this objective into a mathematical portfolio optimization problem. The goal is to determine the optimized time and quantity to buy the aircrafts under various different conditions that can maximize total satisfaction of stakeholders within certain time frame.

### 6.2.2 Problem formulation

To measure the satisfaction of a portfolio, we introduce an exponential utility of the form $U(t) = A(t) + e^{-\gamma x}$, where $x$ is a random variable associated with each factor considered below and $\gamma$ is the coefficient to be determined by both subjective and objective conditions.

We shall consider below factors when measuring utility:

1. Price of the aircraft: Price of the aircraft is determined by market demand and supply of aircrafts in perfect competition market. Due to budget constraint, we assume lower price will give more satisfaction and higher price will give less satisfaction.
2. Maintenance and operating costs: The maintenance and operating costs, similarly, subject to the budget constraint, therefore we assume the target group would prefer less is better.
3. Technology improvement: One assumption is that technology level can only increase over time. An improvement of technology could possibly decrease the purchase price and related costs and therefore increase satisfaction if we buy aircrafts after the technology improvement.
4. Contribution to the mission: Military aircrafts are bought to meet certain military task or mission. The portfolio is better to fit in the mission properly in order to give more satisfaction.
5. Fair value of the aircraft: After purchasing the aircrafts, due to technology change or other factors, the fair value of the aircraft no longer equals to the purchase price. The difference of fair value and purchase price may contribute to satisfaction function as there could be alternative procurement portfolio that allows you to buy the same aircraft with a lower price a few years later.
6. Unexpected events such as wars. If a war happens, the demand for military aircrafts will increase significantly and thus create a completely different utility function.

Each aspect has dynamic values which changes over the time period. The relationship of each factor and the satisfaction may be linear or quadratic or exponential, which should be determined and modeled by the specific stakeholders or scenarios.

The constraints include technology (minimum technology level of procurement), military requirement, and budget limitation (may vary over the time period), etc.

We are going to display the utility function for each aircraft type with respect to the time(year) we buy the aircrafts. In the diagram, we could select each aircraft type and see how the decision of when to buy changes the utility function with considerations of above factors. Using this graph, we could determine the optimized time to buy each type of aircraft.

### 6.2.3 Mathematical formulation

#### 6.2.3.1 Basic variables definition

| Basic variable | Unit | Explanation |
|---|---|---|
| $i$ | no unit | Aircraft type index, e.g. fight jet, attack jet, combat jet, etc |
| $t$ | Year | Year index of when to buy, e.g. t=1 one year after the base year |
| $T$ | Year | The time horizon in years we are considering, e.g. 20/50/100 years |

#### 6.2.3.2 Utility function definition

Utility function $U_{t,i}(P_{t,i}, D_{t,i}, M_{t,i}, O_{t,i}, K_{t,i})$ for an aircraft type $i$ if we buy at time $t$.

#### 6.2.3.3 Decision variables

| Basic variable | Unit | Explanation |
|---|---|---|
| $P_{t,i}$ | \$ | The (relative)purchase price of brand new aircraft i at year t |
| $D_{t,i}$ | \$ | The (relative) depreciation expense of aircraft i at year t |
| $M_{t,i}$ | \$ | The (relative) maintenance expense of aircraft i at year t |
| $O_{t,i}$ | \$ | The (relative) operating expense of aircraft i at year t |
| $K_{t,i}$ | no unit | The technology level (1 to 10) of aircraft i at year t |

#### 6.2.3.4 Constraints

1. UKMOD can only buy aircraft with technology level greater or equal to $Ki*$.
2. Total budget of purchasing aircraft in year $t$: $Bt$.

## 6.3 One Factor Model

Consider just one factor – Price, a decrease in price over year can generate positive utility while an increase in price will generate negative utility in general. We use the utility function

$$U(t) = A(t)e^{-\gamma p(t)},$$

where $p(t)$ is the price of one particular aircraft at year $t$. Consider the price at year zero as 100 percent, the constant vector $A(t)$ is the utility in this situation. The coefficient $\gamma$ is determined by various stakeholders and currently can be inputted manually in the program. Consider the case that the price increases 1 percent, 2 percent, 3 and 4 percent in each following year, the utility decreases exponentially as below.

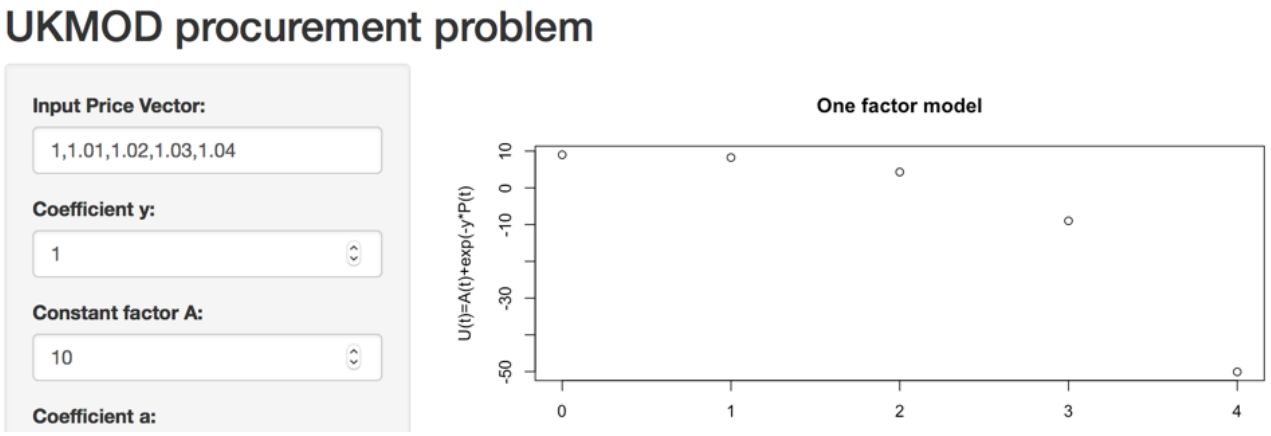


## 6.4 Summary and Further Implementation

Considering an exponential relationship between price and utility, we get a increasing utility function as the price decreases over time. This is insufficient to determine the optimized time to buy each type of aircrafts. Going forward, we will add in other factors and consider the correlation between the factors to maximize the utility.

# Bibliography

[1] J. T. Silva and H. Tadeu, "Real options theory: An alternative methodology applicable to investment analyses in r & d projects," *Australian Journal of Basic and Applied Sciences*, vol. 8, pp. 444–454, Apr. 2014.

[2] S. Howell, A. Stark, D. Newton, D. Paxson, M. Cavus, J. Azevedo-Pereira, and K. Patel, *Real Options - Evaluating Corporate Investment Opportunities in a Dynamic World*, English. Financial Times Prentice Hall, 2001.

# 7 Kinross: Caterpillar haul truck engines - Model selection and decision policy

**Dragan Banjevic, Janet Lam**

In April 2018, C-MORE began a new project with Kinross on the optimal replacement frequency of a fleet of haul truck engines. Kinross supplied event history and a record of inspections gathered at oil changes for its fleet of haul trucks. In the first stage (April – June 2018) the data preparation and analysis have been conducted, including cleanup, identification of anomalies and potential errors. In the second stage, initial model selection was started, and some preliminary results had been presented at the June C-MORE meeting. After June, more data cleaning was performed, mostly to look for "outliers" (spurious measurements, sampling errors), more detailed model selection, and finally, creation of decision policy. The details of this process will be described in this report.

## 7.1 A short summary of the data

- There are two different engine models: 793C and 793D. After discussion with Kinross engineers, it was concluded they can be considered identical for the analysis.
- There are 15 units – 9 are model 793C and 6 are 793D.
- There are 34 histories (chronological data since installation/repair till failure/suspension) of which 8 ended in failure, 13 ended in suspension (due to high hours) and 13 were still in service.
- Inspections are made regularly throughout the lives of all units, 1323 inspections in total
- The data ranges from July 2012 to February 2018.
- There are 37 columns of measurements, mostly metal and oil variables. Several of them (mostly oil variables) are with incomplete (missing) records. They were not included in the analysis.

## 7.2 Outliers analysis

Outliers in measurements are either erroneous records, or unusual records out of range or data trend that are not followed by any signs of engine problems. Erroneous records are either deleted or corrected,

and unusual records (very high, or very low) are often checked by repeated sample. In the historic analysis of the data is important to eliminate those cases, as they may obscure relationship between engine problems and measurements. An example of an outlier in copper (Cu) measurements is shown in fig. 7.1. The data show all Copper records for truck id 815 vs truck hours. A value of 80 ppm Cu is surrounded by values all less that 10ppm. No indication of engine problem (failure or replacement) can be seen on the graph of events, just below it. Another example of an outlier, common at engine installation, is shown on an Iron graph in fig. 7.2. It may be a clean-up value, or an error, more that any indication of a problem. All variables of any interest in the analysis had been checked and the outliers corrected. A common method we use in EXAKT is to replace them with the previous values. In total, we corrected 85 records.

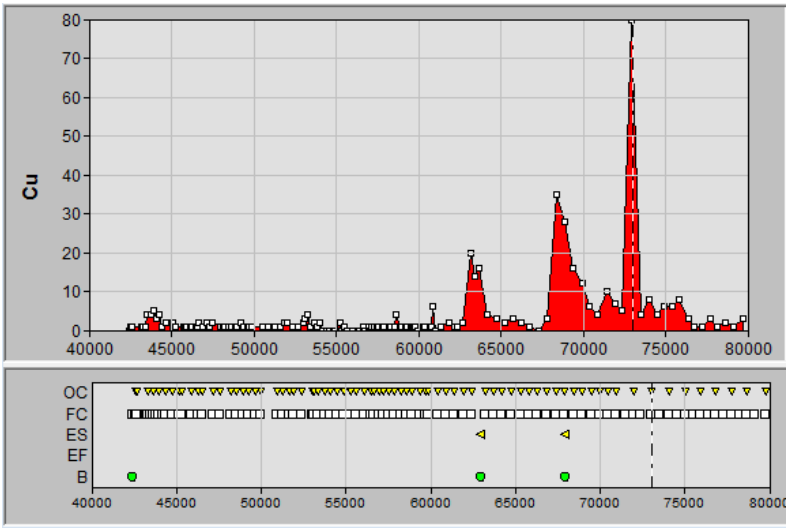


Figure 7.1: Copper records for truck ID 815 vs. truck hours

## 7.3 Default values at events

An important part of the analysis is to set up default values for variables in "clean" oil, just after oil replacement, as they are not measured. This is necessary for analysis of changes of the variable values from one inspection to the next. For wear metals and contaminants, the defaults are set up to zero values (0), and for additives, it depends on oil brand. The following "CovariatesOnEvent" table (table 7.1) was used in our analysis. The default values are also defined for the beginning of any history (at installation or repair). The default values at failure or suspension are used only in some special cases and will not be discussed here.

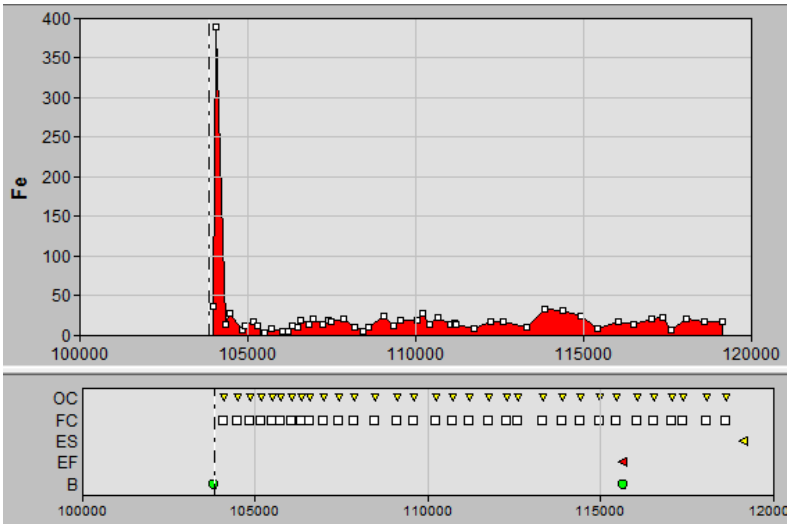


Figure 7.2: Iron records for truck ID 802 vs. truck hours

Table 7.1: Default variable values at events

| Event | Fe | Cu | Pb | Sn | Cr | Ni | Ti | Al | Si | Na | K | B | Ca | Mg | P | Zn | Mo |
|---|---|---|---|---|---|---|---|---|---|---|---|---|---|---|---|---|---|
| EF | 0 | 0 | 0 | 0 | 0 | 0 | 0 | 0 | 0 | 0 | 1.3 | 20 | 1000 | 850 | 1000 | 120 | 43 |
| ES | 0 | 0 | 0 | 0 | 0 | 0 | 0 | 0 | 0 | 0 | 1.3 | 20 | 1000 | 850 | 1000 | 120 | 43 |
| B | 0 | 0 | 0 | 0 | 0 | 0 | 0 | 0 | 0 | 0 | 1.3 | 20 | 1000 | 850 | 1000 | 120 | 43 |
| *ES | 0 | 0 | 0 | 0 | 0 | 0 | 0 | 0 | 0 | 0 | 1.3 | 20 | 1000 | 850 | 1000 | 120 | 43 |
| OC | 0 | 0 | 0 | 0 | 0 | 0 | 0 | 0 | 0 | 0 | 1.3 | 20 | 1000 | 850 | 1000 | 120 | 43 |

## 7.4 Oil change and filter change

Oil change is included in the events data as it affects measurements values. The metal particles accumulate in oil and show increasing trend in subsequent inspections of the same oil, until oil change (OC). As the number of oil samples from the same oil is one or two (sometimes three), the trend is not clearly visible in single histories under normal conditions, due to sampling variations, but can be observed in averages. An effect of filter change on variable values (as they are followed by OC) is considered insignificant, and is not taken into account in the analysis. At every OC, EXAKT augments the data to include the default values, as if they were observed.

## 7.5 Model selection

After data preparation, we can start model selection. The lifetime process of an engine (our equipment, in general) is described by its *hazard of failure* function in the form of proportional hazards model (PHM),

as follows

$$h(t;Z) = \frac{\beta}{\eta}\left(\frac{t}{\eta}\right)^{\beta-1} \exp\left\{\gamma_1 Z_1(t) + \gamma_2 Z_2(t) + \cdots + \gamma_m Z_m(t)\right\}.$$

The variables in the model are $t$ (operating hours - age), and measurements at $t$ (called covariates, in statistics) $Z_1(t), Z_2(t), \ldots, Z_m(t)$. Parameters of the model are $\beta$ (shape), $\eta$ (scale), variables' "weights" $\gamma_1, \gamma_2, \cdots, \gamma_m$. If a "weight" $\gamma_i$ of the covariate $Z_i(t)$ is equal to zero, than this variable "disappears" from the model, that is, it does not influence hazard of failure. In that case, the variable is called *nonsignificant*, otherwise is *significant*. If all weights are equal to zero, then none of the variables is significant and the model is reduced to the classical two-parameter Weibull model

$$h(t;Z) = \frac{\beta}{\eta}\left(\frac{t}{\eta}\right)^{\beta-1}.$$

The goal of model selection is to estimate parameters of the model and find a set of significant variables. The process works mostly through a sequential exclusion of nonsignificant variables from the model. With a large number of variables, and a limited number of histories (and failure events), the procedure can be tedious and time consuming.

### 7.5.1 Two-parameter Weibull model

As a simplest first model, we ignored all covariates, and estimated Weibull model, with shape and scale parameters, as shown in table 7.2. As seen, Shape = 2.313, indicating a process of engine aging (Shape

Table 7.2: Weibull model parameter estimates

| Parameter | Scale | Shape | Mean Life | Med. Life | Char Life | Std. Dev. |
|---|---|---|---|---|---|---|
| Estimate | 23855 | 2.313 | 21134.9 | 20359.3 | 23855 | 9695.9 |

> 1). The mean life of an engine is estimated to be 21,134.9 hours, if it were to run to failure without preventive replacements (due to large hours). The Kinross policy, as seen from the data, is to replace an engine at around 15,000-16,000 operating hours. From this Weibull model, a chance that an engine will survive to 16,000 hours replacement time is around 67%, not far from observed in the data. We will later discuss whether this policy is economically justified.

### 7.5.2 Selection of significant variables

The data includes a non-metal variable "Eval", an evaluation of overall health of the engine, with values as described in table 7.3. We investigated this variable first. The variable is qualitative (non-numerical) and requires a special transformation to check its significance. It appeared as *nonsignificant*, meaning that the described state did not correlate significantly with engines failures. It is not clear how this

Table 7.3: Eval variable description

| Value | Description |
|---|---|
| A | Acceptable |
| B | Minor corrective action required |
| C | Abnormal wear or condition exists, action required |
| X | Extreme wear or degradation of oil properties, immediate action required |

variable was calculated. It may require more detailed analysis.

The **Caterpillar SOS Services table** provided by Kinross suggests monitoring metal particles from Copper (Cu), Iron (Fe), Chromium (Ch), Aluminum (Al), Lead (Pb), Silicon (Si), and Tin (Sn).

We considered all metal variables in our analysis, not only from the Caterpillar table, by grouping them into three categories: Wear metals, Additives, and Contaminants. Some metals may be included in more than one group, such as Cu, Zn, Si, and Sb. After checking one group of metals, significant variables from different groups may be combined for further selection. The problem of models with larger numbers of variables is that the model accuracy may be poor, due to limited number of histories and failures. Typically, with the kind of data set we have here, up to three or four variables can be safely included in the model. In addition to variable selection (significant, nonsignificant), there is a statistical test-model fit applied to validate the overall model accuracy.

> Modelling only with "Caterpillar variables" did not reveal any model that might be hoped for. For example, *Fe* itself (as a single variable in the model) did not appear to be significant, as it was expected to be by the engine wear. When *Fe* values were plotted against failure events, there was no clear connection, such as *Fe* increase before failure. Emilio (from Kinross) asked whether this situation that some variables, such as *Fe*, are not significant, even if expected, is common or uncommon. In our experience it is not uncommon. A possible explanation could be that the trucks are not old enough to show wear metals as significant indicators of failures, or that the other failure modes not related to wear causes are more prevalent, such as contamination.

Of all Caterpillar variables, *only Si appear to be significant by itself*, with a good test-model fit. In combination with Si, still no other variable was significant.

> **Wear metals.** When using a wider list of wear variables, Al and Si appeared jointly significant, but with poor overall test-model fit.
>
> **Additives.** When using additives, Mo, B, Na, and P appear jointly significant, but with poor

overall test-model fit.

**Contaminants.** With contaminants, B, Na and Si (to a lesser degree) appear to be significant, but again with a bad overall test-model fit.

**More advanced methods.** They include variables derived from the original variables, and "historic" transformations, such as differences ("jumps") between inspections, or inclusion of trend through previous measurements (lags). We focused on investigating Fe, and found it is with the value from the previous inspection (Fe and Fe1; Fe1 - first lag of Fe) jointly significant. We tested the other combinations of Fe and other metals, and their lags in the model. Some of them appear to be jointly significant, and some of them with a moderate test-model fit.

**Combined models.** Several other models were created by combination of variables from different groups and tested for model fit, as well as for decision making, such as
[Si], [Mo Si], [Mo B Si], [Fe Fe1], [Fe Si], [Fe Si Mo], [Zn Si Mo Fe].

## 7.6 Decision making modelling

Decision making is a process of deciding whether to continue or stop operation of the engine depending on its age (operating hours) and the condition monitoring measurements (oil analysis data). The decision policy is defined by selection of a threshold on hazard function (hazard level). At every inspection instant the hazard function is calculated and if its value is below the threshold, it is recommended to continue operation. If it is above, it is recommended to stop operation and perform repair/ replacement. The hazard level is selected to optimally balance expected costs of preventive repairs and failure repairs. In simpler words, the policy tries to prevent costly failures by timely preventive repairs, but not to we perform them too soon. The optimal level is calculated by minimizing the expected cost per time unit (in this case, hour).

We need two cost parameters to calculate the optimal hazard level: single cost of preventive repair/ replacement, and a single cost of failure replacement. It is important to note that those cost include all costs related to the replacement, material cost, labour cost, and the downtime cost (lost production – often the largest part of the cost). After a discussion, Brian Wright from Kinross estimated the preventive replacement cost of an engine to $380,000, and the failure replacement cost to $925,000. It makes the cost ratio $925/380 = 2.43$, which is relatively moderate. The larger cost ratio, the more cautious the policy is, but also its saving in comparison with policy of running until failure.

### 7.6.1 Time-based policy

If the replacement policy uses only operating hours (age) information of the engine for replacements, the optimal hazard level is equivalent to optimal preventive replacement time. If we use the estimated

two-parameters Weibull model as reported above, and the replacement cost suggested by Kinross, the optimal preventive replacement time is 18,793 operating hours, somewhat longer than the 16,000 hours effectively applied. Theoretically, the expected saving of applying the optimal policy in comparison with the current one is about 12.5% ($38.6/hour in comparison with $44.2/hour), but the comparison is not very reliable, due to 13 histories still in operation. This increase in the preventive replacement time may be contributed to not very high cost ratio of 2.43, unless the costs of failure replacements are underestimated.

### 7.6.2 Condition-based policy

We have considered several hazard models that may be appropriate for building a reasonable decision policy, notably [Si], [Mo Si], [Mo B Si], [Fe Si], and [Fe Si Mo]. Those models show, at least in theory, savings between 15-20% in comparison with the current policy, but when applied retroactively, saving are smaller, between 1-7%. The actual comparison is not reliable, due to histories in operation. With more decided histories, we would expect savings more close to predicted, as the policy does not favour short replacement times. Of all models we would select [Fe Si Mo] as the main one, although not much better. The model parameters are presented in table 7.4. Fe is included in the model as appeared to be

Table 7.4: Report on hazard function parameters estimation

| Parameter | Estimate | Sign. | Standard Error | Wald | DF | p-Value | Exp of Estimate | 95% CI Lower | 95% CI Upper |
|---|---|---|---|---|---|---|---|---|---|
| Scale | 2.519e+07 | | 9.95e+07 | | | | | 0 | 2.202e+08 |
| Shape | 2.31 | N | 0.6696 | 3.828 | 1 | 0.05041 | | 0.9976 | 3.623 |
| Fe | -0.1003 | N | 0.06655 | 2.273 | 1 | 0.1316 | 0.9045 | -0.2308 | 0.0301 |
| Si | 0.5732 | Y | 0.1623 | 12.48 | 1 | 0.0004113 | 1.774 | 0.2552 | 0.8912 |
| Mo | 0.3449 | Y | 0.1645 | 4.394 | 1 | 0.03606 | 1.412 | 0.02242 | 0.6674 |

reasonable for decisions, even if its p-value is somewhat above the value of 5%. The theoretical saving for this model would be around 15%, and realized with current histories of about 5%, by preventing 3 out of 8 actual failures. An application of the decision policy on actual data is shown in fig. 7.3.

The other models that may be consider for decision policy are [Si], [Mo Si], [Mo B Si] which show predicted saving of 15-25%, but less efficient when effectively applied than [Fe Si Mo]. It is interesting that all those models would prevent 3 out of 8 actual failures.

With more data (histories), the above mentioned models may be re-estimated and decision policies improved and validated.

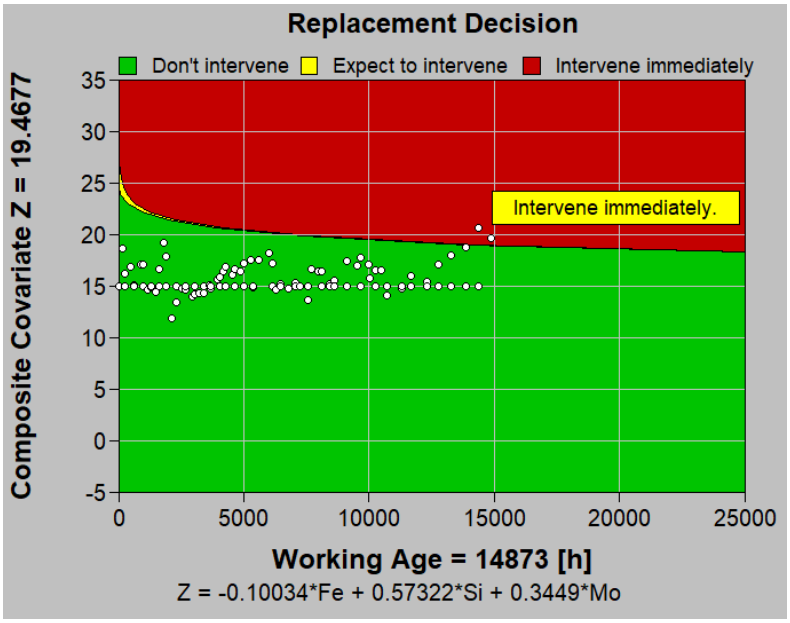


Figure 7.3: Decision policy at work: Intervene immediate (points in red zone)

## 7.7 Conclusion

The Kinross Caterpillar haul truck engines data (oil analysis data, and maintenance records) show promising results for improvement of the engines' replacement policy, by applying the EXAKT model. The saving predicted can be 15-20% of the current policy, but this should be validated by more engine histories. More detailed analysis of engine failure modes would be desirable, as appeared that the oil analysis records are not very informative of engines health, in general. If some of failures are not related to oil variables (e.g., wear), they should be treated differently. The replacement due to age (high hours), if applied at all, could be also improved, by somewhat extending the upper limit from 16,000 hours to more than 18,000 hours, with the suggested cost ratio of 2.43. The estimated average life (MTTF) of an engine, if run until failure is estimate to around 21,000 hours.

# 8 Barrick Veladero pump regression analysis

**Gaoyang Li, Visiting Ph.D. student**

As of June 2018, C-MORE met with Barrick for a further discussion on possibilities with the data that is available, and the results that Barrick wanted to see.

In this report, we summarize our findings on regression analysis of the pump variables.

## 8.1 Background

This project pertains to a pair of pumps that work in tandem. The speed of the pumps is determined by the operator, with the objective of maximum flow.

The maintenance question is to determine the relationship between the variables being measures to better understand how a failure may be predicted.

## 8.2 Introduction

According to the Kernan [1], ideally five parameters should be monitored to understand how a pump is performing: suction pressure, discharge pressure, flow, pump speed, and power. In this dataset, the vibrations, speeds, temperatures, and the discharge pressures of the two pumps are obtained. Detailed information is shown in table 8.1.

## 8.3 Data preprocessing

### 8.3.1 Visualizing missing values

First, some preprocessing was carried out before visualizing the missing values.

- All the error records including the 'No Data', 'Comm Fail', 'Unit Down',' Bad', 'Arc Off-line', and 'Error' were removed.
- Temperature 1 and Temperature 2 before "2011/9/21 18:00:00", and the Temperature 3 and Temperature 4 from "2012/10/2 11:00:00" to "2015/5/26 11:00:00" did not change, which is clearly

Table 8.1: Monitoring variables of the two pumps

| **Pumps** | **Monitoring targets** | **Variables** |
|---|---|---|
| Pump A | Vibration | Vibration #1 –# 4 |
| | Speed | Speed A |
| | Temperature | Temperature #1, #2 |
| | Discharge pressure | Discharge pressure A |
| | Status | Status A |
| Pump B | Vibration | Vibration # 5 – #8 |
| | Speed | Speed B |
| | Temperature | Temperature #3, #4 |
| | Discharge pressure | Discharge pressure B |
| | Status | Status B |
| Others | Overall flow | Flow |
| | Thomas' comments | |

not reasonable. Thus, all the temperature records between these intervals were removed.

The complete (shaded) and missing (blank) values are visualized along the time axis in fig. 8.1. As shown in fig. 8.1, the records between "2016/07/02 16:00:00" and "2017/11/15 00:00:00" best suited for analysis.

### 8.3.2 Removing outliers

Some obvious outliers can be excluded by univariate visualization. For example, it is contradictory when the status is stopped while the speed is not zero, as shown in fig. 8.2. Also, some extremely high temperatures as shown in fig. 8.3 are unreasonable and can be excluded.

### 8.3.3 Data transformation

Data transformation is also necessary for some variables.

- All the data are transformed into the numeric format.
- Only one record is kept of the records with the same timestamps.
- Pump status of running and stopped are replaced with 1 and 0, respectively.

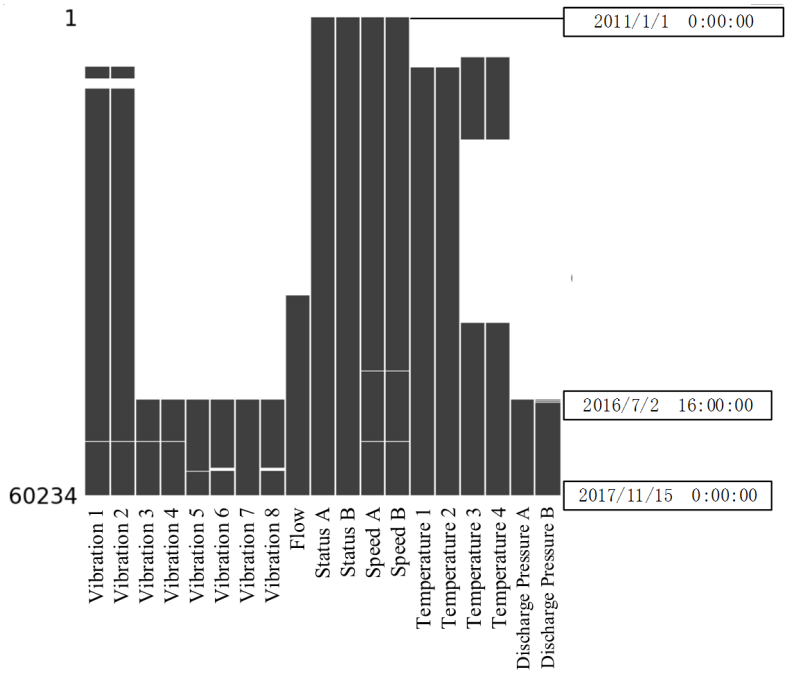


Figure 8.1: Data integrity figure

- The overall flow is divided into Flow A and Flow B with the flowing principle. Flow A and Flow B equal to Flow/2 if both the pumps are running. Flow A equals to Flow if only Pump A is running, and Flow B equals to Flow if only Pump B is running.

- In this study, the seasonality of the temperature is an obvious obstacle for the analysis. As shown in fig. 8.4, the seasonality of Temperature 1 and Temperature 2 are removed with the seasonal_decompose function of the statsmodels library. The residuals are utilized in the following analysis instead of the real temperatures.

## 8.4 Exploratory data analysis

After the data processing, we can do some exploratory data analysis to examine the correlations of the variables.

### 8.4.1 Correlation matrix

First, the correlation matrix among all the variables is shown in fig. 8.5. As shown in fig. 8.5, there are strong correlations between Vibration 1 and Vibration 3, Vibration 2 and Vibration 4, Vibration 5 and Vibration 7, Vibration 6 and Vibration 8, and Temperature 1 and Temperature 2, which imply the installation configuration of the sensors.

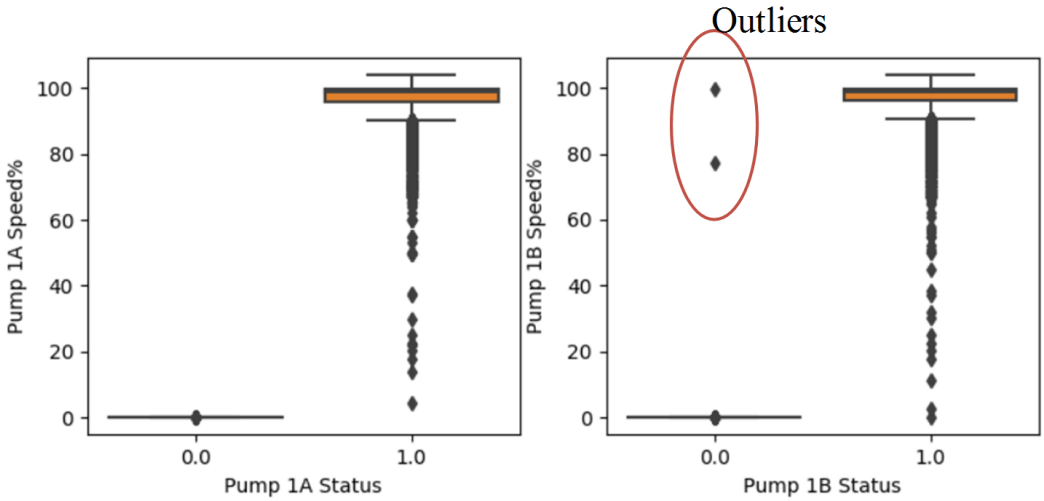


Figure 8.2: Pump speeds vs. status

Additionally, there are some obvious correlations, for example, the status and the speed, the status and the pressure, and the overall flow and the Flow A or Flow B. The speeds of the two pumps keep pace with each other most of the time.

Beyond this, there seem no other strong correlations among the variables. The correlation values between the pressure and speed are relatively high for both the pumps. It appears that the residuals of the Temperature 3 and Temperature 4 have strong relations with Pressure B, but the same phenomenon is not observed in Pump A.

### 8.4.2 Bivariate visualization

Based on the correlation matrix, we can conduct several bivariate visualizations. Figure 8.6 shows the bivariate analysis between the vibrations, and fig. 8.7 shows the relationship between the speeds and pressures, respectively.

### 8.4.3 Multivariate visualization

Furthermore, the multivariate visualization is also a powerful tool for visualizing the correlations among the variables. The multivariate visualization of the speeds, flows and pressures for Pump A and Pump B are shown in figs. 8.8 and 8.9, respectively. Several outliers can be removed in this step.

We can observe a clear connection between the speed and pressure, and a weak correlation between speed and flow.

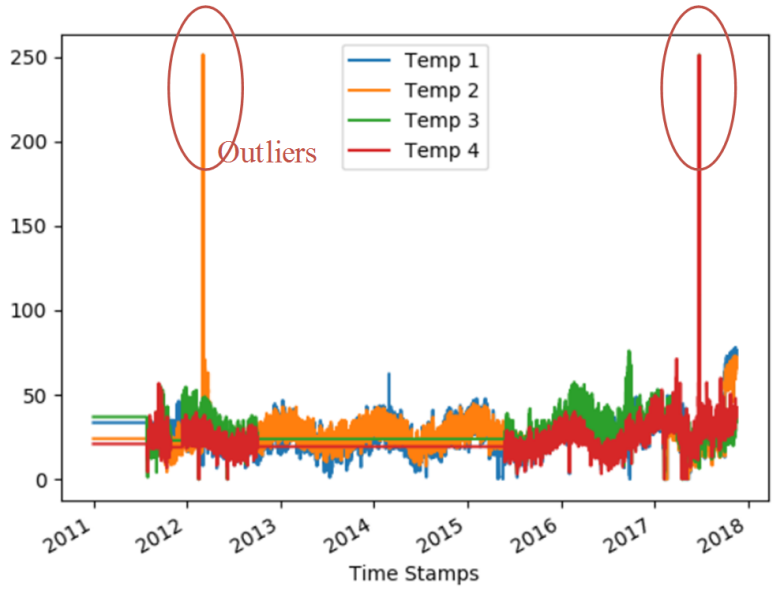


Figure 8.3: Temperature outliers

## 8.5 Models

In this study, we try out several linear models to determine the correlations among the variables.

### 8.5.1 Simple feature engineering

Considering the strong correlations among the vibrations, we create several new variables of V1V3, V2V4, V5V7, and V6V8 by multiplying the vibrations together.

### 8.5.2 Linear models with different target variables

**Model 1:** We start by constructing a simple linear regression model between the speed and the discharge pressure. The heteroscedasticity characteristic is a problem for such a model as shown in fig. 8.7. Fortunately, the heteroscedasticity can be removed with two approaches. The first way is the generalized ordinary least squares algorithm, also known as the weighted ordinary least squares (WOLS) regression. The comparisons between the ordinary least squares (OLS) and WOLS are shown in fig. 8.10. The WOLS assigns higher weights for the data points of lower variances, which makes the regression line closer to the data of lower values. However, in most cases, the heteroscedasticity is caused by the lack of enough explanatory variables. We found that the heteroscedasticity in this problem can be removed by introducing the flow in the regression analysis, which introduces model 2 as follows.

**Model 2:** In this step, the models were built with a two-step regression, which is a convenient and fast way of removing the outliers.

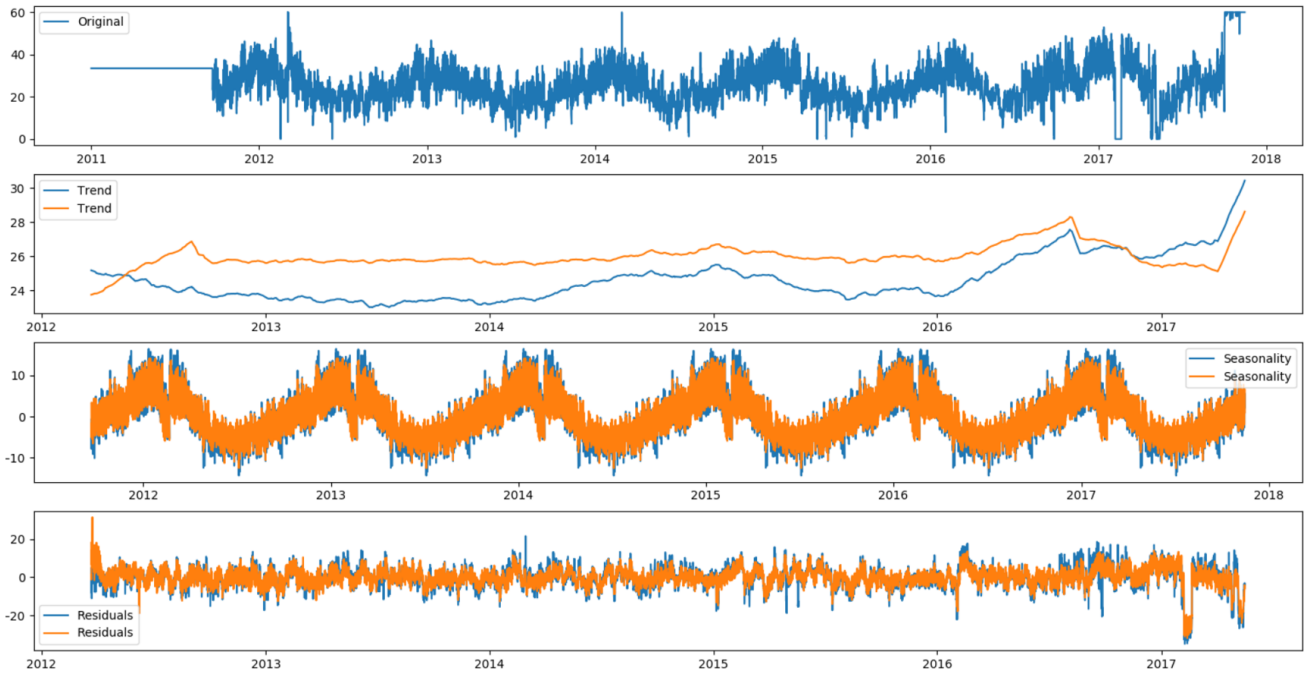


Figure 8.4: Processing the seasonality out of temperature readings

- Build a regression model and remove the data points of higher Cook's distance.
- Build a new regression model with the remaining data.

In statistics, Cook's distance is a commonly used estimate of the influence of a data point when performing an OLS analysis. The points of higher Cook's distance can be seen as outliers.

The data are split into the training set and test set.

As mentioned before, a more reasonable way to remove the heteroscedasticity is to introduce the speed into the regression model. Based on this idea, two regression models are constructed. The first one is

**Speed A, Flow A ⇒ Pressure A**

The first regression step for calculating the Cook's distance is shown in fig. 8.11a, while the second step is in fig. 8.11b. The R-square value of the regression is 0.957 according to the regression analysis in fig. 8.12, which implies that most of the response variable variation can be explained by the model. Similarly, we can build the same model for Pump B.

**Speed B, Flow B ⇒ Pressure B**

The two steps of regression are shown in figs. 8.13a and 8.13b, respectively. As shown in fig. 8.14, the R-square value 0.952 indicates a strong model.

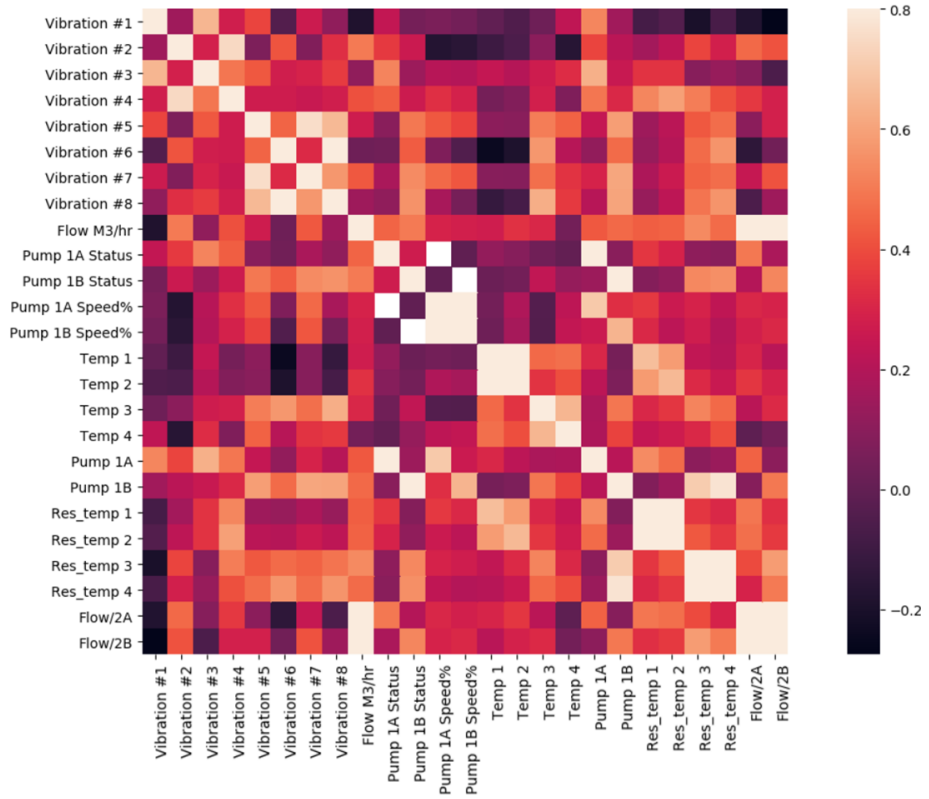


Figure 8.5: Correlation matrix

**Model 3:** In model 3, we attempt to predict the flow based on the speed, vibration, and temperature residuals. First, we try to build a regression model on Pump A with the following variables.

**V1, V2, V3, V4, V1V3, V2V4, Speed A, Res_temp 1, Res_temp 2 ⇒ Flow A**

The regression results of the two steps and the parameter analysis are shown from figs. 8.15a, 8.15b and 8.16. The R-square value 0.794 is not very satisfying but should be enough for the trend prediction.

Similarly, we can build the same model for Pump B.

**V5, V6, V7, V8, V5V7, V6V8, Speed B, Res_temp 3, Res_temp 4 ⇒ Flow B**

The regression results are shown in figs. 8.17a, 8.17b and 8.18. The results are similar to Pump A with an R-square value of 0.770.

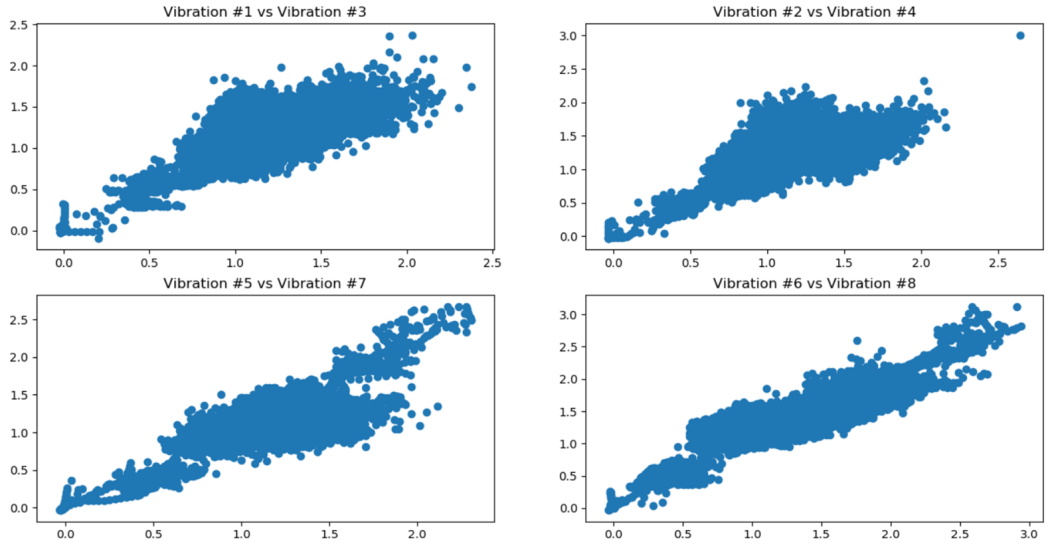


Figure 8.6: Bivariate analysis between vibrations.

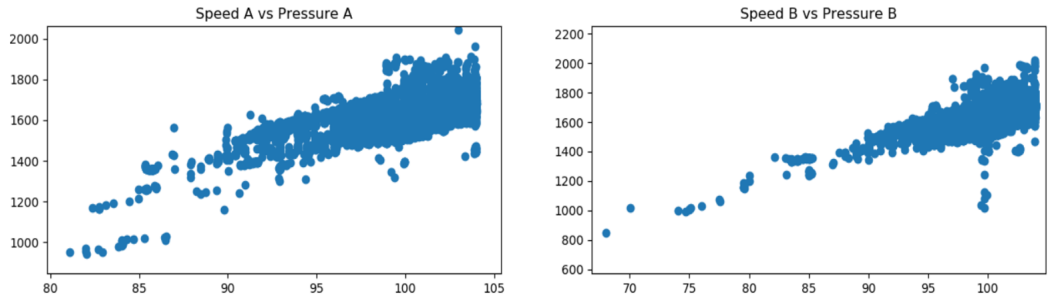


Figure 8.7: Bivariate analysis between speed and pressure

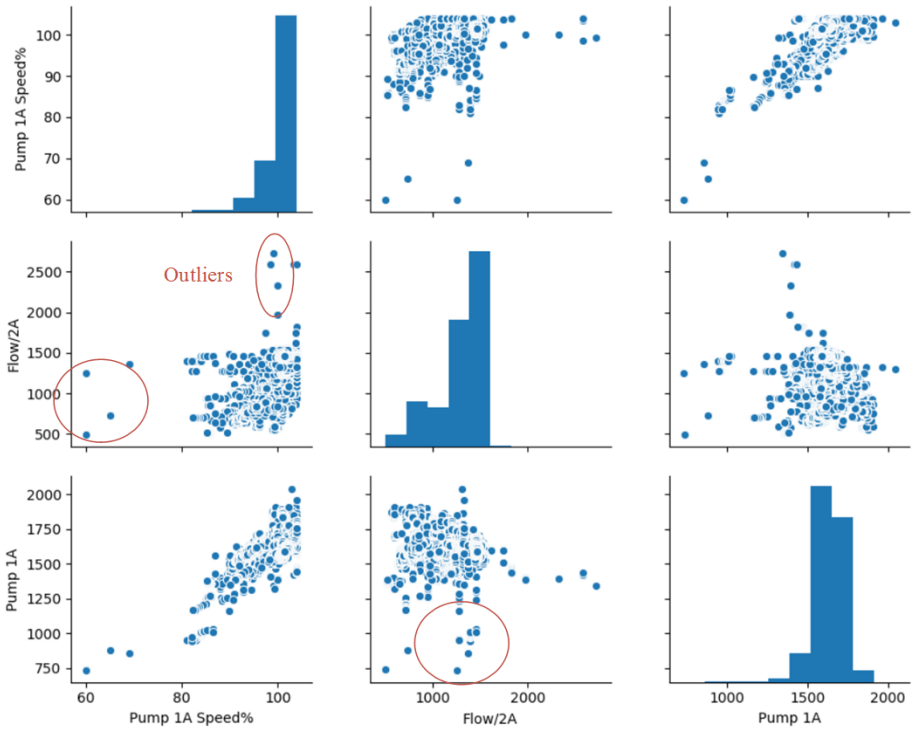


Figure 8.8: Speed, flow and pressure for Pump A

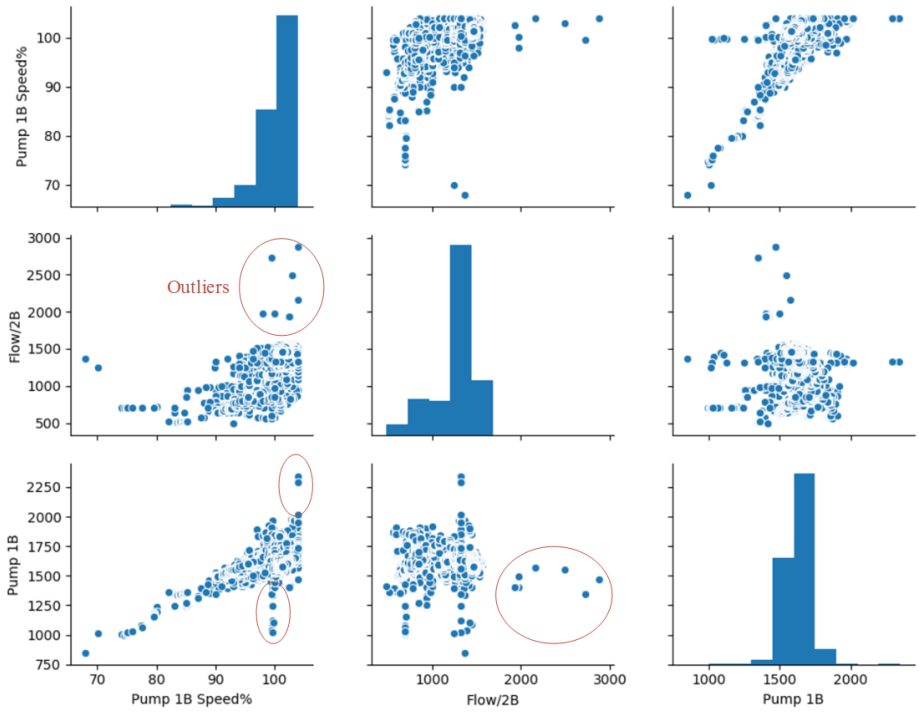


Figure 8.9: Speed, flow and pressure for Pump B

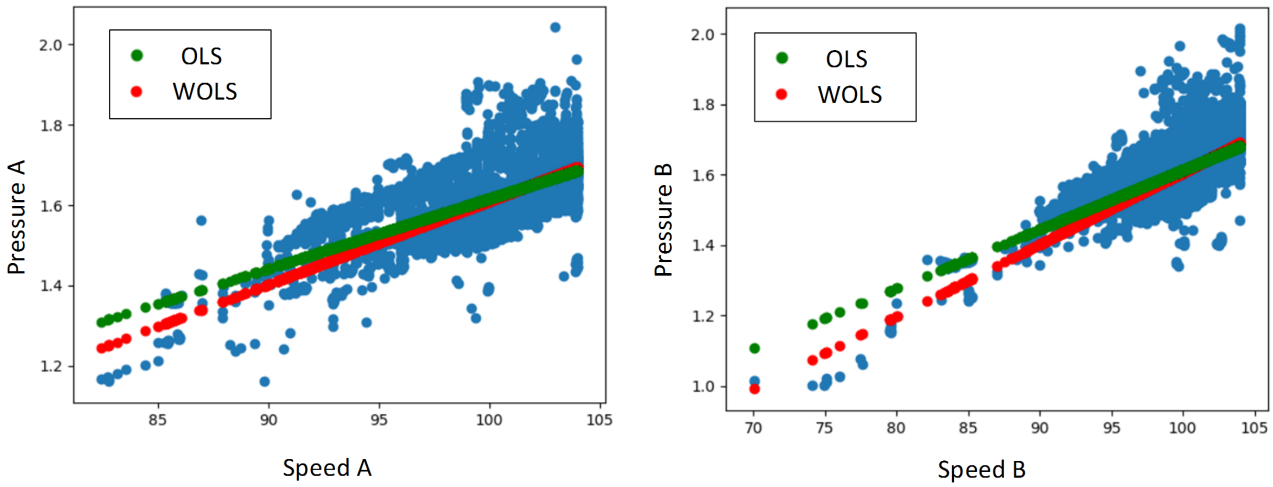


(a) Pump A (b) Pump B

Figure 8.10: Regression model between speed and pressure

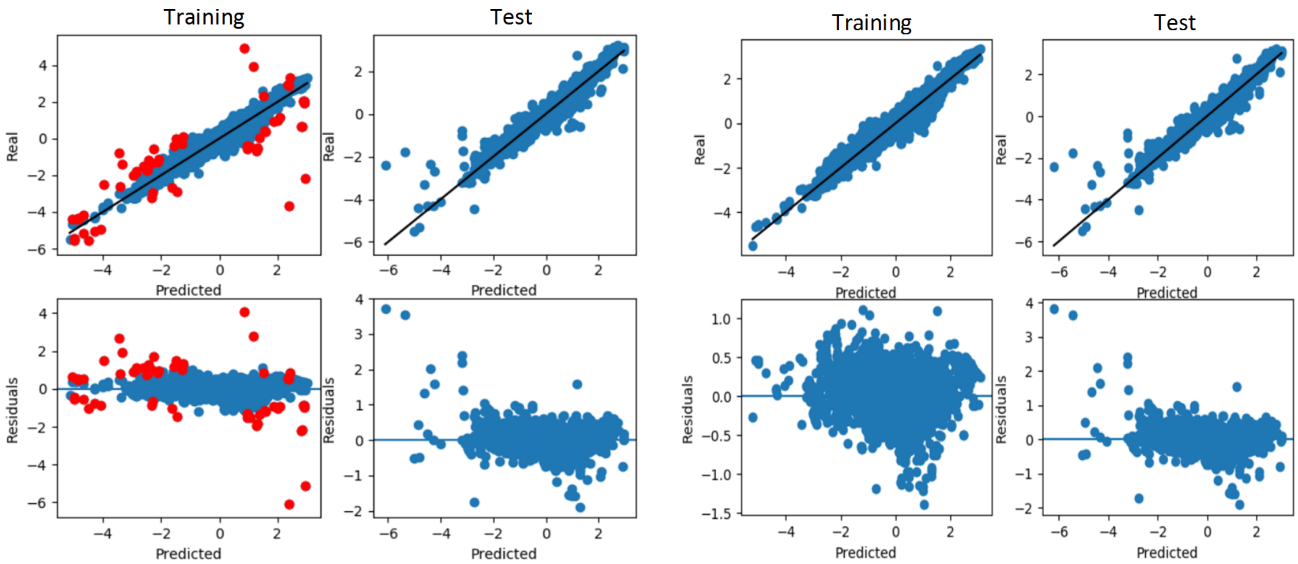


(a) First regression step (b) Second regression step

Figure 8.11: Stepped regression results for pump A

OLS Regression Results

| | | | |
|---|---|---|---|
| Dep. Variable: | y | R-squared: | 0.957 |
| Model: | OLS | Adj. R-squared: | 0.957 |
| Method: | Least Squares | F-statistic: | 8.874e+04 |
| Date: | Sun, 18 Nov 2018 | Prob (F-statistic): | 0.00 |
| Time: | 16:31:06 | Log-Likelihood: | 1440.4 |
| No. Observations: | 8028 | AIC: | -2875. |
| Df Residuals: | 8025 | BIC: | -2854. |
| Df Model: | 2 | | |
| Covariance Type: | nonrobust | | |

| | coef | std err | t | P>\|t\| | [0.025 | 0.975] |
|---|---|---|---|---|---|---|
| const | -0.0004 | 0.002 | -0.177 | 0.860 | -0.005 | 0.004 |
| x1 | 1.3784 | 0.003 | 421.109 | 0.000 | 1.372 | 1.385 |
| x2 | -0.9873 | 0.003 | -305.999 | 0.000 | -0.994 | -0.981 |

| | | | |
|---|---|---|---|
| Omnibus: | 785.936 | Durbin-Watson: | 1.997 |
| Prob(Omnibus): | 0.000 | Jarque-Bera (JB): | 4082.823 |
| Skew: | -0.331 | Prob(JB): | 0.00 |
| Kurtosis: | 6.430 | Cond. No. | 2.41 |

Figure 8.12: Regression results for pump A

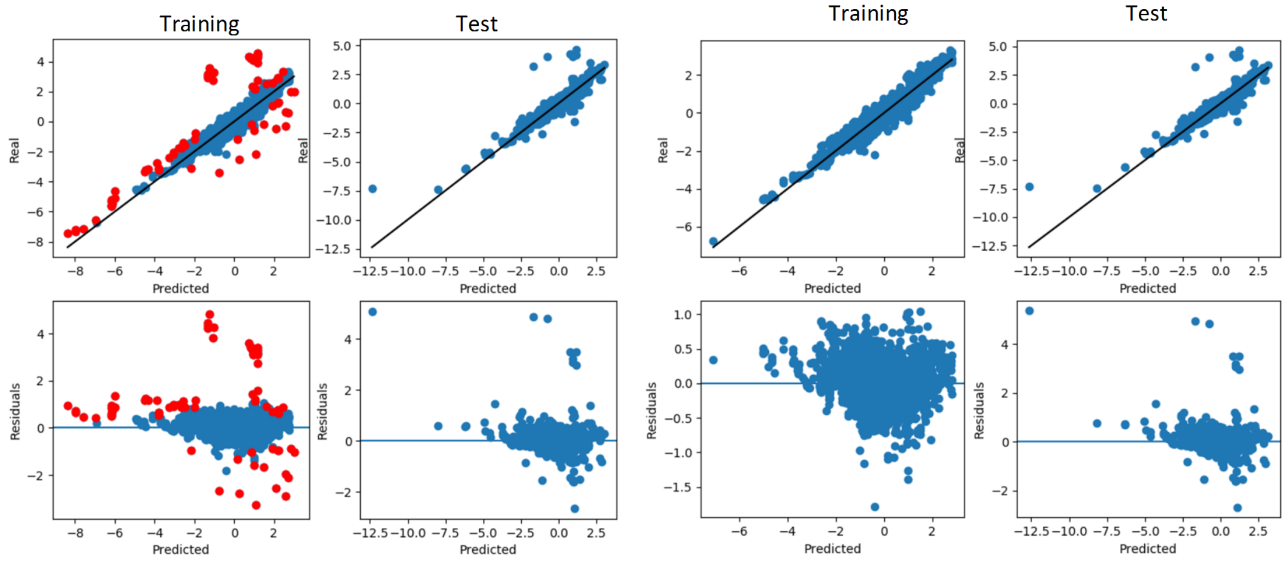


(a) First regression step

(b) Second regression step

Figure 8.13: Stepped regression results for pump B

OLS Regression Results

| | | | |
|---|---|---|---|
| Dep. Variable: | y | R-squared: | 0.952 |
| Model: | OLS | Adj. R-squared: | 0.952 |
| Method: | Least Squares | F-statistic: | 7.837e+04 |
| Date: | Sun, 18 Nov 2018 | Prob (F-statistic): | 0.00 |
| Time: | 16:39:50 | Log-Likelihood: | 1256.9 |
| No. Observations: | 7873 | AIC: | -2508. |
| Df Residuals: | 7870 | BIC: | -2487. |
| Df Model: | 2 | | |
| Covariance Type: | nonrobust | | |

| | coef | std err | t | P>\|t\| | [0.025 | 0.975] |
|---|---|---|---|---|---|---|
| const | -0.0103 | 0.002 | -4.434 | 0.000 | -0.015 | -0.006 |
| x1 | 1.3858 | 0.004 | 395.704 | 0.000 | 1.379 | 1.393 |
| x2 | -0.9920 | 0.003 | -294.547 | 0.000 | -0.999 | -0.985 |

| | | | |
|---|---|---|---|
| Omnibus: | 631.141 | Durbin-Watson: | 2.008 |
| Prob(Omnibus): | 0.000 | Jarque-Bera (JB): | 3821.652 |
| Skew: | -0.014 | Prob(JB): | 0.00 |
| Kurtosis: | 6.413 | Cond. No. | 2.49 |

Figure 8.14: Regression results for pump B

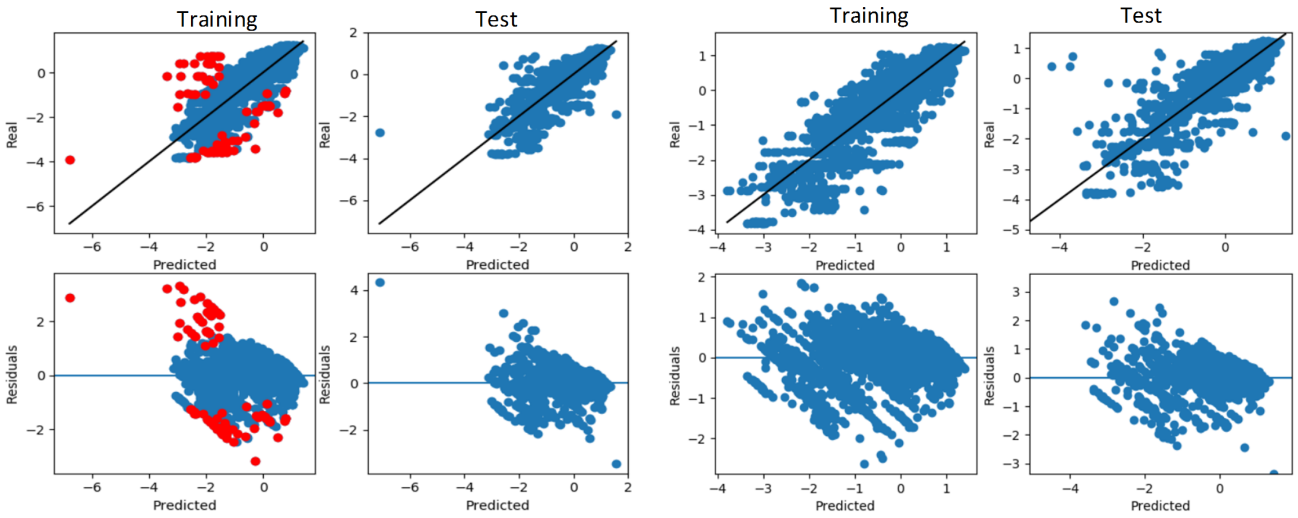


(a) First regression step

(b) Second regression step

Figure 8.15: Stepped regression results for pump A, model 3

OLS Regression Results

| | | | |
|---|---|---|---|
| Dep. Variable: | y | R-squared: | 0.794 |
| Model: | OLS | Adj. R-squared: | 0.793 |
| Method: | Least Squares | F-statistic: | 2115. |
| Date: | Sun, 18 Nov 2018 | Prob (F-statistic): | 0.00 |
| Time: | 16:49:40 | Log-Likelihood: | -2938.6 |
| No. Observations: | 4961 | AIC: | 5897. |
| Df Residuals: | 4951 | BIC: | 5962. |
| Df Model: | 9 | | |
| Covariance Type: | nonrobust | | |

| | coef | std err | t | P>\|t\| | [0.025 | 0.975] |
|---|---|---|---|---|---|---|
| const | -0.0093 | 0.006 | -1.487 | 0.137 | -0.021 | 0.003 |
| x1 | 0.0522 | 0.041 | 1.280 | 0.201 | -0.028 | 0.132 |
| x2 | 0.6488 | 0.057 | 11.432 | 0.000 | 0.538 | 0.760 |
| x3 | -0.3216 | 0.008 | -38.684 | 0.000 | -0.338 | -0.305 |
| x4 | 0.3846 | 0.029 | 13.100 | 0.000 | 0.327 | 0.442 |
| x5 | -0.2564 | 0.055 | -4.674 | 0.000 | -0.364 | -0.149 |
| x6 | -0.7668 | 0.054 | -14.245 | 0.000 | -0.872 | -0.661 |
| x7 | 0.7138 | 0.009 | 77.873 | 0.000 | 0.696 | 0.732 |
| x8 | -0.0941 | 0.014 | -6.580 | 0.000 | -0.122 | -0.066 |
| x9 | 0.3296 | 0.015 | 22.109 | 0.000 | 0.300 | 0.359 |

| | | | |
|---|---|---|---|
| Omnibus: | 882.991 | Durbin-Watson: | 1.981 |
| Prob(Omnibus): | 0.000 | Jarque-Bera (JB): | 2870.292 |
| Skew: | -0.897 | Prob(JB): | 0.00 |
| Kurtosis: | 6.266 | Cond. No. | 27.0 |

Figure 8.16: Regression results for pump A, model 3

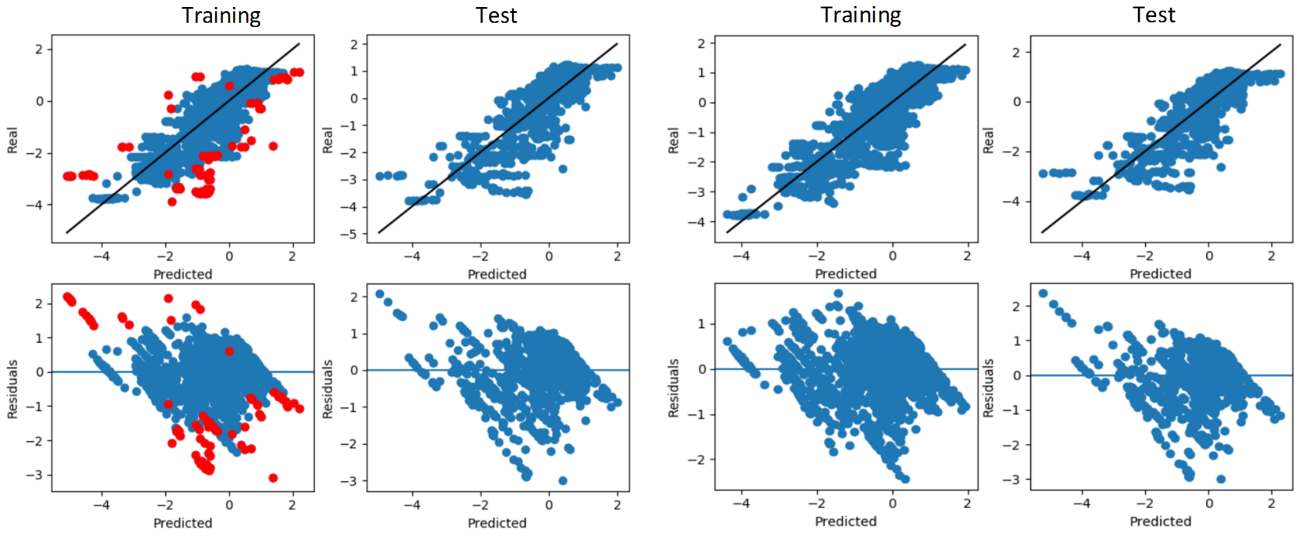


(a) First regression step

(b) Second regression step

Figure 8.17: Stepped regression results for pump B, model 3

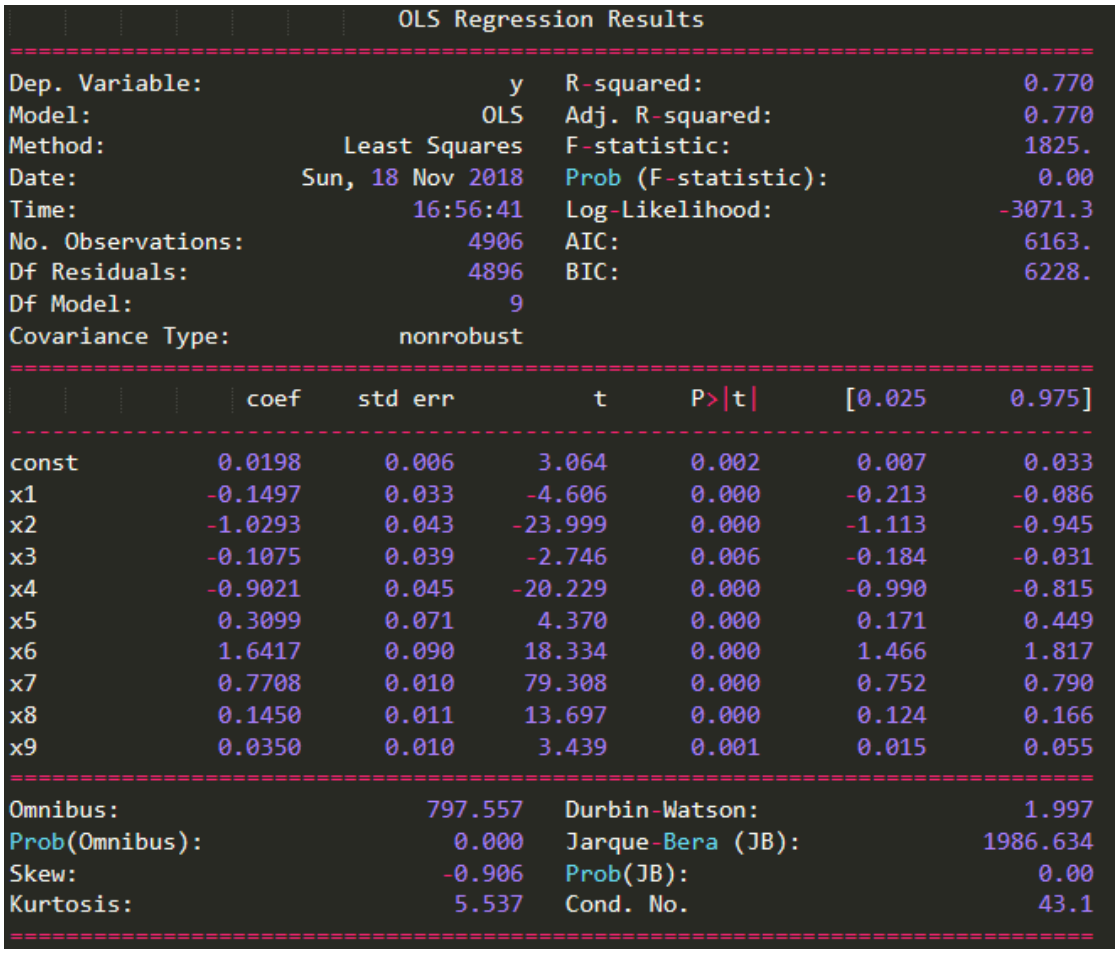

OLS Regression Results

| | | | |
|---|---|---|---|
| Dep. Variable: | y | R-squared: | 0.770 |
| Model: | OLS | Adj. R-squared: | 0.770 |
| Method: | Least Squares | F-statistic: | 1825. |
| Date: | Sun, 18 Nov 2018 | Prob (F-statistic): | 0.00 |
| Time: | 16:56:41 | Log-Likelihood: | -3071.3 |
| No. Observations: | 4906 | AIC: | 6163. |
| Df Residuals: | 4896 | BIC: | 6228. |
| Df Model: | 9 | | |
| Covariance Type: | nonrobust | | |

| | coef | std err | t | P>\|t\| | [0.025 | 0.975] |
|---|---|---|---|---|---|---|
| const | 0.0198 | 0.006 | 3.064 | 0.002 | 0.007 | 0.033 |
| x1 | -0.1497 | 0.033 | -4.606 | 0.000 | -0.213 | -0.086 |
| x2 | -1.0293 | 0.043 | -23.999 | 0.000 | -1.113 | -0.945 |
| x3 | -0.1075 | 0.039 | -2.746 | 0.006 | -0.184 | -0.031 |
| x4 | -0.9021 | 0.045 | -20.229 | 0.000 | -0.990 | -0.815 |
| x5 | 0.3099 | 0.071 | 4.370 | 0.000 | 0.171 | 0.449 |
| x6 | 1.6417 | 0.090 | 18.334 | 0.000 | 1.466 | 1.817 |
| x7 | 0.7708 | 0.010 | 79.308 | 0.000 | 0.752 | 0.790 |
| x8 | 0.1450 | 0.011 | 13.697 | 0.000 | 0.124 | 0.166 |
| x9 | 0.0350 | 0.010 | 3.439 | 0.001 | 0.015 | 0.055 |

| | | | |
|---|---|---|---|
| Omnibus: | 797.557 | Durbin-Watson: | 1.997 |
| Prob(Omnibus): | 0.000 | Jarque-Bera (JB): | 1986.634 |
| Skew: | -0.906 | Prob(JB): | 0.00 |
| Kurtosis: | 5.537 | Cond. No. | 43.1 |

Figure 8.18: Regression results for pump B, model 3

# Bibliography

[1] D. Kernan, "Pumps 101: Operation, maintenance and monitoring basics," ITT Inc., white paper. [Online]. Available: https://www.gouldspumps.com/ittgp/medialibrary/goulds/website/Literature/White%5C%20Papers/ITT_white_paper_Pumps_101_Operation_Maintenance_and_Monitoring_Basics.pdf.

# 9 Teck: Optimal replacement strategy of Komatsu 930E haul trucks

**Janet Lam, C-MORE**

In June, Graeme Dillon from Teck approached C-MORE with a capital equipment replacement strategy problem. Teck's fleet of Komatsu 930E haul trucks were scheduled for replacement at 13 years, but there was a question about the cost optimality of this replacement cycle.

Using capital equipment replacement strategies, we developed a solution that produces an optimal replacement schedule based on the salvage value of the truck at replacement time.

## 9.1 Project description

Teck's fleet of Komatsu 930E haul trucks cost about 5M USD to purchase. Teck has developed a schedule of operating and maintenance (O&M) cost per hour of production and expected annual production hours that increase and decrease with equipment age, respectively. These values are given in table 9.1

Equipment costs more to keep and maintain over time, while running fewer and fewer productive hours, the project question was to find whether there is a most cost-optimal time to replace the haul trucks than the currently prescribed 13 years.

## 9.2 Model development and required information

In order to answer this problem definition, we needed Teck's internal required rate of return (IRR), and the salvage value that Teck could get by selling the truck at each age. The values provided from Teck were

IRR of 8% ($i = 0.08$), and
a salvage value of 200,000 CAD at the end of 13 years.

Since only one salvage value was available, we simply linearly interpolated the salvage value for the intermediate years, converting 5M USD to 6.72M CAD, for a depreciation of 500,000 CAD in salvage

Table 9.1: Komatsu 930E haul truck O&M costs and expected annual productive hours

| Year (from commissioning) | Age bin ('000 production hrs) | O&M cost per production hr (CAD) | Expected annual production hrs |
|---:|---:|---:|---:|
| 1 | 0–6 | 62 | 6000 |
| 2 | 6–12 | 59 | 5933 |
| 3 | 12–18 | 86 | 5800 |
| 4 | 18–24 | 133 | 5733 |
| 5 | 24–30 | 166 | 5667 |
| 6 | 30–36 | 175 | 5533 |
| 7 | 36–42 | 174 | 5533 |
| 8 | 42–48 | 182 | 5400 |
| 9 | 48–54 | 200 | 5333 |
| 10 | 54–60 | 261 | 5267 |
| 11 | 60–66 | 255 | 5400 |
| 12 | 66–72 | 315 | 5133 |
| 13 | 72–78 | 374 | 4867 |

value each year.

In order to find the optimal replacement time, we can use life cycle costing techniques. In this case, we can assume that the project renews itself infinitely, so each time a truck is retired, a new equal truck is purchased for the same price. This way, a longer replacement cycle will result in fewer trucks purchased, but will face higher operating costs.

First, we can compute the annual O&M costs accrued in the $j$-th year

$$C_{o,j} = c_j h_j,$$

where $c_j$ is the hourly O&M cost for the $j$-th year of operation, and $h_j$ is the number of hours available in the $j$-th year. Then, we can compute the present value of the O&M cost in the $j$-th year

$$m_j = C_{o,j} r^j,$$

where $r = 1/(1+i)$ and $i$ is there interest rate.

Since we accrue each year's increasing present value in O&M costs, the total O&M cost for each possible replacement year must be evaluated. If $n$ is the decided age (in years) of the truck at replacement, then

the present value of the total O&M cost is

$$M_n = \sum_{j=1}^{n} m_j.$$

In each possible year of replacement $n$, the resale value of the old truck is different, and the purchase price of the new truck must take place in the replacement year:

$$p_n = (6.72\text{M} - S_n)r^n,$$

where $S_n$ is the salvage value the truck can get after being used for $n$ years.

Then the present value of the total cost of each replacement year is

$$t_n = M_n + p_n,$$

but we can't stop here, because a project that lasts one year cannot directly be compared to a project that lasts 13 years. Consequently, the best way to compare these projects is to assume that they projects renew infinitely:

$$T_n = \frac{t_n}{1 - r^n}.$$

By choosing the replacement year $n$ that produces the least present value total cost over an infinite horizon $T_n$, we can deduce the optimal replacement time of the haul trucks. The results of this calculation are given in table 9.2. The optimal replacement year is highlighted.

## 9.3 Re-evaluating our results

As shown in table 9.2, the optimal replacement year is after each truck's first year of use. Since this is highly undesirable, and frankly questionable, we reconsidered the different components of our calculation.

The most suspicious part of our analysis was the salvage value available at each year of sale. If the truck's purchase price is \$6.72M, then if we were to resell it after only one year of use, by linear interpolation, it could be sold for \$6.22M. We reconsidered whether this was reasonable, and tried different amortization patterns for the salvage value.

**Amortization pattern I:** The first pattern we tried was an immediate drop in price to about half of the original purchase price, followed by a linearly declining resale price until \$200,000 in the 13th year.

With this pattern, the optimal replacement year was after the 9th year, with an optimal project cost of

Table 9.2: Total present value cost over infinite horizon by year of replacement

| Replacement year | Project cost ($) |
|---|---|
| 1 | 9,512,517 |
| 2 | 9,860,627 |
| 3 | 10,395,180 |
| 4 | 11,282,182 |
| 5 | 12,106,823 |
| 6 | 12,632,675 |
| 7 | 12,942,286 |
| 8 | 13,149,468 |
| 9 | 13,353,193 |
| 10 | 13,746,067 |
| 11 | 14,036,081 |
| 12 | 14,406,849 |
| 13 | 14,823,562 |

$14.4M compared to $14.8M if replaced in the 13th year.

**Amortization pattern II:** The second pattern we tried was an immediate drop in price to about two-thirds of the original purchase price, followed by a linearly declining resale price until $200,000 in the 13th year.

With this pattern, the optimal replacement year was after the 8th year, with an optimal project cost of $13.7M compared to $14.8M if replaced in the 13th year.

## 9.4 Conclusions

From our analysis we found that the results are highly sensitive to the salvage values in each year. Since the salvage values described above were simply experimental, and we have deduced the sensitivity to salvage value, we were able to provide an Excel workbook for Teck to enter salvage values directly to the spreadsheet and compute the optimal replacement time given the entered values. Figure 9.1 demonstrates the worksheet. Changing the values in the yellow highlighted column will automatically change the values in the red-green column, along with their colours.

| Year | Sum of accumulated PV O&M costs | Estimated salvage (S)<br><br>Immediate drop to 5M, lose 400K per year | PV of replacement cost ((A-S)$r^n$) | Sum of PV costs (O&M + replacement) | PV of infinite cycles |
|---|---|---|---|---|---|
| | | $6,720,000 | | | |
| 1 | **344,444** | $5,000,000 | **1,489,816** | **1,834,261** | 24,762,517 |
| 2 | **644,553** | $4,600,000 | **1,722,395** | **2,366,948** | 16,591,396 |
| 3 | **1,040,517** | $4,200,000 | **1,912,343** | **2,952,860** | 14,322,607 |
| 4 | **1,600,969** | $3,800,000 | **2,064,700** | **3,665,669** | 13,834,271 |
| 5 | **2,241,209** | $3,400,000 | **2,183,992** | **4,425,201** | 13,854,002 |
| 6 | **2,851,386** | $3,000,000 | **2,274,283** | **5,125,669** | 13,859,514 |
| 7 | **3,413,137** | $2,600,000 | **2,339,214** | **5,752,351** | 13,810,847 |
| 8 | **3,944,113** | $2,200,000 | **2,382,046** | **6,326,159** | 13,760,564 |
| 9 | **4,477,679** | $1,800,000 | **2,405,698** | **6,883,377** | 13,773,612 |
| 10 | **5,114,425** | $1,400,000 | **2,412,776** | **7,527,200** | 14,022,185 |
| 11 | **5,704,996** | $1,000,000 | **2,405,605** | **8,110,601** | 14,201,291 |
| 12 | **6,347,088** | $600,000 | **2,386,257** | **8,733,345** | 14,485,892 |
| 13 | **7,016,393** | 200,000 | **2,356,577** | **9,372,969** | 14,823,562 |

Figure 9.1: Worksheet to compute optimal replacement time

# 10 NDT inspection frequency study for defects by track geometry

**Sophie Tian, PEY research student**
**Janet Lam, C-MORE**

At the last progress meeting, C-MORE submitted an inspection schedule for the non-destructive testing (NDT) team that minimized the time between a defect occurrence and its detection.

In this report, a brief summary of the original report will be followed by new developments with the inclusion of additional track features, including construction and geometry.

## 10.1 Background

The NDT inspection team has a limited number of hours each year to perform tests on the subway track. Currently, there is enough time for the team to perform line-tests on the entire system once per year.

Each night, the NDT team can inspection a single unit of track. The inspection units are usually from the front of one station to the front of the next. There are several exceptions, with King–Queen–Dundas being one unit of measure, due to their close proximity, and some longer lengths, such as Dupont–St. Clair West and Victoria Park–Warden taking two nights of inspeciton. In this report, all mainline track from Lines 1, 2, 3, 4 were considered, except the track North of Sheppard West station on Line 1 (The new Toronto-York Spadina subway extension). Since a single unit of inspection is from the front one station to the front of the next, each station-to-station was considered to be equal.

The objective of the project was to minimize the total average time between a defect occurrence and its detection. This was defined as **unsupervised time** of defects.

By counting the occurrence of new defects per inspection section, we were able to determine the optimal inspection frequency for each section of track.

## 10.2 Next phase: Deeper track information

In the previous phase of the project, the inspection frequency was determined purely by the number of defects and the resource requirement to perform the inspection. However, there are several additional factors that can be considered which will increase the accuracy of the resulting inspection schedule.

- Track geometry: Not all track is shaped in the same way. Defects that occur on a straight length of track may behave differently from defects that occur on tight curves.
- Track construction: Not all track is constructed in the same way. Defects on wood-tie & ballast may behave differently from direct-tie construction.
- Track length: Not all stations are equally spaced apart. Longer sections of track are more likely to have more defects.

For the new phase of the project, we selected track geometry to distinguish the value of each defect. The rationale is that the track geometry is well-defined for the whole system, and verifying this method will allow us to quickly extend the analysis to track construction. Track length requires a different method of analysis.

## 10.3 Mining the asset register

Since the previous analysis did not consider the any characteristics of the tracks, it was necessary to revisit the asset register, and to assign a track geometry to the whole system. The geometry parameters were split up into three main values: tangent (straight track), curves greater than 1000 ft in radius, and curves less than or equal to 1000 ft in radius. Each length of track connecting the subway stations may experience any and all of these geometries multiple times. For example, between St. Clair West station and Dupont station, C123 has a curve radius of 692 ft, and C122 has a radius of 1100 ft, and they're joined by tangent track. (fig. 10.1)

By marking the exact chainage points corresponding to the changes in geometry, we were able to match the number of defects that occur within each of the three types of track geometry. Due to some track information being unavailable, our current analysis is limited to the Bloor-Danforth line, or Line 2. Table 10.1 shows an excerpt of the number of defects within each inspection section stratified by track geometry.

## 10.4 Optimizing the inspection schedule

Given that the TTC has 37 days per year available to inspect Line 2, we are interested in determining the number of inspections that each section of track should receive per year in order to minimize

Table 10.1: Excerpt of number of defects by station and track geometry

| Track | Tangent | Curve >1000 ft | Curve ≤1000 ft | Total defects |
|---|---|---|---|---|
| **Kipling to Islington** | 12 | 2 | 3 | 17 |
| **Islington to Royal York** | 11 | 1 | 0 | 12 |
| **Royal York to Old Mill** | 9 | 5 | 0 | 14 |
| **…** | | | | |
| **Victoria Park to Warden** | 36 | 16 | 0 | 52 |
| **Warden to Kennedy** | 19 | 6 | 0 | 25 |

unsupervised time, weighted by track geometry.

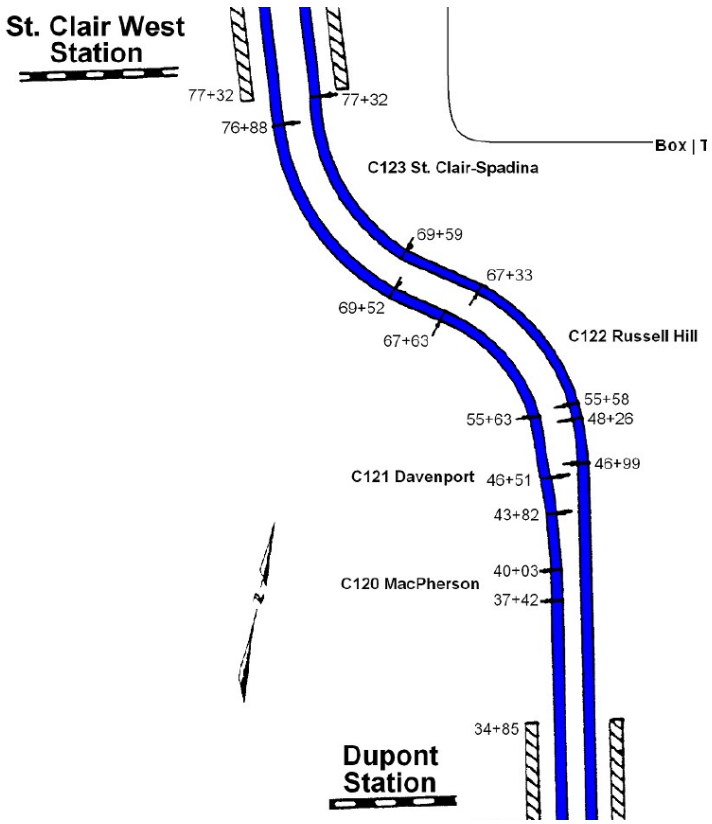


Figure 10.1: Excerpt of detailed track information

Since the risk of a defect increases with the "curviness" of the track, defects on curves with radius less than 1000 ft were given a weight of 1, curves with radius greater than 1000 ft a weight of 0.7, and tangent tract a weight of 0.5. That is, a defect on a tangent with half as risky as one on a tight curve. The respective weights can be easily altered to suit TTC's assessment of relative risk.

### 10.4.1 Computation method

The optimal inspection frequency for each station was computed using a similar method as discussed in the June 2018 meeting. It is summarized here for your convenience:

- For each section of track (between two stations), the weighted defect count was computed. The weights are as described previously for tangent, loose curve and tight curves.

- The relative inspection frequency for the $i$-th inspection section was computed by

$$f_i = \frac{1}{\sum_i \sqrt{d_i w_i}} \sqrt{\frac{w_i}{d_i}}$$

where $d_i$ is the number of days required to inspect the $i$-th section, and $w_i$ is the weighted number of defects for the $i$-th section.

- $f_i$ can be multiplied by $D$, the number of days available per year for mainline inspections, to compute $n_i$, the total number of inspections per year. In this analysis, $D = 37$.

$$n_i = f_i \times D$$

- The optimal inspection interval $I_i$ in days is

$$I_i = \frac{1}{n_i} \times 365$$

- The objective to be minimized in this project is unsupervised time, or the time between a defect occurrence and its detection by the NDT team.

  On a policy in which each section is inspected equally, the unsupervised time $U_e$ in our planning horizon of 1134 days is calculated by

$$U_e = \frac{\sum_i d_i \sum_i w_i}{2D} = 178.1$$

  The unsupervised time for the optimal inspection policy is

$$U^* = \frac{\left(\sum_i \sqrt{d_i w_i}\right)^2}{2D} = 152.75$$

- The resulting percent improvement is

$$E = \left|\frac{U_e - U^*}{U_e}\right| \times 100 = 14.24\%$$

In comparison, with the consideration of priority only, and no track geometry, the optimal inspection policy had an optimal unsupervised time of $U^* = 261.6$ and an equal unsupervised time of $U_e = 349$ with a 25.1% improvement.

## 10.5 Combining geometry with priority

At first glance it seems that stratification by track geometry is not as effective at reducing unsupervised time as priority. However, it is important to note that the results of track geometry did not consider the priority of each defect, and as a result, the defect counts are severely dominated by "delta" defects, or grey defects.

These are very minor defects that do not have a designated response period. Clearly treating all levels of priority as equal does not constitute a holistic analysis. By combining the weights of geometry with priority, our results will value a red defect more highly than a grey defect, but also a tight-curve defect more so than a tangent defect.

By combining the two factors, the resulting optimal unsupervised time is 141, for a 20.7% reduction in unsupervised time compared to an equally distributed inspection schedule. Table 10.2 lists the stations in ascending order of optimal inspection intervals. The shortest inspection interval is just under 5 months from Donlands to Greenwood. The longest inspection interval is just over 45 months in the Kennedy Tail.

## 10.6 Next steps

Due to missing asset registry information, this analysis was limited to Line 2. We would like to extend this work for the whole subway and LRT system. Additionally, a 3rd dimension for stratification is still possible. Track construction that describes a concrete direct tie, or wood tie on ballast, etc. can also affect the risk of a defect. For all these extensions, additional information is required.

Table 10.2: Optimal inspection intervals for Line 2 with track geometry and defect priority

| **Stations** | **Inspection interval (mths)** |
|---|---|
| Donlands to Greenwood | 4.9 |
| Sherbourne to Castle Frank | 5.57 |
| Dundas West to Lansdowne | 6.51 |
| Castle Frank to Broadview | 6.89 |
| Broadview to Chester | 7.82 |
| Victoria Park to Warden | 8.48 |

*Continues on next page*

Table 10.2: Optimal inspection intervals for Line 2 with track geometry and defect priority

| **Stations** | **Inspection interval (mths)** |
|---|---|
| Chester to Pape | 9.11 |
| St. George to Bay | 9.47 |
| Dufferin to Ossington | 9.7 |
| Coxwell to Woodbine | 9.79 |
| Lansdowne to Dufferin | 10.37 |
| Woodbine to Main | 10.67 |
| Yonge to Sherbourne | 11.06 |
| Christie to Bathurst | 11.39 |
| Kipling to Islington | 11.53 |
| Keele to Dundas West | 12.36 |
| Main to Victoria Park | 14.35 |
| Warden to Kennedy | 14.53 |
| Ossington to Christie | 14.96 |
| Pape to Donlands | 15.09 |
| Bathurst to Spadina | 15.28 |
| Bay to Yonge | 15.66 |
| Old Mill to Jane | 16.58 |
| Greenwood to Coxwell | 17.21 |
| Spadina to St. George | 17.55 |
| High Park to Keele | 19.62 |
| Royal York to Old Mill | 25.77 |
| Islington to Royal York | 28.18 |
| Kipling tail | 31.03 |
| Runnymede to High Park | 33.17 |

*Continues on next page*

Table 10.2: Optimal inspection intervals for Line 2 with track geometry and defect priority

| **Stations** | **Inspection interval (mths)** |
|---|---|
| Jane to Runnymede | 43.88 |
| Kennedy Tail | 45.02 |

# 11 Toronto Hydro – Investment Spike Smoothing

**Gary Wang, EngSci thesis student**

In our ongoing project with Toronto Hydro, the objective is to address investment spike issues when a large proportion of assets come due for replacement simultaneously.

As an extension to our last report, this report will present the problem and objectives, and present a brief literature review. Two mathematical approaches to this problem will be presented at the end of this section.

## 11.1 Background, Problem and Objectives

Toronto Hydro, the "company", has a large variety of physical assets in the distribution system; each type of asset has a large and dynamic population. The company has a replacement program(s) for each category of asset. All assets are subject to replacements, reactively and/or proactively, due to failures, failure risks, aging, upgrades, legal obligations, etc. Assets of the same type often have similar useful-lives. Historically, large projects/initiatives have installed assets within a short period of time (or in a cyclical nature of a period of years), which can contribute to spikes in renewal expenditures in the future. Due to capital budget constraints, not all assets can be replaced at or before the optimal/expected replacement time, which further contributes to the spikes in renewal expenditures.

This project will focus on creating an optimization approach to smooth out investment spikes with reasonable economic efficiency. The model should allow analysts and planners to setup constraints that are unique to a specific project/program. The types of constraints should include, but not limited to: capital budgeting constraints, replacement quantity constraints, and investment period constraints. For more details on the proposed constraints, please review section 11.4.

## 11.2 Hypothesis

Toronto Hydro's investment smoothing problem can be solved as an optimization problem with a set of constraints on the difference in budgeting between years. Other constraints, such as, replacement amount and risk levels can also be imposed in the optimization model, if needed.

## 11.3 Literature Review

### 11.3.1 Maintenance Resource Planning for Utility Poles in a Power Distribution Network [1]

A recent report from the Centre for Maintenance Optimization and Reliability Engineering (C-MORE), Maintenance Resource Planning for Utility Poles in a Power Distribution Network, discusses prevention of unexpected increase in demand and resources, optimizing through the use of delayed renewal process [1]. The paper provides insights into preventative planning and risk management in the utility industry. Preventative planning takes on a similar concept as proactive replacement planning where certain proactive and precautionary actions are performed to minimize the risk/cost of outages. The idea of risk management also coincides with the given research objective. The company does proactive replacement planning on a risk basis, prioritizing risky assets over assets that are unlikely to fail in a given period of time.

### 11.3.2 The Equipment-Replacement Problem [2]

An article published by the University of Texas at Dallas (UTDallas) has investigated into an equipment replacement problem. The article breaks dynamic programming into four general stages [2]:

1) Definition of appropriate stages and states.
2) Definition of the optimal-value function.
3) Construction of a recurrence relation.
4) Recursive Computation.

For step 1, it is important to properly define stage variables and state variables. A stage variable should indicate the timeframe/timestamp of an equipment replacement problem. A state variable provides a snapshot of asset conditions at each timestamp [2]. In Toronto Hydro's investment problem, the stage variables are the years that one plans for asset replacement; the state variables are the asset demographics of a given year defined as stage variables. In step 2, an appropriate optimization function must be defined [2]. In the Toronto Hydro investment spike smoothing problem defined earlier, the goal is to minimize risk cost through active replacements while constraining budget expenditures for each year. In step 3 and 4, a recursive function will be created to compute the optimized replacement schedule from the farthest replacement year included in the stage variables to the closest year (to now) [2].

## 11.4 Theoretical Concerns

As a regulated utility company, Toronto Hydro faces many regulations and budgeting constraints. The model should allow analysts and planners to setup constraints that is unique to a specific project/ program. The types of constraints should include, but not limited to: capital budgeting constraints,

replacement quantity constraints, and investment period constraints.

The capital budgeting constraints set limits to annual capital expenditures. This constraint may vary from year to year. All values will be provided in present value.

The replacement quantity constraints set limits annual replacement quantities. This constraint may vary from year to year. The units of quantity may vary, for example, underground cables are measured in meters while transformers are counted as individual units.

The investment period constraints set time limits to the replacement program. These constraints are a set of time variables, these variables indicate the desire time frame to achieve the set objectives.

Given Asset A and B in year $i$, A has a lower risk cost than B in year $i$, but if A has a higher risk cost growth, then in some year $j$, where $j > i$, the risk cost of A may potentially out-grow B's. Thus, it may be more efficient to replace A before B in the long-term as A has a larger risk cost growth. The risk cost growth problem must be taken into consideration when formulating the mathematical optimization.

If an asset is replaced too early, the given asset may not be fully depreciated, the early replacement causes the company to lose value on the replaced asset; if an asset is replaced later, the given asset bear an increasing amount of outage risk due to age-related factors. If an outage occurs, the consequence cost of the outage may be significantly higher than the replacement cost or the asset value. The replacement timing trade-offs will need to be closely examined when developing investment smoothing algorithms.

## 11.5 Proposed Approach

For the investment spike smoothing problem, "risk costs" carried by physical assets will be used to provide snapshots asset demographics/asset health at each stage (current methodology used at Toronto Hydro). Toronto Hydro perform maintenance activities on a fixed cycle, asset replacements will not affect routine maintenance activities. Therefore, maintenance costs will not be factored into this model. Toronto Hydro will provide a consequence cost for each individual asset based on its setup (e.g. carried load, location, outage duration, etc.). A mathematical program will be created to meet the given expenditure constraints while minimizing the risk costs. The model should provide an optimized investment schedule within the given constraints.

### 11.5.1 Non-Linear Programming Approach and Mathematical Formulation

In this approach, the mathematical formulation will the sum of annual risk cost over the investment planning period while setting constraints on annual investment budget to smooth out the investment costs. This formulation considers risk cost growth within the investment period. Due to the non-linearity nature of this mathematical formulation, the program may have a long run-time when dataset

becomes very large.

#### 11.5.1.1 Variables and Definitions

| | |
|---|---|
| $A_{ij}$ | Age, age of asset $i$ in year $j$. |
| $B_j$ | Annual Budget, the forecasted expenditure based on suggested replacement schedule in year $j$. |
| $B\text{max}_j$ | Maximum Annual Budget, the maximum forecasted expenditure in year $j$. |
| $B\text{min}_j$ | Minimum Annual Budget, the minimum forecasted expenditure in year $j$. |
| $C_i$ | Consequence Cost, the cost to Toronto Hydro and customers if asset $i$ fails or malfunctions. |
| $F\text{avg}_j$ | Flexibility (Average), the allowed expenditure differences between the average annual expenditure and the annual budget in year $j$. |
| $F\text{cons}_j$ | Flexibility (Consecutive Years), the allowed expenditure differences between annual budgets of year $j$ and year $j+1$. |
| $HZ_{ij}$ | Hazard Rates, the chance of failure of asset $i$ in year $j$. Derived based on Weibull distributions. |
| $\text{RepAmount}_j$ | Replacement Amount, the number of units replaced for a specific type of assets (major types, e.g. underground transformers) in year $j$. |
| $\text{RepCost}_i$ | Replacement Cost, the cost to replace asset $i$. |
| $\text{RiskCost}_{ij}$ | Risk Cost, is equivalent to Consequence Cost of asset $i$ multiplied by the chance of failure (Hazard Rate) in year $j$. |
| $S_i$ | Scale, a parameter used in the Weibull/Hazard Rate Function for asset $i$. |
| $SF_i$ | Scale Factor, a parameter used in the Weibull/Hazard Rate Function for asset $i$. This parameter is used after assigning Shape to 3. For more details, please see section 11.5.1.2. |
| Shape | Shape, a parameter used in the Weibull/Hazard Rate Function. In FIM model, Shape = 3 for all electrical assets. For simplicity, this parameter will be set to 3 for all assets in this project. |
| $X_{ij}$ | Decision Variable, $X_{ij}$ takes on 0 or 1. If $X_{ij} = 1$, asset $i$ will be replaced in year $j$. If $X_{ij} = 0$, asset $i$ will remain in the system in year $j$. |

#### 11.5.1.2 Mathematical Formulations and Constraints

$$\min \sum_{i,j} \text{RiskCost}_{ij} = C_i \times HZ_{ij}$$

subject to:

$$A_{i,j+1} = (A_{ij} + 1) \times (1 - X_{i,j+1})$$
$$HZ_{ij} = \left(\frac{\text{Shape}}{S_i}\right) \times \left(\frac{A_{ij}}{S_i}\right)^{(\text{Shape}-1)}$$

Most asset types have a *Shape* factor of 3, if Shape is set to 3:

$$\begin{aligned} HZ_{ij} &= \left(\frac{3}{S_i}\right)\left(\frac{A_{ij}}{S_i}\right)^{3-1} \\ &= \left(\frac{3}{s_i^3}\right) A_{ij}^2 \\ SF_i &= \frac{3}{S_i^3} \\ \sum_i X_{ij} &= \text{RepAmount}_j \\ B_j &= \sum_i (X_{ij} \times \text{RepCost}_i) \end{aligned}$$

**The optimization *must* satisfy at least one of the following:**

$$B\min_j \leq B_j = \sum_i (X_{ij} \times \text{RepCost}_i) \leq B\max_j$$
$$\left|\bar{B} - B_j\right| = \left|\bar{B} - \sum_i (X_{ij} \times \text{RepCost}_i)\right| \leq F\text{avg}_j$$
$$\left|B_{j+1} - B_j\right| = \left|\sum_i (X_{i,j+1} \times \text{RepCost}_i) - \sum_i (X_{ij} \times \text{RepCost}_i)\right| \leq F\text{cons}_j$$

### 11.5.2 Linear Programming Approach and Mathematical Formulation

In this approach, the linear programming mathematical formulation with a look-ahead period ($k$ years in a look-ahead period) will be introduced. At each investment year, the program will accumulate risk-cost from current investment year to current investment year plus $k$ years. In each investment, the program will minimize the accumulated risk-cost over the look-ahead period through asset replacement while staying within the budget constraint. A replacement schedule for the current year will be generated and the next year's asset demographics will be updated accordingly. This approach considers risk growth from the beginning for the investment year to the end of investment year plus the number of years in the look-ahead period. This approach has a looser constraint on risk growth than

the previous approach. But due to its linear nature, this program has a short run-time compared to the previous approach.

#### 11.5.2.1 Variables and Definitions

| | |
|---|---|
| $\text{AccumulatedRisk}_{ij}$ | Accumulated Risk, the sum of risk cost for asset $i$ from year $j$ to year $(j+k)$ [$k$ years in look-ahead Period]. |
| $A_{ij}$ | Age, age of asset $i$ in year $j$. |
| $B_j$ | Annual Budget, the forecasted expenditure based on suggested replacement schedule in year $j$. |
| $B\text{max}_j$ | Maximum Annual Budget, the maximum forecasted expenditure in year $j$. |
| $B\text{min}_j$ | Minimum Annual Budget, the minimum forecasted expenditure in year $j$. |
| $C_i$ | Consequence Cost, the cost to Toronto Hydro and customers if asset $i$ fails or malfunctions. |
| $F\text{avg}_j$ | Flexibility (Average), the allowed expenditure differences between the average annual expenditure and the annual budget in year $j$. |
| $F\text{cons}_j$ | Flexibility (Consecutive Years), the allowed expenditure differences between annual budgets of year $j$ and year $j+1$. |
| $HZ_{ij}$ | Hazard Rates, the chance of failure of asset $i$ in year $j$. Derived based on Weibull distributions. |
| $\text{RepAmount}_j$ | Replacement Amount, the number of units replaced for a specific type of assets (major types, e.g. underground transformers) in year $j$. |
| $\text{RepCost}_i$ | Replacement Cost, the cost to replace asset $i$. |
| $\text{RiskCost}_{ij}$ | Risk Cost, is equivalent to Consequence Cost of asset i multiplied by the chance of failure (Hazard Rate) in year $j$. |
| $S_i$ | Scale, a parameter used in the Weibull/Hazard Rate Function for asset $i$. |
| $SF_i$ | Scale Factor, a parameter used in the Weibull/Hazard Rate Function for asset $i$. This parameter is used after assigning Shape to 3. For more details, please see section 11.5.2.2. |
| Shape | Shape, a parameter used in the Weibull/Hazard Rate Function. In FIM model, Shape = 3 for all electrical assets. For simplicity, this parameter will be set to 3 for all assets in this project. |
| $X_{ij}$ | Decision Variable, $X_{ij}$ takes on 0 or 1. If $X_{ij}=1$, asset $i$ will be replaced in year $j$. If $X_{ij}=0$, asset $i$ will remain in the system in year $j$. |

#### 11.5.2.2 Mathematical Formulations and Constraints

Start from the first year within the investment period, after completing the optimization, update next year's asset demographics accordingly. Repeat for all years within the investment period.

$$\min \sum_i \text{AccumulatedRisk}_{ij} \text{ for all } j \text{ in investment period}$$

subject to:

$$\begin{aligned}
\text{AccumulatedRisk}_{ij} &= \sum_{k=0}^{\text{lookAhead}} \text{RiskCost}_{ik} \\
\text{RiskCost}_{ij} &= C_i \times HZ_{ij} \\
HZ_{ij} &= \left(\frac{\text{Shape}}{S_i}\right) \times \left(\frac{A_{ij}}{S_i}\right)^{(\text{Shape}-1)}
\end{aligned}$$

Most asset types have a *Shape* factor of 3, if Shape is set to 3:

$$\begin{aligned}
HZ_{ij} &= \left(\frac{3}{S_i}\right) \times \left(\frac{A_{ij}}{S_i}\right)^{3-1} \\
&= \left(\frac{3}{s_i^3}\right) A_{ij}^2 \\
SF_i &= \frac{3}{S_i^3} \\
\sum_i X_{ij} &= \text{RepAmount}_j \\
B_j &= \sum_i (X_{ij} \times \text{RepCost}_i)
\end{aligned}$$

**The optimization *must* satisfy at least one of the following:**

$$\begin{aligned}
B\text{min}_j \leq B_j = \sum_i (X_{ij} \times \text{RepCost}_i) &\leq B\text{max}_j \\
\left|\bar{B} - B_j\right| = \left|\bar{B} - \sum_i (X_{ij} \times \text{RepCost}_i)\right| &\leq F\text{avg}_j \\
\left|B_{j+1} - B_j\right| = \left|\sum_i (X_{i,j+1} \times \text{RepCost}_i) - \sum_i (X_{ij} \times \text{RepCost}_i)\right| &\leq F\text{cons}_j
\end{aligned}$$

# Bibliography

[1] M. A. Bajestani, N. Montgomery, D. Banjevic, and A. K. Jardine, "Maintenance resource planning for utility poles in a power distribution network," in *Reliability and Maintainability Symposium (RAMS), 2015 Annual*, IEEE, 2015, pp. 1–6.

[2] S.-C. Niu, "The equipment-replacement problem," University of Texas at Dallas, 2003.

# 12 Predictive maintenance study on production testing equipment

**Akshay Vishwakarma, C-MORE M.Eng student**

Starting May 2018, Akshay has worked with teams at Veoneer Canada Inc. and University of Toronto to develop a statistical model to help predict upcoming failures at a specific equipment at Veoneer Canada.

This report discusses about the development of predictive model for manufacturing. When the model is implemented in the manufacturing environment, it will help predict upcoming equipment failures in their manufacturing environment

## 12.1 Project background and description

Veoneer's facility in Markham, Ontario is a high-volume manufacturing facility for electronics safety modules for active and passive safety in automobiles. To keep the production running efficiently Veoneer has control plans in place to react to any failures or abnormal scenarios during scheduled production.

It was realized that being reactive to failures is not very cost-effective, as reaction plan results in longer unscheduled downtime and higher replacement costs which ultimately results in higher operational costs.

### 12.1.1 Project objective

Veoneer has requested to develop prediction model that can use data to predict future machine failures. This predictive model will allow the users to pro-actively address tooling/machine performance issues before it reaches complete failure. The correct use of the application can result in increased product quality, improved cycle time and a reduction in production downtime due to equipment failure.

The constraints of the project are as follows:

- The proposed solution must not affect the cycle time of module production

- The solution must be developed based on data from equipment directly
- The solution must not be able to adapt on the data generated in the future state

### 12.1.2 Stakeholders and their interests

- Senior Management
  - Interested to know how the proposed solution improve their global operational margins
  - Interested to know if similar solution can be deployed to other facilities as well
  - Interested to know the global deployment cost
- Local Management
  - Interested to know how the proposed solution improve their local operational margins
  - Interested to know if similar solution can be deployed to other high value components as well
  - Interested to know the deployment timeline
  - Interested to know cost per deployment
- Production Supervisor
  - Interested to know how the proposed solution will affect their production schedule
  - Interested to know about training for their operators
- Maintenance supervisor
  - Interested to know how the proposed solution will affect their maintenance schedule
  - Interested to know about the training for their mechanics
  - Interested in the interface methods with the system
- Process Engineer
  - Interested to know changes required in equipment to implement the solution
  - Interested in Overall Equipment Efficiency (OEE) for the station where solution is implemented
  - Interested to know the resources or spare parts quantity needed after the implementation of this solutions.
  - Interested to know parameters used for model development
- Maintenance mechanic
  - Interested to know how they will receive the notification for maintenance
  - Interested in the interface methods with the system
- Production operator
  - Interested in the standard work instruction

### 12.1.3 Manufacturing process details

Under the current process, the operator at the manufacturing station picks the module from the upstream station and loads it at the pin check station for testing. The pins of the module engage with the pins of the testing station for various module-related testing.

Through repeated engagement of module pins to the testing station, the pins at station start to degrade over time due to the friction between pins. The contact between the pins creates metal slivers that can lead to shorting with other pins or reduced thickness of test pins which lead to problem of pin engagements.

As a result, these failures cause unexpected downtime during production. Hence company must do reactive maintenance (expensive alternative) to meet their daily production targets. The problem with the maintenance is compounded when the maintenance personnel are busy with maintenance of other equipment.

## 12.2 Exploratory analysis

Before developing any prediction model, it was very important that we investigated all the data to understand the distribution of all the downtimes. Upon developing the distribution of down time (show in fig. 12.1a) we noticed that very high majority of distribution (98.8%) was concentrated under four minutes. Based on discussion with the process engineer, it was concluded that these short downtimes were failures associated to the module and not with testing equipment. In order to focus on equipment failure, it was concluded from the discussion that our downtime of interest was all the entries with failure downtime greater than or equal to four minutes (fig. 12.1b).

Along with the distribution of downtime, it was important that we also do exploratory analysis for the time to failure, or the number of cycles until arriving at a $\geq$ 4 minute downtime. This analysis will help us develop a predictive model for maintenance of the testing equipment. Figure 12.2a shows the distribution of cycles it takes to failure.

Upon looking at the data and discussions with the subject matter expert, it was concluded that data had high variance in the distribution pattern. Hence input from the process engineer was needed to filter the correct data points for analysis and model generation.

After the discussion with the process engineer/subject matter expert it was concluded that failures that took place within 1600 cycles or less are the part of anomalies in operation or metal slivers generated as part of regular daily operation. Cycles greater than 20,000 module tests suggested that routine planned maintenance had been complete. Hence the cycles between 1600 and 20,000 were used in our analysis as cycles that were consistent in character for our problem. Figure 12.2b provides additional details to fig. 12.2a.

## 12.3 Predictive model generation

To develop a prediction model, the age policy model was used. The age policy model is derived from a Weibull distribution that calculates the probability of failure as the cycles of operation increases. Along with the probability of failure, the age policy then incorporates the cost per failure and cost per maintenance cycle to find the optimized cycles for maintenance. The optimized cycles for maintenance are result of cycles at which cost per test is the lowest. The formulas used in the model generation are as follows:

**Total expected cost per cycle**

$$C_p R(t_p) + C_f(1 - R(t_p)),$$

where $C_p$ is the cost of a single cycle ending in a PM, $C_f$ is the cost of a single cycle ending in a failure, and $R(t_p)$ is the probability of the equipment surviving to time $t_p$.

**Expected cycle length**

$$t_p + R(t_p) + \int_{-\infty}^{t_p} tf(t)dt.$$

The resulting expected cost per cycle is the ratio of the above quantities:

$$\frac{C_p R(t_p) + C_f(1 - R(t_p))}{t_p + R(t_p) + \int_{-\infty}^{t_p} tf(t)dt}. \tag{12.1}$$

## 12.4 Results and discussion

### 12.4.1 Distribution

The Weibull distribution was used to see the general distribution of filtered data (fig. 12.3). The graph signifies that as cycles of operations are increases the probability of failure starts to increase as well. The parameters obtained from the fitting were were Scale = 6036 and Shape = 1.587. The scale signifies that there is probability of 63.2% failure of the equipment when the cycles of operation reaches 6036. The shape of 1.587 signifies the skewness towards right (the higher the number the higher it is skewed to right).

In our distribution, along with the skewness to the right some counts were visible at the right tail of the distribution. It means that there were some process anomalies or some maintenance done on the station.

### 12.4.2 Optimal cycles for maintenance

In order to find the optimized cycles for maintenance, following parameters were used:

- Scale: 6036.85
- Shape: 1.587
- Cost of Maintenance: $703.488

  The value was calculated by multiplying the value per minute of production that would be lost ($100/minute) with weights of 79.65% to 5 minutes and 20.349% to 15 minutes

  The values of 5 minutes and 15 minutes was chosen based on the feed back from subject matter expert. The weight of 79.65% was given to all the entries that were less than 15 minutes and 20.349% was given to all the entries that were greater than 15 minutes.

- Cost of Downtime: $1785.932

  The value was calculated by multiplying value per minute of production ($100/minute) with average of all the downtimes in the analysis.

Equation (12.1) was used to develop the fig. 12.4. It was concluded that the optimized cycle to do maintenance is 7461 and the associated cost is $0.32 cents/test.

## 12.5 Conclusion and next steps

Based on the historical data it can be concluded that the optimized cycles to maintenance is 7461. But it should also be kept in mind that due disturbances in data such as process anomalies, improper maintenance, etc. there were assumptions related to data preprocessing was defined. Changes to those assumptions can have significant impact on this model.

Hence it is strongly recommended that to move forward with the implementation of such model, following steps must be done before system goes live:

- Deeper data analysis / cleaning to finalize the data preprocessing steps
- Finalize the equipment for deployment
- Production level development
- Finalize the use of output from the prediction model (how to use the results from this model in manufacturing environment)
- Include method to acknowledge planned maintenance was done.

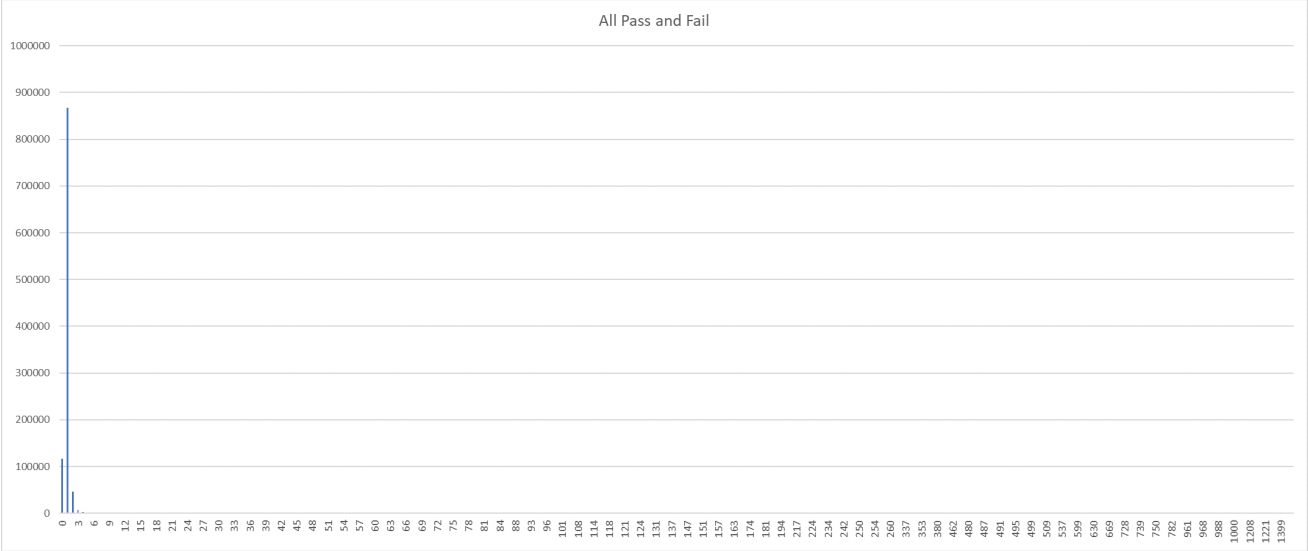


(a) All downtimes

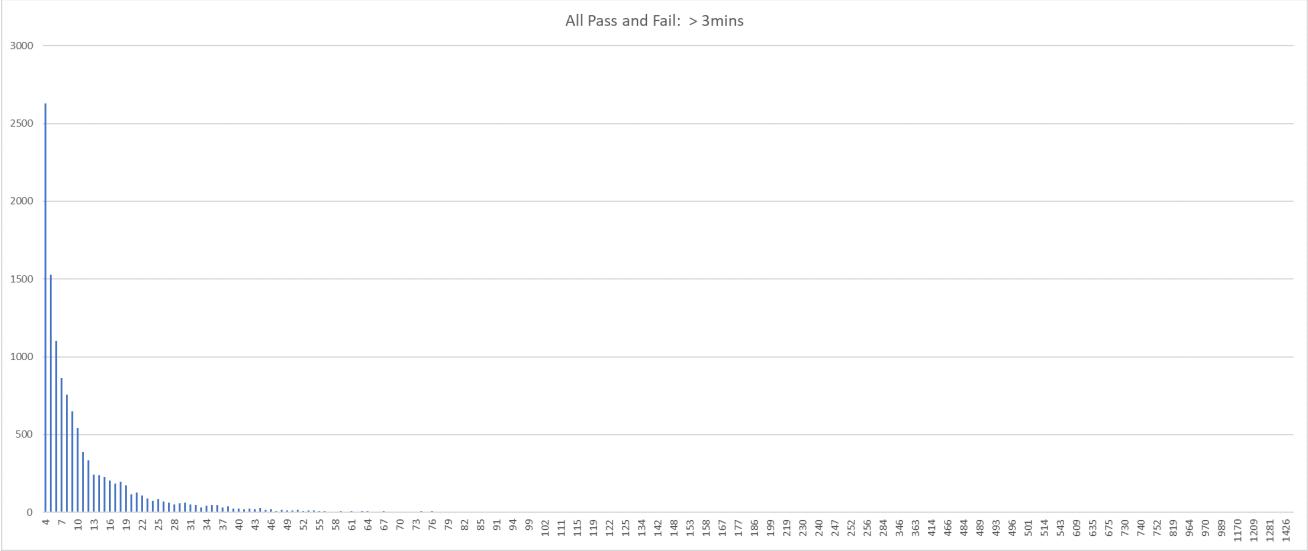


(b) Downtimes $\geq$ 4 minutes

Figure 12.1: Histogram of downtimes

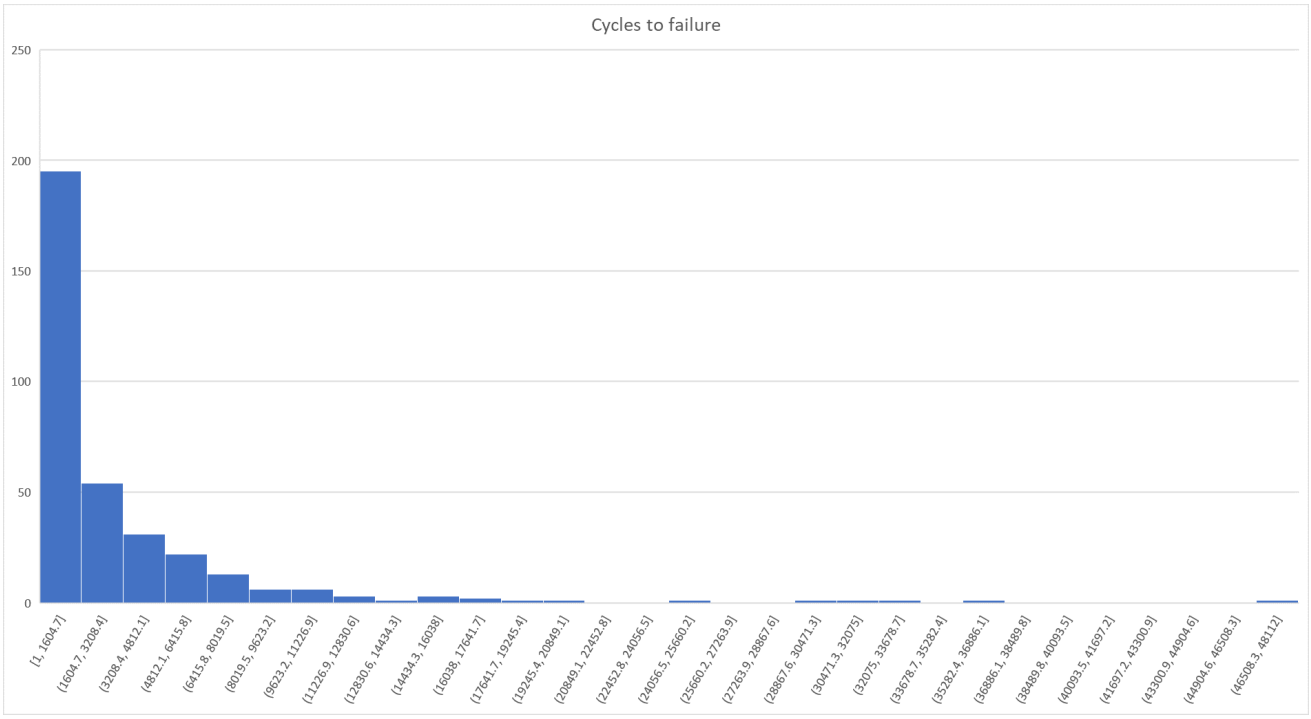


(a) Cycles to failure

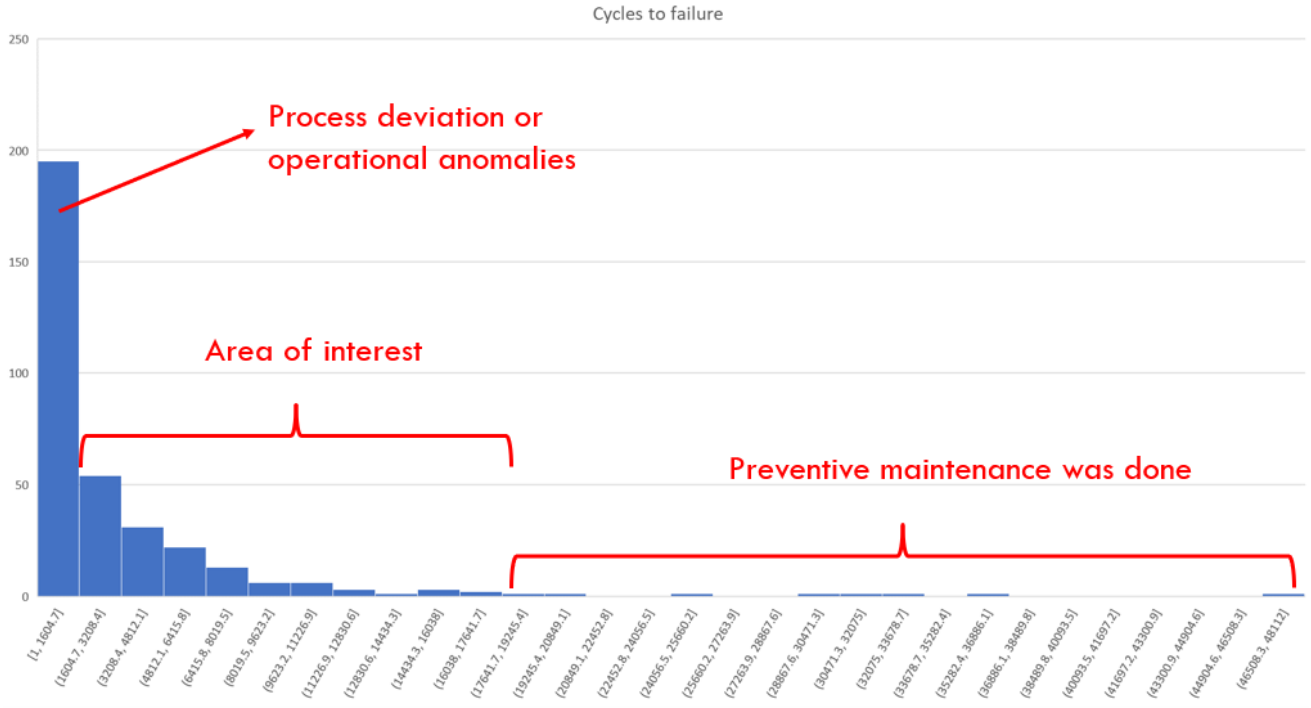


(b) Annotated histogram

Figure 12.2: Histogram of cycles to failure

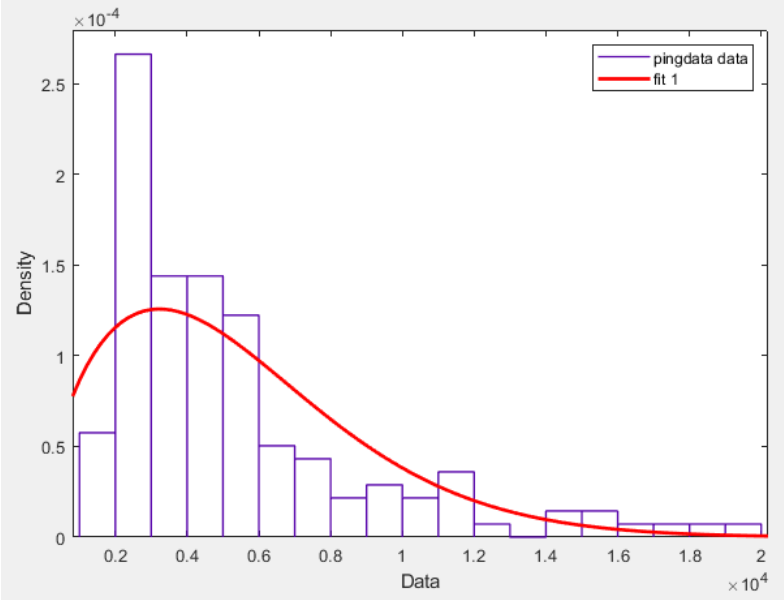


Figure 12.3: Weibull fitting on failure time data

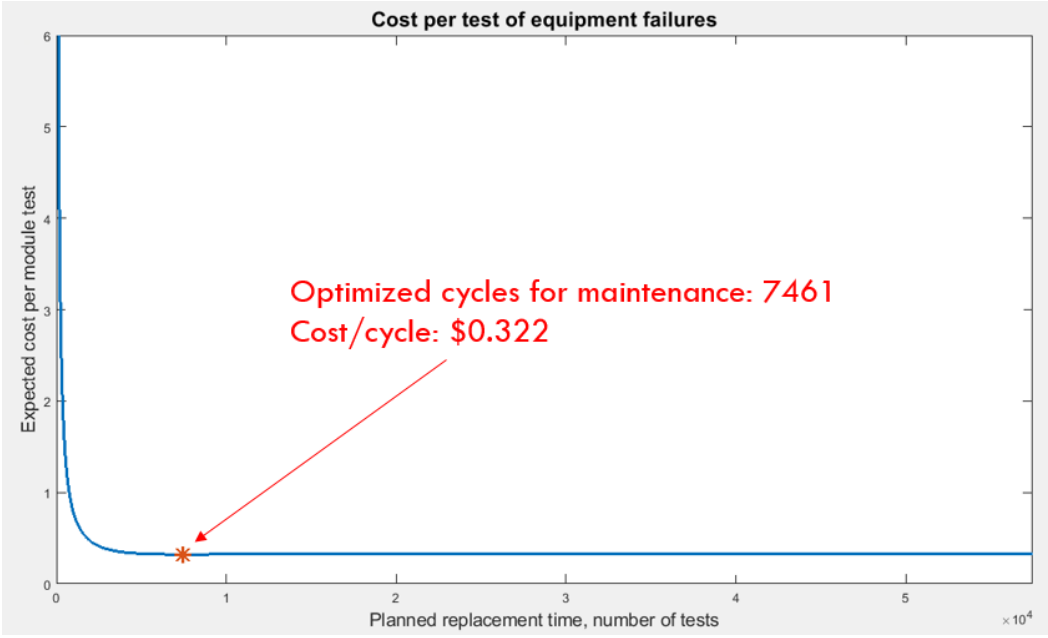


Figure 12.4: Cost per cycle over time to preventive replacment

# 13 Li Yang: research summary

**Li Yang, Postdoctoral fellow**

I joined C-MORE as a postdoctoral fellow under the guidance of Prof. Chi-Guhn Lee in October 2018,

after receiving my Ph.D. in the School of Reliability and Systems Engineering, Beihang University. The title of my doctoral dissertation is "Lifetime modeling and maintenance optimization of complex repairable systems". It focuses mainly on remaining lifetime prognostic, condition-based maintenance and health management of complex industrial systems, such as aircraft, production lines, critical infrastructures. In Jan to April of 2018, I was a visiting student in Department of Industrial and Systems Engineering, University of Singapore, co-advised by Dr. Ye Zhisheng.

Since 2018, I have authored 6 journal papers in the area of industrial engineering, such as European Journal of Operational Research, Reliability Engineering & System Safety, Journal of Manufacturing Systems and Computers & Industrial Engineering. Additionally, there are 4 papers in the status of under revision/review.

## 13.1 Previous research

My previous research in this year concentrates mainly on condition maintenance scheduling and risk management of complex industrial systems. Detailed works include: (a) Hybrid preventive maintenance of competing failures under random environment, where both age-based and condition-based maintenance are incorporated to prevent failures, along with a dynamic control limit; (b) opportunistic condition-based maintenance optimization of production systems considering random production wait time; (c) Mission abort strategies based on early-warning signal, and their applications in unmanned aerial vehicles (UAVs).

### 13.1.1 Hybrid preventive maintenance under random environment

This study investigates an industrial system subject to two typical failure modes, degradation-based failure and sudden failure. The system is operating under a random environment where external shocks arrive according to a Poisson process. The impact of shock damage on system failure is two-fold: (a) increase the hazard rate of sudden failure; (b) cause abrupt degradation increment. The system is preventively replaced when its age attains a pre-determined threshold (age-based replacement), and

undergoes a finite number of condition monitoring (CM) before this replacement. At a CM, the control limit of preventive replacement varies with the number of CM and is determined by a reliability criterion. The objective of this paper is to jointly optimize the replacement interval, monitoring interval and reliability criterion such that the expected cost per unit time is minimized. A case study on oil pipeline is provided to illustrate the applicability of the maintenance strategy.

According to our policy, age-based replacement is executed to prevent sudden failure when the age of the system attains a certain level. Within this replacement interval, CM is performed several times with a constant interval with the purpose of revealing failure and measuring the degradation level. At a CM, if a failure is revealed, a reactive replacement is immediate; Otherwise if the degradation level exceeds the preventive control limit, preventive replacement is immediate. A shifting control limit is also considered, which depends on the distance from the monitoring time to the preventive replacement time.

### 13.1.2 Opportunistic condition-based maintenance optimization of production systems

A variety of production systems experience unavoidable production wait time due to the exhaustion of raw materials or lack of demand, which provides extra opportunities for the execution of maintenance activities. In our research, a novel condition-based maintenance strategy is proposed for a production system whose production waits arrive according to the homogenous Poisson process.

This production system undergoes gradual degradation, which ultimately results in soft failures (capacity reduction). To ensure a flexible and cost-effective maintenance allocation, two levels of maintenance, opportunistic maintenance (during production waits) and regular maintenance are schemed simultaneously along with two separate control limits. The applicability of the proposed strategy is validated by a case study on a crystallizer casting machine. The result illustrates that the proposed maintenance strategy is more cost-effective compared with several classic/advanced strategies.

### 13.1.3 Mission abort strategies based on early-warning signal

The mission abort is an effective action to reduce the risk of casualties and enhance the survivability of mission-based systems such as aircrafts, submarines, and unmanned aerial vehicles (UAVs). A main task in real operations is to strive for balance between the mission reliability and the system survivability via elaborate mission abort plans.

In this research, we design the optimal mission abort policies based on the information of early-warning signals, which indicates the possible forthcoming fatal malfunction. Depending on the acquisition time of such information, the operator may immediately abort the mission, or ignore the information and continue the task. Within the framework of a constant mission duration, we carry out an economic analysis for the above problem. The optimal abort decision that minimizes the expected total economic

loss is investigated. We further extend the proposed model to the scenario of a random mission duration and derive the corresponding optimal abort decisions. A case study on a UAV executing power-grid inspection missions is used to illustrate the applicability of the abort policies.

## 13.2 Ongoing research

My ongoing research concentrates mainly on prognostic and health management of wind farms. The whole research framework contains four steps as follows.

**Step 1: Signal processing and data analysis**
In this step, we aim to extract some useful features from the data collected in wind farm, e.g., vibration data, temperature data. Based on that, the degradation trend of turbine components are formulated.

**Step 2: Remaining useful lifetime prediction and parameter estimation**
In this step, we are devoted to predict the RUL of each component in a turbine based on some machine learning technology, including recurrent neutral network, reinforcement learning etc

**Step 3: Dynamic maintenance interval programming at the component level**
This step dynamically determined the optimal maintenance interval for each component of a turbine based on newly updated RUL and reliability parameters.

**Step 4: Rolling approach for group maintenance optimization of several turbines in the farm.**
Using the sub-optimal maintenance interval obtained in step 3, a rolling approach method is used for group maintenance optimization in a given period. The main purpose is to share the set-up cost and downtime cost of different components.

## 13.3 List of papers published/submitted

[1] Yang Li, Ye Zhisheng, Chi-guhn Lee, Yang Sufen, Peng Rui, A two-phase preventive maintenance policy considering imperfect repair and postponed replacement, *European Journal of operational Research*, 2018. (accepted, DOI: 10.1016/j.ejor.2018.10.049)

[2] Yang Li, Zhao Yu, Peng Rui, Ma Xiaobing, Hybrid preventive maintenance of competing failures under random environment, *Reliability Engineering and System Safety*, 2018, 174: 130-140.

[3] Yang Li, Zhao Yu, Peng Rui, Ma Xiaobing, Opportunistic maintenance of production systems subject to random wait time and multiple control limits, *Journal of manufacturing systems*, 2018, 47: 12-34.

[4] Yang Li, Zhao Yu, Ma Xiaobing, Multi-level maintenance strategy of deteriorating systems subject to two-stage inspection, *Computers & Industrial Engineering*, 2018, 118: 160-169.

[5] Yang Li, Zhao Yu, Ma Xiaobing, Qiu Qingan, An optimal inspection and replacement policy for a two-unit system, *Journal of Risk and Reliability*, 2018, DOI:10.1177/1748006X18761488

[6] Qiu Qingan, Cui Lirong, Yang Li*. Maintenance Policies for Energy System Subject to Complex Failure Processes and Power Purchasing Agreement. *Computers & Industrial Engineering*, 2018, 119: 193-203 (corresponding author).

[7] Yang Li, Sun Qiuzhuang, Ye Zhisheng, Designing Mission Abort Strategies based on Early-Warning Signal-Application to UAV, *IEEE Transactions on Industrial Informatics*, 2018. (under review)

[8] Yang Li, Zhao Yu, Ma Xiaobing, Advanced maintenance scheduling of a two-component system with failure interaction, *Applied Mathematical Modeling*, 2018. (under 2nd review)

[9] Ma Xiaoyang, Yang Li*, Peng Rui. Reliability analysis and condition-based maintenance of a warm standby cooling system, *Reliability Engineering & System Safety*, 2018 (under revision)

[10] Wu Tianyi, Ma Xiaobing, Zhao Yu, Yang Li. Maintenance scheduling of a production system in consideration of production wait time. *International journal of production research*, 2018 (under review)

# 14 Ongoing Research on the Remaining Useful Life Prediction for High Voltage Circuit Breakers

**Gaoyang Li, Visiting Ph.D. student**

## 14.1 Introduction

High voltage circuit plays a crucial role in the safety and stability of the energy transmission. The life-cycle management of high voltage circuit breakers, which aims to provide optimal management to enhance the equipment's reliability and reduce the cost during the life circle relies on accurate information about the remaining useful life of the circuit breakers. According to the surveys conduct by the CIGRE, mechanism and its control circuit account for most of the defects. Thus mechanism life is one of the limits of the useful life of the circuit breakers.

The health status of the circuit breakers has a close relationship with its remaining useful life. One simple way to define the status of the circuit breaker is the percentage of the remaining useful life. Traditional methods to predict the remaining useful life of machines are basically based on statistical methods by fitting the life time of several samples with a probability distribution, of which the Weibull and exponential distribution are the most widely used. However, the information like mean time to failure provided by the statistical methods is a kind of statistical averaging, which lacks the ability to offer personal guide for each equipment. One evolution of the statistical methods is the proportional hazard model. By multiplying an exponent of the health parameters with the life distribution function, the model gets the ability to provide amendment to predict the reliability or remaining useful life. But an unavoidable problem is that enough data must be provided to fit the distribution function well. In recent years, with the development of sensor and signal processing technique, the online monitoring data become another promising treasury to diagnose the health status of the circuit breakers. Furthermore, combined with machine learning method, the data mining on monitoring data shows great ability to provide depth-layer information about the machine's failure.

Despite the wealth of information found in these literature, the features extracted depend on expertise and there lacks a comprehensive features selection and extraction method based on real accelerated life tests. In this study, we endeavor to build a feature selection and extraction framework based on the real

accelerated life test data.

## 14.2 Model description

As a routine maintenance item in the power grid, large amounts of mechanical characteristic data, including the displacement curves of the movable contacts and the control current curves of the coils, have been accumulated during the operations. In this study the feature set consists of two parts, including the extracted feature from the raw curves and the direct exported parameters from the mechanical characteristic tester.

For the coil current curves, the key points include the starting rising point, the first local minimum point, starting and ending points of the plateau and the ending point of the current. Besides, the starting point, ending of the acceleration phase, ending of the uniform phase and the ending point of the displacement curves are considered to be the key points of the displacement curves.

The health status centered feature extraction are based on two criterions, the monotonicity and consistency. Monotonicity implies that the changing direction of the selected parameter must unidirectional because the health status's deterioration is an irreversible process. Consistency is another criterion of small volatility between different circuit breakers.

*Monotonicity:* Monotonicity is the combination of the Pearson's coefficient, Spearman's rank correlation coefficient and Kendall tau's rank correlation coefficient.

*Consistency:* The consistency coefficients are simply defined as the standard deviations of the coefficients

*Feature selection:* By Combining the monotonicity coefficients and the consistency coefficients, the final feature selection standard for Pearson's coefficient is defined as:

$$I_{\text{pearson}} = \frac{|\rho_{\text{pearson}}|}{a(\sigma(\rho_{\text{pearson}}) + b}$$

where $b$ deci des how much the consistency coefficient affects the final decision, and $a$ limits the scale of the final coefficient.

The decision coefficient is defined as the weighted average of the absolute value of the three coefficients above, where the weight of Pearson is set to be 0.5 to assign equal attention to linear and nonlinear correlation. Finally, Support Vector Regression (SVR) is utilized to map from an input to the output based on the training set.

## 14.3 Summary

In this work, a new feature selection and extraction framework is proposed for the health status diagnosis of the mechanism of high voltage circuit breakers. Firstly, among 44 closing features extracted based on the key points, 6 features are selected based on monotonicity and consistency. Then the features are fed into a SVR model for training and predicting remaining useful life of a new mechanism. The visualization results show that the proposed method can capture the deterioration of the mechanism accurately and the mean square error of the diagnosis result is 15.6%.

# Bibliography


[1] T. Lindquist, L. Bertling, and R. Eriksson, "A method for age modeling of power system components based on experiences from the design process with the purpose of maintenance optimization," in *Reliability and Maintainability Symposium, 2005. Proceedings. Annual*, IEEE, 2005, pp. 82–88.

[2] X. Zhang, E. Gockenbach, Z. Liu, H. Chen, and L. Yang, "Reliability estimation of high voltage sf6 circuit breakers by statistical analysis on the basis of the field data," *Electric Power Systems Research*, vol. 103, pp. 105–113, 2013.

[3] H. T. Pham, B.-S. Yang, T. T. Nguyen, *et al.*, "Machine performance degradation assessment and remaining useful life prediction using proportional hazard model and support vector machine," *Mechanical Systems and Signal Processing*, vol. 32, pp. 320–330, 2012.

[4] Y. Peng, M. Dong, and M. J. Zuo, "Current status of machine prognostics in condition-based maintenance: A review," *The International Journal of Advanced Manufacturing Technology*, vol. 50, no. 1-4, pp. 297–313, 2010.

[5] D. Zhang, W. Li, X. Xiong, and R. Liao, "Evaluating condition index and its probability distribution using monitored data of circuit breaker," *Electric Power Components and Systems*, vol. 39, no. 10, pp. 965–978, 2011.

[6] X. Wang, M. Rong, J. Qiu, D. Liu, B. Su, and Y. Wu, "Research on mechanical fault prediction algorithm for circuit breaker based on sliding time window and ann," *IEICE transactions on electronics*, vol. 91, no. 8, pp. 1299–1305, 2008.

[7] C.-J. Lin, R.-C. Weng, *et al.*, "Simple probabilistic predictions for support vector regression," 2004.

# A Automatic Learning of Inter-Task Mappings for Transfer Learning in Model-Free Tasks

**Michael Gimelfarb, Ph.D. Student, Member of C-MORE Lab and D3M Lab**

## A.1 Introduction

Over the last several decades, reinforcement learning has become a popular approach for multi-period decision making and planning in stochastic and non-stationary environments. The development of deep learning techniques has allowed reinforcement learning to be applied successfully to MDPs with continuous or large state spaces ([1]), which would otherwise be intractable to solve with traditional dynamic programming.

Roughly speaking, reinforcement learning can be broken down into two main categories: model-based and model-free. In model-based RL, the agent observes the model directly or learns the model prior to finding an optimal plan or policy. In model-free RL, the agent does not make an effort to learn the model, but rather learns the optimal policies directly through interaction with the environment.

Model-free RL has become popular since it does not require knowledge of the underlying model, which can often be too complex to model directly. However, despite the improvements in deep learning and the exponential growth in computing power, model-free RL methods are sample inefficient and often require millions of training examples and days of computation time on parallel clusters to solve. Neural networks are typically trained with back-propagation using gradient descent, which leads to instabilities or convergence to local minima, all of which can lead to sub-optimal policies.

In order to accelerate the convergence and improve robustness of RL algorithms, a variety of frameworks have been introduced over the years for incorporating prior knowledge of the domain in various forms. Reward shaping transforms a sparse reward structure into a dense one while preserving the optimal policies ([2]). Policy shaping assumes that a human expert is able to provide demonstrations directly, or otherwise can critique actions selected by the learning agent ([3]). Transfer learning applies the knowledge obtained from solving source task(s) to solve similar target task(s) ([4]), often using inter-task mappings ([5]) which describe the similarity of states or actions between tasks. When differ-

ent tasks or observations of varying complexity are available for transfer, curriculum learning is often used to order them ([6]). Finally, in multitask learning, an agent simultaneously solves multiple tasks while exploiting the similarities between the tasks ([7]).

The remainder of the report is organized as follows: Section A.2 presents the review of some relevant literature, Section A.3 presents some necessary definitions, Section A.4 presents the objectives and general timeline for the thesis, Section A.5 discusses the main contributions in the RL community, Section A.6 discusses the relevance of the work, and Section A.7 presents a first attempt at the problem.

## A.2 Relevant Work

### A.2.1 Shaping of Rewards and Policies

Given an MDP $(\mathcal{S}, \mathcal{A}, R, P, \gamma)$ with reward function $R$, the idea of reward shaping is to instead learn the MDP with reward function $R + F$ where $F$ is a shaping function that incurs additional reinforcement reward. Unfortunately, [8] showed that arbitrary reward shaping can lead to positive-reward cycles that change the optimal policy. [2] showed that potential-based reward shaping (PBRS) is both necessary and sufficient for policy invariance in arbitrary MDPs. Later, policy invariance guarantees for PBRS were established for multi-agent systems ([9]), time-dependent potentials ([10]), and action-dependent potentials ([11]). The discovery of the equivalence of PBRS with Q-value initialization ([12]), led to a brief decline in the interest of reward shaping. However more recently, methods for learning and representing advice have made use of PBRS in different forms. [13], for example, showed how arbitrary reward signals can be transformed into a potential function for PBRS.

While reward shaping is based on transferring knowledge of value functions, policy shaping is based on transferring knowledge of the policy ([3]). Here, the agent communicates via a noisy channel with a human expert, who rates an action as either good or bad, and updates the belief about the optimal policy in a Bayesian framework.

### A.2.2 Using Shaping for Transfer Learning

There has been some work applying shaping to transfer learning between tasks in model-free settings. [14] provides a reward to the learning agent in a state-action pair proportional to the probability that the mapped state-action pair is selected according to the transferred policy. These additional rewards are used to learn a potential function in the framework of [13] which is used for the target task. However, this requires the use of predetermined inter-task mappings, which we want to learn. [15] combine reward shaping with demonstrations. [16] learns a function from a problem-independent descriptor, called "agent-space", to the reward space. Modelling the agent-space, however, requires knowledge of semantics that are common across source and target task(s).

### A.2.3 Automatic Learning of Inter-Task Mappings

There has been some recent work on learning the inter-task mapping under some assumptions. In the first class of papers, some knowledge of the source and target domains are known. In [17], for instance, the domain is represented as Qualitative Dynamic Bayes Network (QDBNs) (in which only dependencies between variables are represented). [18] uses a similarity metric between states in two MDPs defined in terms of their reward and transition functions. In the second class of papers, data is used to learn the mapping, rather than prior model assumptions. [19] provides a set of possible inter-task mappings between state spaces and a mechanism to learn the best mapping from the set. However, the complexity of the algorithm depends on the number of inter-task mappings, which grows rapidly as the tasks become more complex. A data-driven approach in [20] learns the inter-task mapping by first learning a transition model of the target task which is then used to learn an inter-task mapping. This method also does not scale too well, and does not apply in online settings. Other approaches are detailed in [21].

### A.2.4 Dealing with Negative Transfer

One challenge when transferring knowledge between two tasks is *negative transfer* ([4]). When the source and target tasks are dissimilar, the transferred knowledge can misguide the learning agent and slow down convergence. One simple solution, called *option-based transfer*, is to give the decision maker the option to trust the transferred knowledge or reject it ([22]). Another approach is to choose a source task that is related to the target task prior to transfer ([23]).

## A.3 Definitions

### A.3.1 Reinforcement Learning

Given an MDP $(S, A, R, P, \gamma)$ and policy $\mu$, the agent can learn the value function for the policy $\mu$

$$Q^{\mu}(s,a) = \mathbb{E}_{s_t \sim P, a_t \sim \mu}[\sum_{t=0}^{\infty} \gamma^t R(s_t, a_t, s_{t+1}) | s_0 = s, a_0 = a] \tag{A.1}$$

from observations $(s_t, a_t, s_{t+1}, r_t)$ using temporal difference (TD) learning

$$Q_{t+1}(s_t, a_t) = Q_t(s_t, a_t) + \alpha \left[\tilde{R}_t(s_t) - Q_t(s_t, a_t)\right], \tag{A.2}$$

where $\alpha \in [0, 1]$ is a learning rate and $\tilde{R}_t$ is an improved estimator of future rewards. For Q-learning, for example, this estimate is given by $\tilde{R}_t(s) = r_t + \gamma \max_{a \in A} Q_t(s_{t+1}, a)$ where $r \sim R$. A more detailed presentation is given in [24].

### A.3.2 Potential-Based Reward Shaping

In order to transfer knowledge from source to target task, we follow the potential-based reward shaping framework introduced in [2]. Specifically, given an MDP with reward function $R(s, a, s')$, the agent solves the corresponding MDP with reward function $R(s, a, s') + F(s, a, s')$, where $\Phi : \mathcal{S} \to \mathbb{R}$ and

$$F(s, a, s') = \gamma\Phi(s') - \Phi(s),\ s, s' \in \mathcal{S}. \tag{A.3}$$

Recall that $\Phi$ can be time ([10]) and action ([11]) dependent.

### A.3.3 Transfer Learning and Inter-Task Mappings

We assume that a source task MDP $\mathcal{M}_{src}$ has been learned and the optimal value function $V^*_{src}$ or $Q^*_{src}$ is available to the agent. The agent wants to incorporate $Q^*_{src}$ as potential-based reward shaping advice to learn a target MDP $\mathcal{M}_{tar}$. However, since the state spaces of the source and target tasks differ, it is not possible to use $Q^*_{src}$ directly on the target task.

In order to address this issue, we follow the framework of [5] and introduce an inter-task state (and possibly action) mapping $\mathcal{X} : \mathcal{S}_{tar} \times \mathcal{A}_{tar} \to \mathcal{S}_{src} \times \mathcal{A}_{src}$. Intuitively, the inter-task state/action mapping identifies states/actions in the source task that are most similar to states/actions in the target task. A more powerful generalization, which we want to explore in this work, incorporate the idea of mappings on subsets of states between the two tasks ([25]). Given $Q^*_{src}$ and $\mathcal{X}$, the agent can initialize Q-values in the target task according to $Q^*_{src}(\mathcal{X}(s, a))$. However, since Q-value initialization is theoretically equivalent to reward shaping ([12]), it is equivalently possible to apply potential-based reward shaping on $\mathcal{M}_{tar}$ using potential $\Phi_{\mathcal{X}} = Q^*_{src} \circ \mathcal{X}$. This view is particularly useful when $\mathcal{X}$ is changing over time, such as in the case when it is being learned. What information we transfer between tasks, and how to transfer it, in order to learn $\mathcal{X}$ is the main question that we would like to address in this research program.

## A.4 Objectives and Outline of Proposal

In this program, we want to derive a mathematical framework and algorithms for learning inter-task mappings $\mathcal{X}$ between solved source tasks, and a target task which is learned online in a model-free setting. The inter-task mapping, in conjunction with the optimal value function from the source task, is incorporated as reward shaping advice into the target task to improve the quality of convergence. The main research question has two main aspects: (1) *what* minimal information/abstraction about the tasks do we need to learn (policies, values, state-space features) in order to learn the task mapping? (2) *how* do we transfer this knowledge to learn a good task mapping online and efficiently in a way that works well on a variety of tasks?

### A.4.1 Long-Term Plan

There are many ways to address these questions from different points of view. While there are many different frameworks for incorporating advice besides reward shaping, we believe that augmenting the reward structure using PBRS has many key advantages. Firstly, there are policy invariance guarantees which hold for general MDPs and general potential functions ([2]). Secondly, it is possible to use PBRS to transfer a variety of information, including value functions, policies ([14]) or even individual examples ([15]). Thirdly, we note that a related work on reward shaping with expert advice has already been accepted to a top journal (NIPS) by the candidate and advisors ([26]). A four-year research program could consist of the following.

**Year 2**: We begin by studying the problem in which the information we transfer is based only on the value functions between tasks. Using empirical evaluation, we first try to understand when and why this approach leads to positive transfer in some cases and negative transfer in others (e.g. scale and location invariance of the value functions in the source and target tasks, information lost when transferring state by state or action by action). For example, we want to investigate the use of adaptive standardization or normalization of the data and the source value function to allow scale and location invariant learning. We will want to develop assumptions on the tasks under which this kind of transfer works effectively and prove that our algorithm converges asymptotically to the best mapping. We also want to investigate the combination of this idea with option-based transfer.

**Year 3**: Since information on value functions may still not be sufficient, we then try to incorporate the knowledge of the optimal policy from the source task rather than just the values alone (see, e.g. [14]) and learn the corresponding state and action inter-task mappings. Also, by treating value and policy advice as two different experts, it may be possible to apply the Bayesian reward shaping techniques we developed in our previous work ([26]). One formal way to learn mapping between two different MDPs with different reward functions and transition functions is to use the *bisimulation metric* ([18], [27]). Unfortunately, this metric is expensive to compute and is only applicable for transfer in model-based RL. However, it is not the only way to learn the mapping between MDPs. One promising approach we want to investigate is to learn a *soft* (or probabilistic) mapping between state spaces ([28]). By defining a suitable smooth parameterization of this soft mapping, we believe it will be possible to use Bayesian methods to learn the optimal parameters of this mapping from data. This will constrain the space of possible mappings in the hypothesis space to those which are continuous rather than arbitrary, which will reduce the over-fitting or noise in the learned mappings and make them more effective for transfer.

**Year 4**: A final approach we want to investigate in this work is whether higher-level abstractions of the source and target MDPs can be learned online, and how they can be used for value or policy transfer in a reward shaping framework. For example, instead of learn a mapping between single states, it can be more effective to learn a mapping between subsets of states in the two tasks based on reward information ([25]). This can be seen as a more general case of the inter-task mapping framework. Another

approach is to learn more abstract features of the state spaces and use this knowledge to guide the exploration policy of the target task. Transfer learning in supervised tasks by learning a latent representation using variational autoencoders has already been investigated by [29], but to our knowledge, no detailed investigation of these techniques for reinforcement learning have been investigated so far.

## A.5 Contributions

To the best of our knowledge, there have been no major attempts to learn the inter-task mapping in a reward shaping framework directly from data, nor in a deep learning framework. While most of the existing work focuses on exploiting some known structural properties of the MDPs being solved, our work focuses on the less-explored issue of how to transfer directly from feedback of the learning process, when no structural properties are known in advance. We believe that this work is a step forward in developing truly "independent" agents that learn from experience rather than direct human intervention or guidance.

## A.6 Relevance of Research

This work will be useful for time-sensitive and complex tasks, where we don't know the underlying dynamics of the system (so we cannot specify the task mappings a prior), but one where we can leverage prior knowledge of solution(s) on related task(s). For example, suppose that a robot is used for search and rescue in a complex and dangerous environment, such as a building. The inputs are sensory data (e.g. visual, temperature, audio). If the robot has already performed search and rescue in different situations, it may transfer the optimal values or policies from this task. Since the environment is uncertain and we do not know in advance what the dangers may be, or where the victim is located, we may not understand how to map between the tasks. The robot might want to learn the associations between the tasks as it explores.

## A.7 First Attempts

In order to learn $\mathcal{X}$, we first make the observation that the optimal potential function $\Phi$ for any given task is the true optimal value function $Q^*_{src}$. Therefore, given estimates of optimal values $Q^*_{src}$ and $Q^*_{tar}$ from source and target tasks, respectively, we solve the general optimization problem $\min_{\chi \in \mathcal{X}} \|Q^*_{src} \circ \mathcal{X} - Q^*_{tar}\|$. We propose to learn $\mathcal{X}$ online from observations $(s_t, a_t, s_{t+1}, r_t)$ obtained while learning the target task. Since tabular and deep learning are inherently different in nature, we present slightly different approaches.

### A.7.1 The Tabular Case

Here, Q-values $Q_t(s,a)$ are stored in a table and learned using (A.2). We implement $\mathcal{X}$ as a table of assignments between observed target state and source states. In particular, we follow the Bayesian Q-learning framework ([30]) and assume that Q-values $q_{s,a}$ for the target task follow Gaussian distributions conditional on the state-action pair $(s_{src}, a_{src}) \in \mathcal{S}_{src} \times \mathcal{A}_{src}$ in the source task,

$$\mathbb{P}(q_{s,a,t} = q | s_{src}, a_{src}) = \mathcal{N}(q; Q^*_{src}(s_{src}, a_{src}), \theta_{s,a}) \tag{A.4}$$

where $\theta_{s,a} > 0$ is a problem-dependent parameter. Given data $\mathcal{D}_{s,a} = \{q_{s,a,t};\ t = 1, 2 \dots T\}$, we compute the maximum a-posteriori estimator assuming conditional independence of $q_{s,a,t}$ and uniform prior on $s_{src}, a_{src}$

$$\log \mathbb{P}(s_{src}, a_{src}, \theta_{s,a} | \mathcal{D}_{s,a}) = \log \mathbb{P}(\theta_{s,a}) - \frac{T}{2} \log \theta_{s,a} - \frac{1}{2\theta_{s,a}} \sum_{t=1}^{T} \left( q_{s,a,t} - Q^*_{src}(s_{src}, a_{src}) \right)^2 + C. \tag{A.5}$$

Clearly, we can first obtain the solution for $s_{src}$ and $a_{src}$, and then find the optimal $\theta_{s,a}$. Since $\sum_t (x_t - y)^2$ is convex in $y$ and symmetric about its global optimum point $\frac{1}{T}\sum_t x_t$, the unique solution for $s_{src}, a_{src}$ is independent of $\theta_{s,a}$ and is $(s^*_{src}, a^*_{src}) = \arg\min_{(s',a')} \left| Q^*_{src}(s', a') - \frac{1}{T}\sum_{t=1}^{T} q_{s,a,t} \right|$. This leads to an efficient algorithm for learning the transfer function from data (Algorithm 1). Here $\mathcal{X}$ could be initialized in different ways, based on a prior belief, at random, or to the state with near-zero values. $\theta_{s,a}$ could be later used to develop confidence estimates. By ordering pairs $(s,a)$ according to $Q^*_{src}$, it is possible to find $(s^*_{src}, a^*_{src})$ using binary search in time $O(\log|\mathcal{S}_{src}| + \log|\mathcal{A}_{src}|)$ (see, e.g. [31]); this is `BinarySearchMin`.

**Algorithm 1** `ComputeTransfer`

**input** $\mathcal{U}_{src} = \{(s_{src}, a_{src}) \in \mathcal{S}_{src} \times \mathcal{A}_{src}\}$ sorted according to $Q^*_{src}$
**input** $\mathcal{D}_{s,a}$ for observed $s \in \mathcal{S}_{obs}, a \in \mathcal{A}_{obs}$ in the target task
**input** $\mathcal{X}$ from previous episode or initialized based on prior belief
**for** $(s,a) \in \mathcal{S}_{obs} \times \mathcal{A}_{obs}$ **do**
    $\mu_{s,a} = \frac{1}{|\mathcal{D}_{s,a}|} \sum_{q \in \mathcal{D}_{s,a}} q$
    $(s^*_{src}, a^*_{src}) =$ `BinarySearchMin`$(\mu_{s,a}, \mathcal{U}_{src})$
    set $\mathcal{X}[s,a] \leftarrow (s^*_{src}, a^*_{src})$
**return** $\mathcal{X}$

### A.7.2 The Value Function Approximation Case

Here, the transfer function $\mathcal{X} = \mathcal{X}(s; \mathbf{w}^{tar})$ and the optimal value function on the source task $Q^*(s,a;\mathbf{w}^{src})$ are both feed-forward neural network. Given a sequence of state-value observations on the target task, $(s_i, V_i)$, we want to minimize the mean-squared-error (MSE)

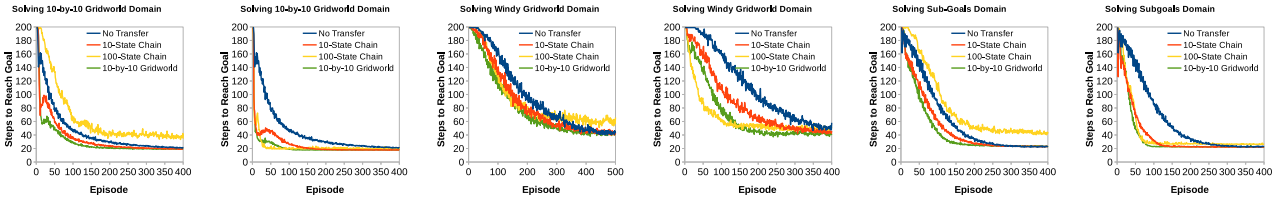


Figure A.1: Performance (steps required to reach the final goal) on all three target tasks (basic grid-world, windy grid-world, sub-goals), using each of the source tasks for transfer; shows both random and constant initialization of the transfer function. Averaged over 100 independent runs using Q-learning.

$$\mathcal{L}(\mathbf{w}^{tar}) = \frac{1}{2}\sum_i \left(V_i - V^*_{src}(\mathcal{X}(s_i;\mathbf{w}^{tar});\mathbf{w}^{src})\right)^2. \tag{A.6}$$

The composition $V^*_{src}(\mathcal{X})$ is also a neural network, with input network $\mathcal{X}$ which is connected to an output network $V^*_{src}$. The optimal parameters $\mathbf{w}^{tar}$ of $\mathcal{X}$ would be found by optimizing $\mathcal{L}$ using stochastic gradient descent; here the connections associated with $V^*_{src}$ would be frozen during training while those of $\mathcal{X}$ would be trained to minimize A.6.

### A.7.3 Preliminary Empirical Results

In our preliminary simulations, we considered three target tasks: (1) a 10-by-10 deterministic grid-world problem with a fixed initial and fixed goal state, (2) a 10-by-10 "windy" grid-world where the agent has probability 0.3 of moving to the cell above, and (3) the 5-by-5 domain with sub-goals from [2]. For each target task, we considered three source tasks: (1) a 10-state linear chain, (2) a 100-state linear chain, and (3) a deterministic 10-by-10 grid-world. As seen in Figure A.1, initialization of $\mathcal{X}$ is critical for good performance. More work needs to be done to develop a method that can detect and avoid negative transfer.

# Bibliography


[1] Y. Li, "Deep reinforcement learning: An overview," *arXiv preprint arXiv:1701.07274*, 2017.

[2] A. Y. Ng, D. Harada, and S. Russell, "Policy invariance under reward transformations: Theory and application to reward shaping," in *ICML*, vol. 99, 1999, pp. 278–287.

[3] S. Griffith, K. Subramanian, J. Scholz, C. L. Isbell, and A. L. Thomaz, "Policy shaping: Integrating human feedback with reinforcement learning," in *Advances in neural information processing systems*, 2013, pp. 2625–2633.

[4] M. E. Taylor and P. Stone, "Transfer learning for reinforcement learning domains: A survey," *Journal of Machine Learning Research*, vol. 10, no. Jul, pp. 1633–1685, 2009.

[5] M. E. Taylor, P. Stone, and Y. Liu, "Transfer learning via inter-task mappings for temporal difference learning," *Journal of Machine Learning Research*, vol. 8, no. Sep, pp. 2125–2167, 2007.

[6] Y. Bengio, J. Louradour, R. Collobert, and J. Weston, "Curriculum learning," in *Proceedings of the 26th annual international conference on machine learning*, ACM, 2009, pp. 41–48.

[7] R. Caruana, "Multitask learning," *Machine learning*, vol. 28, no. 1, pp. 41–75, 1997.

[8] J. Randløv and P. Alstrøm, "Learning to drive a bicycle using reinforcement learning and shaping.," in *ICML*, Citeseer, vol. 98, 1998, pp. 463–471.

[9] S. Devlin and D. Kudenko, "Theoretical considerations of potential-based reward shaping for multi-agent systems," in *The 10th International Conference on Autonomous Agents and Multiagent Systems-Volume 1*, International Foundation for Autonomous Agents and Multiagent Systems, 2011, pp. 225–232.

[10] ——, "Dynamic potential-based reward shaping," in *Proceedings of the 11th International Conference on Autonomous Agents and Multiagent Systems-Volume 1*, International Foundation for Autonomous Agents and Multiagent Systems, 2012, pp. 433–440.

[11] E. Wiewiora, G. W. Cottrell, and C. Elkan, "Principled methods for advising reinforcement learning agents," in *Proceedings of the 20th International Conference on Machine Learning (ICML-03)*, 2003, pp. 792–799.

[12] E. Wiewiora, "Potential-based shaping and q-value initialization are equivalent," *Journal of Artificial Intelligence Research*, vol. 19, pp. 205–208, 2003.

[13] A. Harutyunyan, S. Devlin, P. Vrancx, and A. Nowé, "Expressing arbitrary reward functions as potential-based advice.," in *AAAI*, 2015, pp. 2652–2658.

[14] T. Brys, A. Harutyunyan, M. E. Taylor, and A. Nowé, "Policy transfer using reward shaping," in *Proceedings of the 2015 International Conference on Autonomous Agents and Multiagent Systems*, International Foundation for Autonomous Agents and Multiagent Systems, 2015, pp. 181–188.

[15] T. Brys, A. Harutyunyan, H. B. Suay, S. Chernova, M. E. Taylor, and A. Nowé, "Reinforcement learning from demonstration through shaping.," in *IJCAI*, 2015, pp. 3352–3358.

[16] G. Konidaris and A. Barto, "Autonomous shaping: Knowledge transfer in reinforcement learning," in *Proceedings of the 23rd international conference on Machine learning*, ACM, 2006, pp. 489–496.

[17] Y. Liu and P. Stone, "Value-function-based transfer for reinforcement learning using structure mapping," in *Proceedings of the national conference on artificial intelligence*, Menlo Park, CA; Cambridge, MA; London; AAAI Press; MIT Press; 1999, vol. 21, 2006, p. 415.

[18] P. S. Castro and D. Precup, "Using bisimulation for policy transfer in mdps," in *Proceedings of the 9th International Conference on Autonomous Agents and Multiagent Systems: volume 1-Volume 1*, International Foundation for Autonomous Agents and Multiagent Systems, 2010, pp. 1399–1400.

[19] V. Soni and S. Singh, "Using homomorphisms to transfer options across continuous reinforcement learning domains," in *AAAI*, vol. 6, 2006, pp. 494–499.

[20] M. E. Taylor, G. Kuhlmann, and P. Stone, "Autonomous transfer for reinforcement learning," in *Proceedings of the 7th international joint conference on Autonomous agents and multiagent systems-Volume 1*, International Foundation for Autonomous Agents and Multiagent Systems, 2008, pp. 283–290.

[21] M. E. Taylor and P. Stone, "An introduction to intertask transfer for reinforcement learning," *Ai Magazine*, vol. 32, no. 1, p. 15, 2011.

[22] T. Croonenborghs, K. Driessens, and M. Bruynooghe, "Learning relational options for inductive transfer in relational reinforcement learning," in *International Conference on Inductive Logic Programming*, Springer, 2007, pp. 88–97.

[23] E. Talvitie and S. P. Singh, "An experts algorithm for transfer learning.," in *IJCAI*, 2007, pp. 1065–1070.

[24] R. S. Sutton, A. G. Barto, F. Bach, *et al.*, *Reinforcement learning: An introduction*. MIT press, 1998.

[25] D. Foster and P. Dayan, "Structure in the space of value functions," *Machine Learning*, vol. 49, no. 2-3, pp. 325–346, 2002.

[26] M. Gimelfarb, S. Sanner, and C.-G. Lee, "Reinforcement learning with multiple experts: A bayesian model combination approach," in *Proceedings of the 32nd Annual Conference on Advances in Neural Information Processing Systems (NIPS-18)*, To appear., Montreal, QC, Canada, 2018.

[27] N. Ferns, P. Panangaden, and D. Precup, "Metrics for finite markov decision processes," in *Proceedings of the 20th conference on Uncertainty in artificial intelligence*, AUAI Press, 2004, pp. 162–169.

[28] J. Sorg and S. Singh, "Transfer via soft homomorphisms," in *Proceedings of The 8th International Conference on Autonomous Agents and Multiagent Systems-Volume 2*, International Foundation for Autonomous Agents and Multiagent Systems, 2009, pp. 741–748.

[29] F. Zhuang, X. Cheng, P. Luo, S. J. Pan, and Q. He, "Supervised representation learning: Transfer learning with deep autoencoders.," in *IJCAI*, 2015, pp. 4119–4125.

[30] R. Dearden, N. Friedman, and S. Russell, "Bayesian q-learning," in *AAAI/IAAI*, 1998, pp. 761–768.

[31] D. E. Knuth, *The art of computer programming: sorting and searching*. Pearson Education, 1997, vol. 3.

# B Digital twin of reheat furnace

**Kuilin Chen, C-MORE Ph.D. student**

Digital twin is one of the core concepts in Industrial 4.0 with the integration of Internet of Things, artificial intelligence and optimal decision making. The definition and application of digital twin is reviewed at the beginning of this article, followed by detailed design and development of digital twin for a reheat furnace through data-driven modelling. Finally, the potential application of sequential Monte Carlo is discussed with the consideration of the real-time synchronization feature in digital twin.

## B.1 Literature review

In recent years, Industry 4.0 has become an emerging concept with the amazing growth and advancement in digital technologies that allow the integration of Internet of Things (IoT), cloud computing and artificial intelligence, etc. [1], [2]. In this fourth wave of industrial revolution, traditional manufacturing companies make huge investment to digitize their assets to take the advantage of smart factory, decentralized organization and flexibility to increase their efficiency and profitability in competition [3]–[5]. Among several fundamental concepts within Industrial 4.0, digital twin (DT) plays a central role because it bridges the assets and processes in the physical world with the models and analytics at the virtual space in the real-time fashion [6]. Essentially, DT can provide company with complete digital footprint of their products and equipment for the entire life cycle, leading to deep understanding of product development and equipment health conditions [7]. With the real-time synchronization of floor shop in physical world and integrated models and software in virtual space, manufacturing companies are able to detect and solve physical issues in product and equipment sooner, predict outcomes at high fidelity, design and build better products, and, ultimately, better serve their customers. Therefore, the DT concept becomes more and more prevalent in both industry and academia by boosting company's revenue through rapid product development, improved operation efficiency, reduced defect rate and optimized maintenance schedule.

### B.1.1 Definition of digital twin

Although DT is a very new concept without a universal definition, researchers from different areas have attempted to define it in several different ways based on problems and issues they want to solve within the Industrial 4.0 framework in their area. The conceptual model of a virtual, digital equivalent to a physical product is proposed in 2003, with the expectation that all the data and information of a physical system could be replicated in software for simulation and analysis. [8], [9] That conceptual model, though not being called as DT, but embodies all essential parts of DT, such as the physical space, the virtual space, and the linkage or interface between the two spaces [10], [11]. DT is formally defined through a case study by NASA and US air force as an integrated simulation models of an as-built vehicle based on the best available information, and history data to reflect wear and tear of its corresponding physical twin while in use communicated by sensor updates [12], [13]. Researchers in aerospace community develop various digital twins to mirror the health conditions of a aircraft or parts by integration with other aspects such as product life-cycle management (PLM), feedback from real world, and prognostics and diagnostics activities [13]–[15]. The concept of digital twin is expanded as a digital counterpart product to its physical instance, which could be used for products from any manufacturing industries, though their research focus is still on manufacturing of air vehicles [16]. Thanks to the rapid development in data acquisition, cloud computing and big data technologies in manufacturing industries, DT is also developed and defined in manufacturing industries as a virtual counterpart of production resources based on coupled models to simulate the condition of the equipment and machines [17]. In parallel, the idea of DT is closely integrated with some ongoing research of cyber-physical system (CPS) and virtual factory (VF) in smart manufacturing area [18]. Simulation is a core functionality of DT in manufacturing, which provides seamless assistance and support for operation and service by means of direct linkage of operation data [19]. Along with the view of simulation, DT is composed of very realistic models of the process current state and its behavior in interaction with the environment in the real world [20]. On the other hand, DT also provides a new mechanism to manage IoT with virtual substitutes of real world objects consisting of virtual representations and communication capabilities making up smart objects acting as intelligent nodes inside the internet of things and services [21], [22].

### B.1.2 Application of digital twin

By definition, DT is designed to model sophisticated assets or processes with iteration to external environment, which are very difficult to quantify by traditional methodologies. As such, it is beneficial to review the current application of DT in a wide range of contexts to understand why and how DT is created and implemented before actually developing DT for any particular assets or processes.

DT is initially developed for aerospace vehicles because it's impossible to reproduce the extreme thermal, mechanical, and acoustical loadings in a laboratory environment to understand the health condition of the vehicle. However, health condition of the aerospace vehicle cannot be obtained from tra-

ditional simulation methods because they are not able to integrate the sub-models at different scale or handle the stochastic input data from external environment. Therefore, an integrated multiphysics, multiscale, probabilistic simulation of an as-built vehicle is developed as a digital twin to mirror the conditions of aerospace vehicle in actual flying [12]. The finite element method (FEM) model for local structural loads and computational fluid dynamics (CFD) model for artificially flying the aircraft, at different geometric scale, are closely coupled together to predict the local structural damage and material state in repose to flight conditions, with the auxiliary of computer aided design (CAD) [13], [23], [24]. Nevertheless, neither mathematical modelling details nor performance statistics of DT is provided in those early papers. Recently, an FEM based DT with modelling details is presented to monitor structural health condition. Heuristic optimization algorithm is utilized to identify key parameters in the model, leaning to accurate monitoring results with comparison to real reference data [25]. The aforementioned aircraft or airframe health condition monitoring is based on deterministic physical models within DT, which cannot handle epistemic uncertainty due to lack of knowledge. Consequently, machine learning algorithms such as particle filter driven dynamic Bayesian network is developed as an extra layer above the physical model based DT to get accurate prognostics and diagnostics results through stochastic input-output data from DT [26].

Besides the aerospace field, DT is also well received in smart manufacturing environment, especially with the wave of promoting Industry 4.0. DT has been endowed with new functionality and usage when applied to industrial processes in manufacturing area, beyond the scope of prognostics and diagnostics activities. Apart from acting as digital replica for physical assets at floor shop, DT of manufacturing processes is also developed to provide insightful guidance to improve production efficiency. For instance, a DT of an additive manufacturing process, using multiple analytical sub-models including heat transfer models and fluid dynamics models, is built to predict the spatial and temporal variations of metallurgical parameters, which is proved to be highly accurate with validation of experiment data [27], [28]. Meanwhile, a rapid DT design framework is proposed by adopting the idea of reference models, which refers to producing a copy of a production line and using it for reasoning about other instances of the similar production line. A DT based on such rapid development provides decoupling analytics for a hollow glass production line, as well as multi-objective optimization towards decision making [29].

### B.1.3 Gap in current research

Since the idea of DT was proposed in 2010s, a dozen of papers have been published around this topic. However, after thorough literature review, it is found that most of them are review and introduction papers about potential application of DT in different areas without any detailed examples. Table B.1 lists all reviewed original research papers, which propose methodologies to build DT for a specific system or process.

Table B.1: Digital Twin examples

| Reference | Methodology | Model Details | Performance Statistics |
|---|---|---|---|
| Tuegel, Ingraffea, Eason, *et al.* [13] | FEM and CFD | No | No |
| Glaessgen and Stargel [12] | 3D FEM, quantum mechanics and molecular dynamics | No | No |
| Kraft [24] | physics-based model and experiment | No | No |
| Li, Mahadevan, Ling, *et al.* [26] | FEM and CFD | No | No |
| Seshadri and Krishnamurthy [25] | FEM and genetic algorithm | Yes | Yes |
| Knapp, Mukherjee, Zuback, *et al.* [27] | analytical sub-models, heat transfer model and fluid dynamics model | Yes | Yes |
| DebRoy, Zhang, Turner, *et al.* [28] | heat transfer model | No | Yes |
| Tao and Zhang [30] | FEM and CFD | No | No |
| Zhang, Liu, Chen, *et al.* [29] | reference models | No | Yes |

Although mathematical model is an essential part of DT and almost every DT example listed in table B.1 uses different forms of mathematical models, the majority of current published papers do not provide any model details. No matter model details are provided or not, first-principle models or physical models are used in aforementioned examples. Identification of such models with nonlinear equations is a non-trial mathematical optimization problem. Apart from one paper explicitly using genetic algorithm, none of them illustrates how to identify the parameters in models. Such practice in current DT literature makes it extremely difficult to duplicate the methods proposed by those DT papers, though it is understood that some systems, products and processes contain highly confidential and sensitive information in business and military. In addition, development of DT upon first-principle models requires in-depth knowledge of the system or process, and takes significant effort and time of experienced engineers. It is inevitable that some knowledge is not available for some very complex systems, leading to epistemic uncertainty in models due to lack of knowledge. Furthermore, less than half of the papers in table B.1 present the performance statistics of DT by comparison to its twin in physical world. DT itself is meaningless without high fidelity output compared with the physical system. Development of DT is not a one-time deal. Mismatch between the DT and physical system can happen due to equipment deterioration and external environmental change. How to develop an adaptive DT has not been studied yet.

It is an overwhelming task to develop DT for all processes and equipment in a manufacturing company

all at once. A reasonable plan for digitalization of a tradition manufacturing company is to develop an initial DT for one chosen process along with its equipment, deliver value there, and continue to develop for other processes. The remaining of this article is organized as follows. Development of DT for a reheat furnace in a steel manufacturing company is discussed in details in the next section, followed by some preliminary results. Finally, we conclude our current work and propose some research ideas regarding development of DT for reheat furnace.

## B.2 Design of digital twin for reheat furnace

The fundamental goal of the digital twin is to predict the output (slab drop-out-temperature and throughput) of reheat furnace with high fidelity. Due to the complexity of the reheat furnace system, the digital twin of reheat furnace can be decomposed into combustion system model, slab temperature model,control systems and simplified down stream model. In addition, the output of one subsystem can be the input for another subsystem. The mathematical details of subsystem models are presented in following subsections.

### B.2.1 Combustion zone model

The reheat furnace consists of 12 combustion zones which control the zone temperature independently. In principle, the combustion zone temperature change $\Delta z_t$ between current zone temperature $z_t$ and last zone temperature $z_{t-1}$ is drive by the air flow $a_t$ and gas flow $g_t$ through an unknown mapping function $f_p(\cdot)$ as follows

$$\begin{aligned} \Delta z_t &= f_p(a_t, g_t) \\ z_t &= z_{t-1} + \Delta z_t + \epsilon_{z_t} \end{aligned} \tag{B.1}$$

where $\epsilon_{z_t}$ is the noise or disturbance. The air flow $a_t$ and gas flow $g_t$ are controlled by the zone temperature set point $sp_t$ via a proportional-integral-derivative (PID) controller as follows

$$\begin{aligned} a_t &= K_{p_a} e_{z_t} + K_{i_a} \sum_{i=1}^{t} e_{z_i} + K_{d_a}(e_{z_t} - e_{z_{t-1}}) + \epsilon_{a_t} \\ g_t &= K_{p_g} e_{z_t} + K_{i_g} \sum_{i=1}^{t} e_{z_i} + K_{d_g}(e_{z_t} - e_{z_{t-1}}) + \epsilon_{g_t} \end{aligned} \tag{B.2}$$

where $e_{z_t} = sp_t - z_t$ is the difference between the temperature set point and actual zone temperature, $K_{p_a}$, $K_{i_a}$, $K_{d_a}$, $K_{p_g}$, $K_{i_g}$ and $K_{d_g}$ are the proportional, integral and derivative gains for air flow $a_t$ and gas flow $g_t$ respectively. It is not desirable to identify $f_p(\cdot)$ and predict zone temperature $z_t$ using eq. (B.1) and eq. (B.2) for several reasons.First, the model requires data from infinite past due to the integral part in eq. (B.2). Second, the actual air and gas flows are subject to random disturbance, variation in air and

gas composition and actuator failure which cannot be characterized by eq. (B.2). The zone temperature prediction may not be accurate due to the propagation of errors. Third, it's very difficult or intractable to optimize the slab temperature performance or throughput based on this digital twin because the order of decision variable (temperature set point) is too large.

The best practice in control system optimization is to identify a transfer function $f_c(\cdot)$ between the input and output variables. Equation (B.1) and eq. (B.2) are equivalent to the transfer function as follows

$$z_t = f_c(z_{t-1}, z_{t-2}, ..., sp_{t-1}, sp_{t-2}, ...) + \epsilon_{z_t}$$

For a meaningful model, the orders of zone temperature and set points are truncated to $r$ and $s$, respectively. Let vector $\mathbf{x}_t = [z_{t-1}, \dots, z_{t-r}, sp_{t-1}, \dots, sp_{t-s}]^T$ denotes the stacked past temperature and set points. The combustion zone model can be expressed as follows

$$z_t = f_c(\mathbf{x}_t, \omega) + \epsilon_{z_t}$$

where $\omega$ denotes the vector for model parameters and $\epsilon_{z_t}$ is the model error term between measured zone temperature $z_t$ and modelled zone temperature $\hat{z}_t = f_c(\mathbf{x}_t, \omega)$. The task of combustion zone model design is to find an appropriate model structure and model order ($r$ and $s$) based on available data and knowledge about the combustion system to obtain minimized prediction error from the identified combustion zone model. The identification process is to find a $f_c(\cdot)$ with given structure and model orders by minimizing the error term as follows

$$J(\omega) = \frac{1}{N}\sum_{t=1}^{N}(\hat{z}_t - z_t)^2$$
$$\hat{\omega} = \arg\max_{\omega} J(\omega)$$

where $N$ is the total available number of samples and $\hat{\omega}$ is the estimated model parameter vector.

Different from traditional simulation models, digital twin can be synchronized with the physical system. The frequency of synchronization depends on the purpose of digital twin. Due to the randomness in combustion system, the output from the digital twin can never be the same as the physical system. At each round of synchronization, the current predicted output can be calibrated by the real output data from physical system. The calibrated value can be used for future prediction. In addition, the dynamics in the transfer function is subject to change because the combustion system is a stochastic system. $\hat{\omega}$ can be updated to capture the current dynamics in the system using the latest data from synchronization.

### B.2.2 Slab temperature model

After a slab is charged into reheat furnace, it goes through different combustion zones when it travels from the charge side to discharge side. Due to the nature of digital computer control, the slab temperature model $s_t$ is a discrete time model computed at a fixed time interval (30 seconds) as follows

$$\begin{aligned} \Delta s_t &= f_s(\hat{s}_{t-1}, z_{t-1}, h) \\ \hat{s}_t &= \hat{s}_{t-1} + \Delta s_t \\ s_t &= \hat{s}_t + \epsilon_{s_t} \end{aligned}$$

where $\hat{s}_t$ is the predicted slab temperature, $\epsilon_{s_t}$ is the error term, $h$ is the heat transfer coefficient based on thickness and chemistry composition of slab and $f_s(\cdot)$ is a known nonlinear heat transfer function available on reheat furnace control system. Note that only the initial charge temperature $s_0$ and final drop-out-temperature $s_T$ can be measured. The future slab temperature is predicted based on current predicted slab temperature because no slab temperature measurement is available inside the furnace.

The design of slab temperature model in digital twin can be as simple as duplicating $f_s(\cdot)$ from reheat furnace control system. The input to the model is initial charge temperature $s_0$ and zone temperature $z_t$ that can be calculated by model described in appendix B.2.1.

### B.2.3 Control system

The control system sets up the heating trajectory for each slab at charge time and computes the combustion zone set points for all zones and reheat furnace pacing dynamically at a fixed time interval (30 seconds). The set point of a combustion zone is calculated based on the temperature of all slabs in that zone with respect to their current temperature targets from the heating trajectory as follows

$$\begin{aligned} e_t &= \sum_{j=1}^{K} (s_t^j - t_t^j) \\ sp_t &= g_s(e_t) \end{aligned} \tag{B.3}$$

where $j = \{1, \dots, K\}$ denotes all slabs at one zone. Meanwhile, pace rate is calculated for each slab inside the furnace based on their current temperature and target. The furnace pacing is dominated by the slowest slab inside the furnace.

$$\begin{aligned} e_t^j &= s_t^j - t_t^j \\ p_t^j &= g_p(e_t^j) \\ p_t &= \min(e_t^1, e_t^2, ..., e_t^N) \end{aligned} \tag{B.4}$$

where $j = \{1, \dots, N\}$ denotes all slabs inside the furnace, $p_t^j$ represents the pace rate for an individual slab, $p_t$ is the pace rate for the furnace. Equations (B.3) and (B.4) should be duplicated in the digital twin of reheat furnace to get the same control action behavior as the physical system.

### B.2.4 Simplified downstream model

The reheat furnace requires downstream processing time. On the one hand, the slab temperature target relies on the predicted downstream processing time. On the other hand, the actual throughput is also affected by the downstream processing time because a slab cannot be extracted if the downstream processing is not complete. A simplified model can be developed to predict the downstream processing time.

$$t = g_d(d_1, d_2, c)$$

where $d_1$ is the original dimension (width, thickness and length) of the steel before downstream processing, $d_2$ is the final dimension of steel, $c$ is a vector of slab characteristics such as chemistry composition, hardness, steel grade and special processing requirement. The input to $g_d(\cdot)$ includes both continuous and categorical data, and the relationship between input and output can be quite nonlinear. In this case, deep neural network could be a good candidate for simplified downstream model to predict the processing time.

## B.3 Preliminary example for combustion zone model

A preliminary example of combustion zone model is demonstrated in this section. It can be treated as a toy example for digital twin of reheat furnace. Several transfer function identification methods are considered and compared in this section, including Box-Tiao transformation based ARMAX model, PEM based ARX model and gated recurrent unit (GRU) network. Diebold-Mariano test is used to compare the prediction accuracy between models. Finally, future research path is discussed based on pros and cons of all methods on the numerical performance on temperature control system identification.

### B.3.1 System identification of combustion zone

System identification is the process of using appropriate mathematical models and optimization algorithms to determine a relationship between future outputs $y_t$ and past observations of inputs $u_{t-i}$ and outputs $y_{t-i}$ by minimizing the error between measured outputs and model outputs. Without loss of generality, the input-output relationship can be expressed as follows

$$\begin{aligned} &y_t = f(y_{t-1}, ..., y_{t-p}, u_{t-b}, ..., u_{t-b-s}, \epsilon_{t-1}, ..., \epsilon_{t-q}) + \epsilon_t \\ &r \geq 1, b \geq 0, s \geq 0, d \geq 0 \end{aligned}$$

where $\epsilon_t$ is the error between measured and predicted system output at time $t$, while $b$, $p$, $r$ and $d$ denote input delay, input lag, output lag and error lag, respectively.

### B.3.2 ARMAX model

Liner transfer function can be an Auto-Regressive Moving-Average with eXogenous input (ARMAX) model, which relates the current model output, past inputs, past outputs and past prediction errors [31]. The ARMAX model can be expressed as follows:

$$y_t = \sum_{i=1}^{p} \phi_i y_{t-i} + \sum_{i=b}^{s} \omega_i u_{t-i} + \sum_{i=1}^{q} \theta_i \epsilon_{t-i} + \epsilon_t \tag{B.5}$$

where $\phi_i$, $\omega_i$ and $\theta_i$ are the ARMAX model parameters. The ARMAX model can be identified by the Box-Tiao method in an iterative way [32].

1. Develop an ordinary least squares (OLS) model between $y_t$ and $u_t$

$$y_t = \sum_{j=1}^{s} v_j u_{t-j} + e_t \tag{B.6}$$

   where $e_t$ is the residual of the OLS model and $v_j$ is the impulse response function of the system.

2. Identify an ARMA model for $e_t$ using Box-Jenkins method

$$\begin{aligned} \phi(B) e_t &= \theta(B) a_t \\ \phi(B) &= 1 - \phi_1 B - ... - \phi_p B^p \\ \theta(B) &= 1 + \theta_1 B +, ... + \theta_q B^q \end{aligned} \tag{B.7}$$

   where $a_t$ is white noise.

3. Get filtered $\tilde{y}_t$ and $\tilde{u}_t$ using the ARMA model in eq. (B.7) as follows

$$\begin{aligned} \tilde{y}_t &= \frac{\phi(B)}{\phi(B)} y_t \\ \tilde{u}_t &= \frac{\phi(B)}{\phi(B)} u_t \end{aligned}$$

4. Run the OLS regression of eq. (B.6) on $\tilde{y}_t$ and $\tilde{u}_t$ in Step 1.

5. If the residuals from the previous step is uncorrelated, the model estimation is complete. Otherwise, Step 2 - 4 should be repeated.

A group of preliminary AR orders $p$ and MA orders $q$ can be selected on autocorrelation function (ACF) plot and partial autocorrelation function (PACF) plot. The final model order is determined by Akaike information criterion (AIC). The prediction residuals of ARMAX model identified by Box-Tiao method is guaranteed to be uncorrelated.

### B.3.3 PEM model

Since a transfer function may be used to make long horizon predictions (many-step-ahead predictions), Moving-Average (MA) part is usually not included in the transfer function model because future errors between measured and predicted outputs are not available. Therefore, Auto-Regressive with eXogenous input (ARX) model is the most widely used type of model for linear transfer function. ARX model can be presented as

$$y_t = \sum_{i=1}^{r} \delta_i y_{t-i} + \sum_{i=b}^{s} \omega_i u_{t-i} + \epsilon_t \tag{B.8}$$

Equation (B.8) can be put in vector format as

$$\begin{aligned} y_t &= \Phi^T \mathbf{x}_t \\ \Phi^T &= [\delta_1, ..., \delta_r, \omega_b, ..., \omega_s] \\ \mathbf{x}_t &= [y_{t-1}, ..., y_{t-r}, ..., u_{t-b}, ..., u_{t-b-s}]^T \end{aligned} \tag{B.9}$$

$y_t = \Phi^T \mathbf{x}_t$ where $\Phi^T$ is the parameter vector and $\mathbf{x}_t$ is the regressor vector. The identification process is to find an appropriate estimated parameter vector $\hat{\Phi}^T$ which minimizes the squared error between measured output $y_t$ and estimated output $\hat{y}_t = \hat{\Phi}^T \mathbf{x}$. In the field of control theory and engineering, the error term $\epsilon_t$ is treated as unknown external disturbance to the system. Therefore, $\epsilon_t$ is zero mean but may not be uncorrelated in this model. Parameters in ARX model cannot be computed by OLS because the regressor variables are highly correlated. Prediction error method (PEM) proposed by [33] can be utilized to estimate the model parameters by solving the following non-convex optimization problem:

$$\begin{aligned} J(\Phi) &= \frac{1}{n} \sum_{t=1}^{n} (\Phi^T \mathbf{x}_t - y_t)^2 \\ \hat{\Phi}^T &= \arg\max_{\Phi} J(\Phi) \end{aligned} \tag{B.10}$$

where $n$ is the number of training samples. The optimization problem in eq. (B.10) is usually solved by Gauss-Newton algorithm.

Linear transfer function may not be sufficient to capture the dynamics of real physical systems because they are nonlinear in nature. Although it's possible to build nonlinear ARX (NARX) models, it's very difficult to determine the nonlinear structure for such systems with accurate parameters.

### B.3.4 GRU network

Neural network has been widely used for time series forecasting since 1980s due to its strong capability to approximate nonlinear relationship between past and future data [34], [35]. The recent emergence of deep learning and efficient learning algorithms have enhanced the modelling and prediction capability of NN, but traditional feedforward NN cannot use its reasoning about previous input-output data to inform future ones. Recurrent neural networks (RNN) are perfect for time-series forecasting because they are networks with loops inside them, allowing memory of past information to persist [36]. In fig. B.1, input $\mathbf{x}_t$ is fed to a neural network unit $A$ with an output value $h_t$. The output of current step of the network is passed to the next step. The directed acyclic graph of RNN can be unrolled as fig. B.1 and the unrolled chain-like structure reveals that it's intimately related to time series.

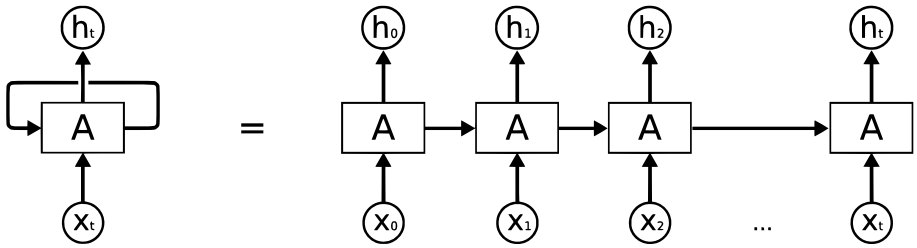


Figure B.1: Unfolded recurrent neural network[1]

In practice, RNN is not able to handle the long-term dependencies in time series well and it also suffers from gradient vanishing problem. The long short-term memory (LSTM) networks are a special kind of RNN, with recurrent gates called forget gates to avoid the long-term dependency problem [37]. LSTM also prevents gradient vanishing or exploding in network training. More recently, GRU without an output gate is developed as one of the most notable LSTM variants [38]. GRU is chosen in this study because it has simpler structure and fewer parameters but leads to better performance than traditional LSTM [39], [40]. The structure of a GRU is shown in fig. B.2 and the mathematical details are presented below.

$$
\begin{aligned}
z_t &= \sigma(W_z \cdot [h_{t-1}, \mathbf{x}_t] + b_z) \\
r_t &= \sigma(W_r \cdot [h_{t-1}, \mathbf{x}_t] + b_r) \\
h_t &= z_t \circ h_{t-1} + (1 - z_t) \circ \tanh\left(W_h \cdot [r_t \circ h_{t-1}, \mathbf{x}_t] + b_h\right)
\end{aligned}
$$

where $\circ$ denotes denotes the Hadamard product, $\sigma(\cdot)$ is sigmoid function, $f_t$ is the forget gate's activation, $i_t$ is the input gate's activation, $C_t$ is the cell state, $\tilde{C}_t$ is the new candidate cell state, $o_t$ is the output gate's activation, $W_*$ and $b_*$ are weight and bias term for each gate to be identified through network

[1] Adapted from `http://colah.github.io/posts/2015-08-Understanding-LSTMs/`

training.

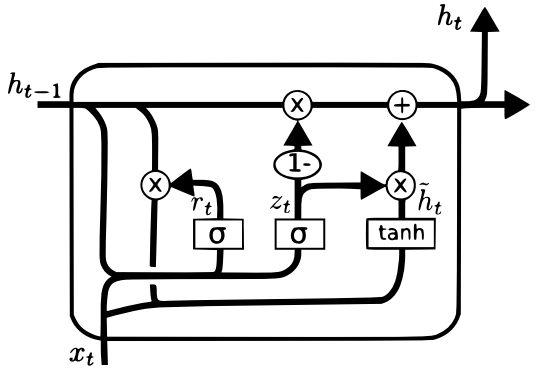


Figure B.2: GRU [2]

The neural network training process is to find the optimal network parameters ($\Phi = [\mathbf{W}, \mathbf{b}]$) by minimizing a cost function, which can be the mean squared error between network's predicted output $\hat{y}_t = h_t$ and measured output $y_t$,

$$\begin{aligned} J(\Phi) &= \frac{1}{n}\sum_{t=1}^{n}(\hat{y}_t - y_t)^2 + \lambda\|\Phi\|_2 \\ \hat{\Phi}^T &= \arg\max_{\Phi} J(\Phi) \end{aligned} \tag{B.11}$$

where $\lambda$ is a regularization term to prevent overfitting. Stochastic gradient descent (SGD) algorithm is utilized to update the each parameter in the direction of negative gradient of the cost function with respect to the corresponding parameter as follows

$$\Phi_{k+1} = \Phi_k - \alpha\nabla_{\Phi}J(\Phi)$$

where $\alpha$ is the learning rate in SGD algorithm [41]. A local minima can be found by SGD algorithm because eq. (B.11) is a high-dimensional non-convex optimization problem. In order to find the best parameters of GRU, parameters are initialized at different values randomly in various training rounds.

### B.3.5 Numerical results

Part of the training and test time-series data is presented in fig. B.3.

A preliminary OLS model is developed between SP and TC. It is found that ARMAX(7,1) leads to best prediction performance in this case. In parallel, ARX(7) model identified by PEM method achieves the best performance after trying different orders in ARX model.

GRU does not require all lagged past output to be fed at each step. Instead, the state of the system

[2]Adapted from `http://colah.github.io/posts/2015-08-Understanding-LSTMs/`

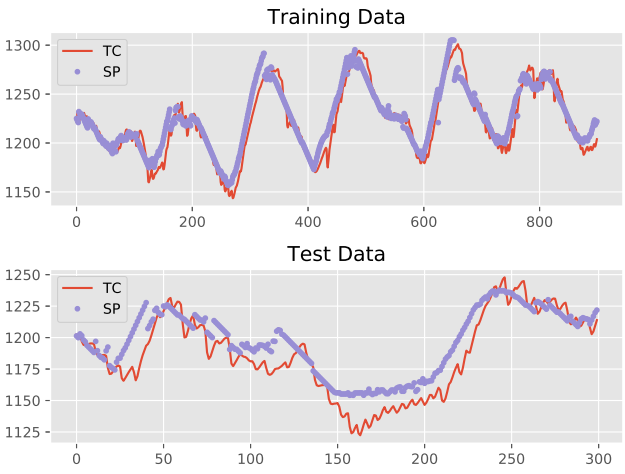


Figure B.3: Training and test time-series data

is captured by the internal cell state based on the memory of past input-output data. The root mean squared error (RMSE) of predicted future temperature by three methods are shown in table B.2.

Table B.2: Prediction performance - RMSE

| Case | ARMAX | ARX | GRU |
|---|---|---|---|
| Training | 2.26 | 2.21 | 2.13 |
| Test | 3.11 | 3.01 | 2.75 |

In addition, Diebold-Mariano test is utilized to compare the prediction accuracy between models [42]. The null hypothesis $H_0$ is that the prediction accuracy is the same for both models. The null hypothesis can be rejected based on the p-values in table B.3, except for comparison with ARX model in test data set. It is obvious that GRU method achieves the best results in both training and test data sets. In addition, the the predicted temperature by GRU are plotted against the TC measurements in Fig fig. B.4. The predicted values by GRU method closely follow the true value of the measured values.

Table B.3: Diebold-Mariano test

| DM Test | DM | p-value |
|---|---|---|
| GRU vs ARMAX Train | -2.8373 | 0.003054 |
| GRU vs ARMAX Test | -2.9871 | 0.001452 |
| GRU vs ARX Train | -4.7281 | 2.098e-06 |
| GRU vs ARX Test | -1.7753 | 0.0023 |

The prediction residuals of ARMAX model are uncorrelated because the identification steps in Box-Tiao transformation explicitly remove the correlation in residuals. However, ARMAX model renders the worst prediction performance because the prediction error is not guaranteed to be minimizes. On the other hand, the ARX model identified by PEM method, with very similar model structure as ARMAX model, results in smaller prediction errors because the model error is explicitly minimized. Last but not the least, GRU obtains the best prediction performance for several reasons. First, it can capture the long-term dependency between past and future input-output sequence beyond limited number of lag orders. Second, the nonlinear activation function is able to characterize potential non-linearity in the system dynamics. Third, the prediction error is minimized with a parameter regularization term to get optimal forecasting accuracy while preventing overfitting.


Figure B.4: Predictions by GRU model

## B.4 Future research

The reheat furnace is a complex manufacturing system subject to variation in external environmental change, equipment wear and failure. If constant model parameter $\Phi$ is used, digital twin may not be able to predict future combustion zone temperature accurately when the dynamics of the combustion zone system changes due to aforementioned reasons. As such, the digital twin for reheat furnace should be modelled as stochastic system with time-variant parameters. For example, the combustion system model can be formulated in the state space model form as follows

$$\Phi_t = \Phi_{t-1} + v_t \tag{B.12}$$

$$y_t = f(\mathbf{x}, \Phi_t) + w_t \tag{B.13}$$

where eq. (B.12) is the state transition equation for unobserved model parameters, and eq. (B.13) is measurement equation for observed combustion zone temperature. $f(\cdot)$ in eq. (B.13) can be, but not limited to, ARMAX, ARX or GRU. Given the state transition and measurement equations, the unobserved model parameters can be estimated by sequential Monte Carlo methods [43], [44]. The procedure is described as follows.

For time steps $t = 1, 2, 3, ...$

1. Initialization: for $i = 1, 2, ..., N_p$, sample $\Phi_0^{(i)} \sim p(\Phi_0)$, $W_0 = 1/N_p$.
2. Importance Sampling: for $i = 1, 2, ..., N_p$, draw samples $\hat{\Phi}_t^{(i)} \sim p(\Phi_t | \Phi_{t-1}^{(i)})$.
3. Weight update: calculate the importance weight $W_t^{(i)} = p(y_t | \hat{\Phi}_t^{(i)})$.
4. Weight normalization: $\tilde{W}_t^{(i)} = W_t^{(i)} / \sum_{j=1}^{N_p} W_t^{(j)}$.
5. Resampling: generate $N_p$ new particles $\Phi_t^{(i)}$ from the set $\{\hat{\Phi}_t^{(i)}\}$ according to the importance weight weights $\tilde{W}_t^{(i)}$.
6. Repeat 2 to 5 for each time step.

A preliminary example is demonstrated here using one sequential Monte Carlo method. One combustion zone temperature dynamics dramatically due to the partial failure of fuel value. As shown in fig. B.5, the actual zone temperature cannot follow the temperature set point.

If the original model is used, the digital twin tends to over predict the temperature due to the model mismatch. With the real-time synchronization with physical system in digital twin, the model parameters can be recursively updated using sequential Monte Carlo. Figure B.6 shows that the model updated by sequential Monte Carlo achieves much better prediction accuracy than the original model under the new system dynamics.

Currently, the sequential Monte Carlo method is used to update the model parameters in ARX model in this preliminary example. It can be applied to GRU so that adaptive neural network based digital twin can be developed. In addition, it is noticed that the predicted values by sequential Monte Carlo is noisy though it's better than the original model. The prediction accuracy can be increased by specifying more appropriate state transition equation for the model parameters. It's anon-trivial task for models with large parameter space, such as GRU.

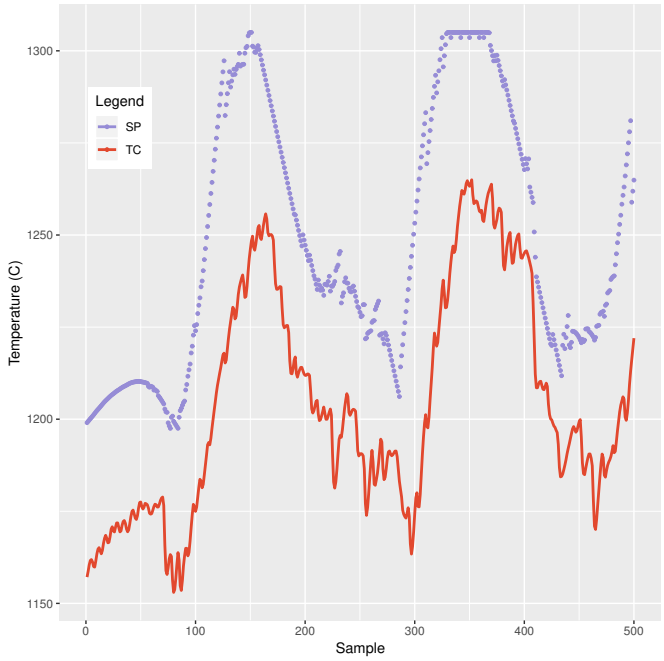


Figure B.5: Temperature dynamics under partial valve failure

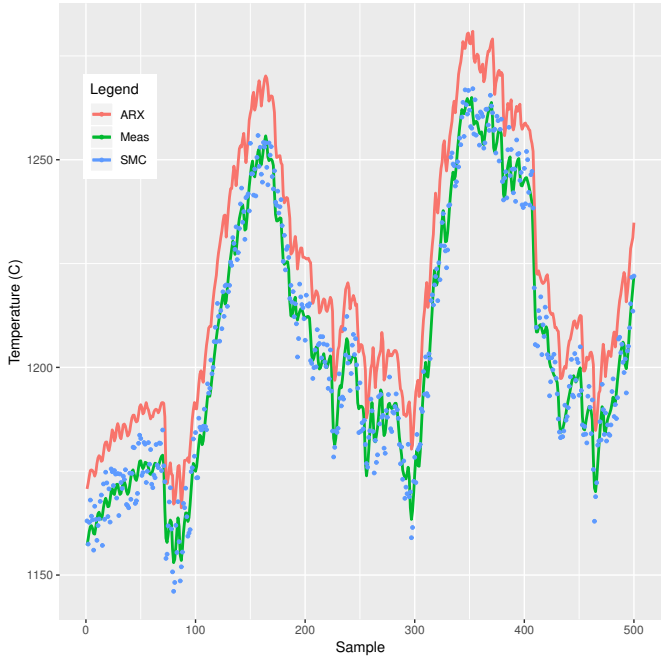


Figure B.6: Temperature prediction under partial valve failure

# Bibliography


[1] H. Lasi, P. Fettke, H. Kemper, T. Feld, and M. Hoffmann, "Industry 4.0," *Business & Information Systems Engineering*, vol. 6, no. 4, pp. 239–242, 2014.

[2] N. Jazdi, "Cyber physical systems in the context of industry 4.0," in *Automation, Quality and Testing, Robotics, 2014 IEEE International Conference on*, IEEE, 2014, pp. 1–4.

[3] R. Drath and A. Horch, "Industrie 4.0: Hit or hype?" *IEEE industrial electronics magazine*, vol. 8, no. 2, pp. 56–58, 2014.

[4] J. Wan, S. Tang, Z. Shu, D. Li, S. Wang, M. Imran, and A. V. Vasilakos, "Software-defined industrial internet of things in the context of industry 4.0," *IEEE Sensors Journal*, vol. 16, no. 20, pp. 7373–7380, 2016.

[5] K. Zhou, T. Liu, and L. Zhou, "Industry 4.0: Towards future industrial opportunities and challenges," in *Fuzzy Systems and Knowledge Discovery (FSKD), 2015 12th International Conference on*, IEEE, 2015, pp. 2147–2152.

[6] R. F. Babiceanu and R. Seker, "Big data and virtualization for manufacturing cyber-physical systems: A survey of the current status and future outlook," *Computers in Industry*, vol. 81, pp. 128–137, 2016.

[7] Q. Qi and F. Tao, "Digital twin and big data towards smart manufacturing and industry 4.0: 360 degree comparison," *IEEE Access*, vol. 6, pp. 3585–3593, 2018.

[8] M. Grieves, *Virtually perfect: Driving innovative and lean products through product lifecycle management*. Space Coast Press, 2011.

[9] M. Grieves and J. Vickers, "Digital twin: Mitigating unpredictable, undesirable emergent behavior in complex systems," in *Transdisciplinary perspectives on complex systems*, Springer, 2017, pp. 85–113.

[10] A. Cerrone, J. Hochhalter, G. Heber, and A. Ingraffea, "On the effects of modeling as-manufactured geometry: Toward digital twin," *International Journal of Aerospace Engineering*, vol. 2014, 2014.

[11] M. Bajaj, B. Cole, and D. Zwemer, "Architecture to geometry-integrating system models with mechanical design," in *AIAA SPACE 2016*, 2016, p. 5470.

[12] E. Glaessgen and D. Stargel, "The digital twin paradigm for future nasa and us air force vehicles," in *53rd AIAA/ASME/ASCE/AHS/ASC Structures, Structural Dynamics and Materials Conference 20th AIAA/ASME/AHS Adaptive Structures Conference 14th AIAA*, 2012, p. 1818.

[13] E. Tuegel, A. Ingraffea, T. Eason, and S. Spottswood, "Reengineering aircraft structural life prediction using a digital twin," *International Journal of Aerospace Engineering*, 2011.

[14] B. Gockel, A. Tudor, M. Brandyberry, R. Penmetsa, and E. Tuegel, "Challenges with structural life forecasting using realistic mission profiles," in *53rd AIAA/ASME/ASCE/AHS/ASC Structures, Structural Dynamics and Materials Conference 20th AIAA/ASME/AHS Adaptive Structures Conference 14th AIAA*, 2012, p. 1813.

[15] K. Reifsnider and P. Majumdar, "Multiphysics stimulated simulation digital twin methods for fleet management," in *54th AIAA/ASME/ASCE/AHS/ASC Structures, Structural Dynamics, and Materials Conference*, 2013, p. 1578.

[16] J. Ríos, J. Hernández, M. Oliva, and F. Mas, "Product avatar as digital counterpart of a physical individual product: Literature review and implications in an aircraft.," in *ISPE CE*, 2015, pp. 657–666.

[17] J. Lee, B. Bagheri, and H. Kao, "A cyber-physical systems architecture for industry 4.0-based manufacturing systems," *Manufacturing Letters*, vol. 3, pp. 18–23, 2015.

[18] K. Alam and A. El Saddik, "C2ps: A digital twin architecture reference model for the cloud-based cyber-physical systems," *IEEE Access*, vol. 5, pp. 2050–2062, 2017.

[19] R. Rosen, G. Von Wichert, G. Lo, and K. D. Bettenhausen, "About the importance of autonomy and digital twins for the future of manufacturing," *IFAC-PapersOnLine*, vol. 48, no. 3, pp. 567–572, 2015.

[20] T. Gabor, L. Belzner, M. Kiermeier, M. T. Beck, and A. Neitz, "A simulation-based architecture for smart cyber-physical systems," in *Autonomic Computing (ICAC), 2016 IEEE International Conference on*, IEEE, 2016, pp. 374–379.

[21] A. Canedo, "Industrial iot lifecycle via digital twins," in *Proceedings of the Eleventh IEEE/ACM/IFIP International Conference on Hardware/Software Codesign and System Synthesis*, ACM, 2016, p. 29.

[22] M. Schluse and J. Rossmann, "From simulation to experimentable digital twins: Simulation-based development and operation of complex technical systems," in *Systems Engineering (ISSE), 2016 IEEE International Symposium on*, IEEE, 2016, pp. 1–6.

[23] E. Tuegel, "The airframe digital twin: Some challenges to realization," in *53rd AIAA/ASME/ASCE/AHS/ASC Structures, Structural Dynamics and Materials Conference 20th AIAA/ASME/AHS Adaptive Structures Conference 14th AIAA*, 2012, p. 1812.

[24] E. M. Kraft, "The air force digital thread/digital twin-life cycle integration and use of computational and experimental knowledge," in *54th AIAA Aerospace Sciences Meeting*, 2016, p. 0897.

[25] B. R. Seshadri and T. Krishnamurthy, "Structural health management of damaged aircraft structures using digital twin concept," in *25th AIAA/AHS Adaptive Structures Conference*, 2017, p. 1675.

[26] C. Li, S. Mahadevan, Y. Ling, S. Choze, and L. Wang, "Dynamic bayesian network for aircraft wing health monitoring digital twin," *AIAA Journal*, vol. 55, no. 3, pp. 930–941, 2017.

[27] G. Knapp, T. Mukherjee, J. Zuback, H. Wei, T. Palmer, A. De, and T. DebRoy, "Building blocks for a digital twin of additive manufacturing," *Acta Materialia*, vol. 135, pp. 390–399, 2017.

[28] T. DebRoy, W. Zhang, J. Turner, and S. Babu, "Building digital twins of 3d printing machines," *Scripta Materialia*, vol. 135, pp. 119–124, 2017.

[29] H. Zhang, Q. Liu, X. Chen, D. Zhang, and J. Leng, "A digital twin-based approach for designing and multi-objective optimization of hollow glass production line," *IEEE Access*, vol. 5, pp. 26 901–26 911, 2017.

[30] F. Tao and M. Zhang, "Digital twin shop-floor: A new shop-floor paradigm towards smart manufacturing," *IEEE Access*, vol. 5, pp. 20 418–20 427, 2017.

[31] G. E. Box, G. M. Jenkins, G. C. Reinsel, and G. M. Ljung, *Time series analysis: forecasting and control*. John Wiley & Sons, 2015.

[32] G. E. Box and G. C. Tiao, "Intervention analysis with applications to economic and environmental problems," *Journal of the American Statistical Association*, vol. 70, no. 349, pp. 70–79, 1975.

[33] L. Ljung, *System Identification: Theory for the User (2nd Edition)*. Prentice Hall PTR, 1998.

[34] K. J. Hunt, D. Sbarbaro, R. Zbikowski, and P. J. Gawthrop, "Neural networks for control systems–a survey," vol. 28, no. 6, pp. 1083–1112, 1992.

[35] K. Narandra and K. Parathasarathy, "Identification and control of dynamic systems using neural networks," *IEEE Trans. on Neural Networks*, vol. 1, no. 1, pp. 4–27, 1990.

[36] K.-i. Funahashi and Y. Nakamura, "Approximation of dynamical systems by continuous time recurrent neural networks," *Neural networks*, vol. 6, no. 6, pp. 801–806, 1993.

[37] S. Hochreiter and J. Schmidhuber, "Long short-term memory," *Neural computation*, vol. 9, no. 8, pp. 1735–1780, 1997.

[38] K. Cho, B. van Merrienboer, C. Gulcehre, D. Bahdanau, F. Bougares, H. Schwenk, and Y. Bengio, "Learning phrase representations using rnn encoder–decoder for statistical machine translation," in *Proceedings of the 2014 Conference on Empirical Methods in Natural Language Processing (EMNLP)*, 2014, pp. 1724–1734.

[39] K. Greff, R. K. Srivastava, J. Koutník, B. R. Steunebrink, and J. Schmidhuber, "Lstm: A search space odyssey," *IEEE transactions on neural networks and learning systems*, vol. 28, no. 10, pp. 2222–2232, 2017.

[40] R. Jozefowicz, W. Zaremba, and I. Sutskever, "An empirical exploration of recurrent network architectures," in *International Conference on Machine Learning*, 2015, pp. 2342–2350.

[41] I. Goodfellow, Y. Bengio, A. Courville, and Y. Bengio, *Deep learning*. MIT press Cambridge, 2016, vol. 1.

[42] F. X. Diebold, "Comparing predictive accuracy, twenty years later: A personal perspective on the use and abuse of diebold–mariano tests," *Journal of Business & Economic Statistics*, vol. 33, no. 1, pp. 1–1, 2015.

[43] J. Liu and R. Chen, "Sequential Monte Carlo methods for dynamic systems," *J. Amer. Statist. Assoc.*, vol. 93, pp. 1032–1044, 1998.

[44] M. Arulampalam, S. Maskell, N. Gordon, and T. Clapp, "A tutorial on particle filters for online nonlinear/non-Gaussian Bayesian tracking," *IEEE Trans. Signal Process.*, vol. 50, pp. 174–188, 2002.